Gesellschaft für Anlagen-
und Reaktorsicherheit
(GRS) mbH

Self-sealing Barriers of Clay/Mineral Mixtures in a Clay Repository

SB Experiment in the Mont Terri Rock Laboratory

Final Report of the Pre-Project

Tilmann Rothfuchs
Norbert Jockwer
Rüdiger Miehe
Chun-Liang Zhang

May 2005

Remarks:

This report was prepared under contract No. 02 E 9713 with the Bundesministerium für Wirtschaft und Arbeit (BMWA).

The work was conducted by the Gesellschaft für Anlagen- und Reaktorsicherheit (GRS) mbH.

The authors are responsible for the content of this report.

GRS - 212
ISBN 3-931995-79-8

Foreword

A couple of years ago, GRS performed laboratory investigations on the suitability of clay/mineral mixtures as optimized sealing materials in underground repositories for radioactive wastes /JOC 00/, /MIE 03/.

The investigations yielded promising results so that plans were developed for testing the sealing properties of those materials under representative in-situ conditions in the Mont Terri Rock Laboratory (MTRL). The project was proposed to the "Projektträger Wassertechnologie und Entsorgung (PtWT+E)", and finally launched in January 2003 as the SB project ("**S**elf-sealing **B**arriers of Clay/Mineral-Mixtures in a Clay Repository").

The project was divided in two parts, a pre-project running from January 2003 until June 2004 under contract No. 02E9713 with PtWT+E and the main project running from January 2004 until December 2008 as a cost shared action of PtWT+E (contract No. 02E9894) and the European Commission (contract No. FI6W-CT-2004-508851). The SB project is part of the EC Integrated Project ESDRED.

This report presents the results achieved in the SB pre-project which was mainly characterized by preceding laboratory investigations for the final selection of suited material mixtures, the development of a testplan for the envisaged in-situ experiments at the Mont Terri Rock Laboratory (MTL) in Switzerland and the preparation of mock-up tests to be performed in advance to the in-situ experiments in the geotechnical laboratory of GRS in Braunschweig. Preparation of the mock-up tests included scoping calculations with regard to the assessment of measurement ranges to be expected as well as analyses of saturation time needed by use of different material mixtures.

In the course of the pre-project it was decided to incorporate the envisaged SB main project into the new EC Integrated Project ESDRED (Engineering Studies and Demonstrations of Repository Designs) performed by 11 European project partners within the 6th European framework programme.

Table of contents

1 Introduction

1.1 Background of the SB project

For about two decades now, geological clay formations have been investigated on their suitability to host a repository for high-level radioactive waste. To seal the waste completely from the biosphere various disposal concepts relying on a multiple barrier system including the geological barrier and engineered barrier systems (EBS) have been developed. Some of those concepts involve highly compacted bentonite buffers between the waste containers and the wall of almost circular disposal drifts or boreholes.

Considering those concepts in more detail, there is a concern about gas pressure built-up in the near-field once formation water reaches the waster canisters after re-saturation of the buffer. Hydrogen gas will be generated by anaerobic corrosion of the canisters and/or by radiolysis of the formation water. According to Rübel et al. (2003), clay formations like the Opalinus clay provide enough water to completely corrode the vitrified HLW canisters in a disposal borehole. Up to 481 m^3 of hydrogen gas would be produced per canister by its complete corrosion. Because of the high swelling pressure of the bentonite buffer and its very low permeability to gas after re-saturation, gas migration is hindered and a higher gas pressure may evolve. In case the least principal stress and the tensile strength are exceeded fracturing and disintegration of the host rock may take place.

Although there are good reasons to assume that the gas pressure might be limited because of low gas generation rates and continuous gas transport by advect-ion/diffusion and two phase flow through the EBS and the host rock, engineering measures can be used to make the system more robust.

Moderately compacted clay/sand mixtures have been found to represent a suitable alternative to the afore-described concepts. In contrast to highly compacted bentonite buffers clay/sand mixtures exhibit a high permeability to gas in the unsaturated state and a comparably low gas entry/break through pressure in the saturated state while providing an adequate self-sealing potential due to swelling of the clay minerals after water uptake from the host rock. By using optimized material mixtures, the evolution of

high gas pressure in the repository near-field will be avoided and possible migration of radionuclides in the liquid phase from the waste matrix through the buffer will be diffusion controlled just like in the host rock.

The sealing properties of clay/sand mixtures have been investigated in detail in the geotechnical laboratory of GRS within two projects, the “Two-Phase Flow” Project /Jockwer et al., 2000/ and the KENTON project /Miehe et al., 2003/. Sealing properties such as permeability to water and gas, gas entry and break-through pressure, and swelling pressure have been determined for different mixing ratios and different degrees of compaction. Adequate sealing properties have been obtained by proper adjustment of the clay/sand ratio.

A further advantage of the clay/sand mixtures lies in the fact that they can be loosely emplaced in conventionally mined disposal drifts with non-circular, but irregular shape and rough surfaces and then reasonably be compacted to get a homogeneous seal with the required density. Hence, conventional mining would be sufficient and costly mining of circular disposal drifts is not required.

The results of GRS’ laboratory investigations were found quite promising and it was thus concluded to qualify and quantify the sealing function of clay/sand mixtures under representative in-situ conditions. Hence, in summer 2003, GRS started the SB (**S**elf-sealing **B**arriers) project, the in-situ part of which to be performed at the Mont Terri Underground Rock Laboratory (MTRL).

For the successful execution of the project, a test plan had to be developed within the pre-project on basis of information available from preceding projects and the literature as well as of intensive discussion with potential project partners or expert organizations. The test plan represents a guideline for project relevant R&D work and contains plans for needed laboratory investigations, mock-up tests, scoping calculations for the mock-up and the in-situ test as well as the in-situ investigations. The following working steps are foreseen in the project:

- Laboratory investigations for final selection of suited clay/sand mixtures

In those preceding laboratory investigations the material mixtures exhibiting the desired material properties with regard to installation density, swelling pressure, permeability to gas and water, and gas break-through pressure will be determined first. Then, the

saturation behaviour of the selected material mixtures will be determined with special respect to the time needed for achieving full saturation of the seal in the mock-up and the in-situ tests.

- Large-scale laboratory mock-up testing for the development of suited material installation techniques and testing of measuring instrumentation

In advance to the start of the in-situ experiments, the transferability of the results obtained on small samples will be tested in large-scale mock-up tests at the GRS laboratories in Braunschweig.

- Material parameter determination and calibration and scoping calculations for the conduction of mock-up and field tests

This work package is mostly concerned with the determination of material parameters needed for the model calculations to predict the large-scale mock-up tests and the field experiments. Modelling will be done by GRS using the code CODE_BRIGHT /OLI 96, UPC 02/ which requires the determination of a series of material parameters including various test equipment, the selected seal material, and the host rock.

Scoping calculations will be done for the mock-up tests and the in-situ experiments. With regard to the project phases, the numerical simulations will involve design calculations, model calibrations, and simulations for supporting appropriate interpretation of the in-situ experiments.

- Field testing in vertical boreholes under representative in-situ conditions in the MTRL.

The realization of the required installation density, the water saturation in interaction with the surrounding host rock, the resulting swelling pressure and the gas break-through pressure of the actually used sealing materials will be demonstrated in up to four test boreholes in a specially excavated test field in the MTRL. First, the installation and measuring techniques will be tested in two preceding test boreholes which will be incorporated in the experimental programme if found representative and successful.

After termination of the in-situ tests, samples will be drilled from the seal and the surrounding host rock for post-test laboratory analyses of the conditions achieved in the demonstration tests (saturation, homogeneity of the saturation, porosity…).

Finally, the whole project will be evaluated and all project data and experiences will be documented in a final summary report. On the basis of results obtained from the SB project, proposals will be made for the sealing of disposal boreholes, drifts and rooms in a clay repository.

1.2 Project objectives and material functional requirements

The overall objective of the project is to test and demonstrate that the sealing properties of clay/sand mixtures determined preliminarily in the laboratory can technically be realized and maintained under repository relevant in-situ conditions (installation density, saturation, swelling pressure, overburden pressure).

The most important material properties that need to be met in a repository and demonstrated in the SB in-situ experiments are listed in the following:

Permeability to gas and diffusivity

The buffer should have a high permeability to gas. One way to avoid the development of a high gas pressure in the disposal rooms is to allow the generated gases to migrate through the seal. Right after material installation, the permeability to gas in the unsaturated state ranges between 10^{-13} and 10^{-15} m^2. According to preliminary lab investigations, it remains above 10^{-17} m^2 after gas break-through in the saturated state.

Permeability to water

The buffer should have a low permeability to water. After water uptake from the host rock, the water permeability of the material reduces because of the swelling of the clay minerals. An initial value of about 10^{-17} and 10^{-18} m^2 would be sufficient in analogy to the permeability of 10^{-14} and 10^{-16} m^2 of the excavation disturbed zone (EDZ) in the host rock /Bossart et al., 2001/. It is expected that the permeability to water will reduce further as a result of ongoing rock creep with healing of the EDZ and compaction of the sealing material.

Gas break-through pressure

As the seal is designed to act as a gas vent the gas entry/break-through pressure of the sealing material must be low enough in comparison to the gas entry pressure of the

host rock to ensure gas migration through the seal. According to NAGRA (2002), the gas entry pressure in the undisturbed Opalinus clay at 600 m depth below ground amounts to about 5 MPa and thus the gas entry/break-through pressure of the seal in such a situation should be lower than 5 MPa.

The conditions at the MTRL differ significantly from those conditions. According to Thury et al. (1999), the overburden pressure at Mont Terri yields a vertical stress of only 7.25 MPa with a horizontal minor stress component of about 2 MPa. Also the porewater pressure only amounts to about 2 MPa so that the **gas entry/break-through pressure** of the seal in the envisaged SB-experiment **has to be kept at a Mont Terri specific level of well below 2 MPa** which can be considered as conservative design value if the necessary sealing effectiveness can be demonstrated for this condition.

Swelling characteristics of the buffer

Adequate swelling pressure to obtain the desired sealing effectiveness against formation water inflow. The sealing material will seal itself by swelling when taking up water. The material fills the entire space between the waste canister and the drift wall and any gap remaining from seal construction. High swelling pressure and the capacity for large volumetric strains under free swelling conditions are considered very advantageous /Pellegrini et al., 1999/. On the other hand, laboratory experiments suggest that gas penetration of an initially water-saturated clay buffer occurs only when the gas pressure slightly exceeds the sum of the swelling pressure and the groundwater pressure /Rodwell et al., 1999/. Consequently, in order to cause the gas to flow preferentially through the seal and not into the host rock, the swelling pressure should not exceed the gas entry pressure of the host rock.

1.3 Preliminary design of the in-situ experiments

The SB experiments at Mt. Terri will be performed in a test niche of 5 m width, 4 m height and 8 m length (Figure 1-1). About four vertical boreholes of 0.31 m diameter will be drilled in the test room floor to a depth of 3 m (Figure 1-2). All the boreholes will be sealed with suitable clay/mineral mixtures and will be equipped with other components. Instruments for measuring different hydro-mechanical parameters will be installed as well.

The lower part of the boreholes, the injection volume, will be filled with a porous material (e.g. alumina beads or sand). On top of the porous medium a filter frit will be placed for ensuring a homogeneous distribution of the injected water over the entire borehole cross section. Above the filter frit, the clay-sand seal will be installed in several layers to a height of 1 m. Above the seal a further filter frit will be installed for water and gas collection. The whole borehole will be sealed against the ambient atmosphere by a gastight packer. The most upper part of the test borehole is grouted for keeping the packer in place at higher swelling pressure of the SB seal.

For saturation or desaturation of the seal water or gas is injected through an injection tube running from a valve panel in the test room via an inclined borehole into the lower injection volume.

The water or gas flowing through the seal is collected in the upper collection volume by a further tube running back to the control valve panel where gas and water flow rates and pressures will be controlled and measured.

Details of the foreseen test procedures are presented in section 5.

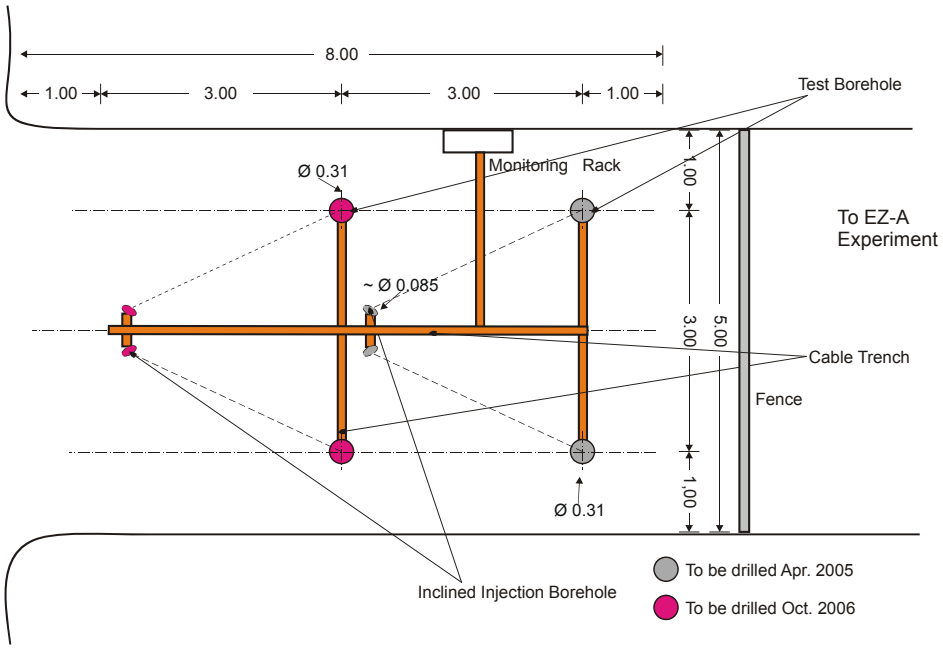

Figure 1-1 Layout of the SB test niche at Mt. Terri

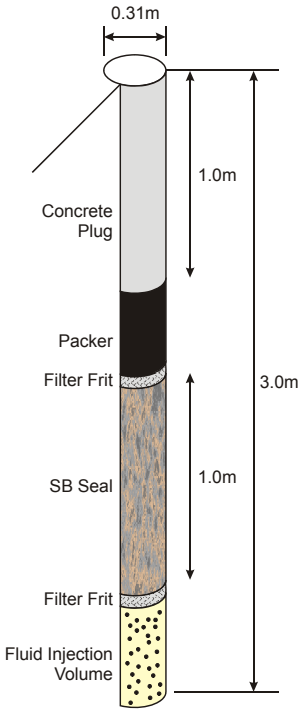

Figure 1-2 Principle design of an SB experiment

1.4 Work programme of the SB pre-project

The SB pre-project was mainly characterized by preceding laboratory investigations for the final selection of suited material mixtures, the development of a test plan for the envisaged in-situ experiments at the Mont Terri Rock Laboratory (MTL) in Switzerland, and the preparation of mock-up tests to be performed in advance to the in-situ experiments in the geotechnical laboratory of GRS in Braunschweig.

In the following, information is given about

- the laboratory results achieved until June 2004,
- the modelling work programme,
- the design of the mock-up tests including some scoping calculations and finally
- the envisaged in-situ test procedures.

2 Laboratory Programme

So far, different materials as for instance bentonite and clay/mineral mixtures have been investigated as sealing materials in repositories in clay, granite and salt. Within the framework of preceding GRS-projects /JOC 00/, /MIE 03/, the hydro-mechanical properties of different clay/mineral-mixtures were determined.

To select suitable material mixtures for the SB project that fulfil the various requirements for a successful demonstration of the sealing effectiveness of the clay/sand mixtures under representative in-situ conditions a preceding laboratory programme was performed in the SB pre-project.

2.1 Definition of petrophysical properties

Measurements of grain density, dry density, bulk density, porosity, water content and degree of water saturation were made according to ISRM suggested testing methods /ISR 81/, see also /ZHA 04/. The above mentioned physical properties are defined as:

- Grain density

$$\rho_s = \frac{M_s}{V_s} \tag{2.1}$$

with M_s = mass of solids, V_s = volume of solids.

- Bulk density

$$\rho_b = \frac{M}{V} = \frac{M_s + M_w}{V} \tag{2.2}$$

with M = mass of bulk sample, V = volume of bulk sample, M_s = mass of solids, M_w = mass of water.

- Dry density

$$\rho_d = \frac{M_s}{V} \tag{2.3}$$

with M_s = mass of solids, V = volume of bulk sample.

- Porosity

$$\phi = \frac{V_v}{V} 100 = \left(1 - \frac{\rho_d}{\rho_s}\right) \cdot 100 \ (\%) \tag{2.4}$$

with V_v = volume of voids, V = volume of bulk sample, ρ_d = dry density, ρ_s = grain density.

- Permeability to gas

$$k_g = \frac{2 \cdot q_g \cdot \mu_g \cdot l \cdot p_0}{A \cdot \left(p_1^2 - p_0^2\right)} \tag{2.5}$$

with:

k_g permeability measured with gas, m^2
q_g flow rate of the gas, m^3/s
p_1 injection pressure, Pa
p_0 atmospheric pressure, Pa
μ_g viscosity of the gas, Pas
l sample length, m
A cross sectional area of the sample, m^2

- Permeability to water

$$k_w = \frac{q_w \cdot \mu_w \cdot l}{A \cdot \Delta p} \tag{2.6}$$

with:

k_w water permeability, m^2
q_w flow rate of the water, m^3/s
Δp pressure difference, Pa
μ_w viscosity of the water, Pas
l sample length, m
A cross sectional area of the sample, m^2

- Water content

$$w = \frac{M_w}{M_s} 100 \ (\%) \tag{2.7}$$

with M_w = mass of water, M_s = mass of solids.

- Relationship between bulk density, dry density and water content

$$\rho_d = \frac{\rho_b}{1 + w/100} \tag{2.8}$$

- Degree of water saturation

$$S = \frac{V_w}{V_v} 100 \ (\%) \tag{2.9}$$

with V_w = volume of pore water, V_v = volume of voids.

- Relationship between degree of saturation and the other physical characters

$$S = \frac{w}{\rho_w} \frac{1}{\left(1/\rho_d - 1/\rho_s \right)} = \frac{\rho_d w}{\rho_w \phi} 100 \ (\%) \tag{2.10}$$

with ρ_w = density of pore water.

- Water content of fully-saturated sample (S = 100 %)

$$w_{sat} = 100 \cdot \rho_w \cdot \left(\frac{1}{\rho_d} - \frac{1}{\rho_s} \right) 100 \ (\%) \tag{2.11}$$

2.2 Measurements and evaluation

The laboratory investigations for the selection of the suitable seal material included the determination of petrophysical properties like installation density, gas and water permeability, gas break-through pressure, swelling pressure as well as saturation behaviour of clay/sand mixtures with different clay contents.

Natural Ca-Bentonite Calcigel produced by Süd-Chemie AG in Germany and pure quartz sand were used to produce the sealing materials of interest. So far, three mixtures with clay/sand ratios of 35/65, 50/50 and 70/30 were tested.

2.2.1 Installation density and porosity

First, the installation densities of the sealing materials were investigated on small samples in an oedometer cell with a diameter of 50 mm. Sample preparation was made by mixing and compaction by hand. The mixtures were also used for the determination of further petrophysical parameters.

To optimize the preparation procedure, clay and sand were mixed together in an electric mixer (Figure 2-1 A) and installed in a tube with a diameter of about 290 mm similar to that of the planned boreholes. The material was emplaced in a plexiglass® tube by layers and compacted by a vibrator (Figure 2-1 B and C). According to the installed mass and volume of the material, the installation density was determined.

From the results, the other state parameters of the compacted material such as grain density, water content and porosity can be determined.

The grain density of the grinded material was determined with helium using an air comparison pycnometer after Beckman (Figure 2-2).

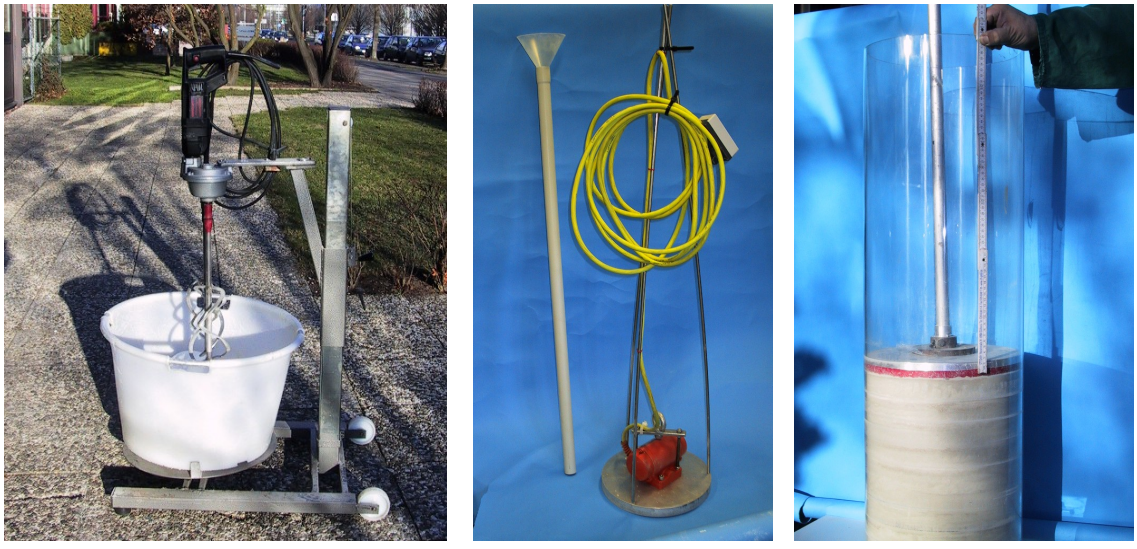

A
Preparation by a mixer

B
Electric vibrator and funnel

C
Compaction by layers in a plexiglass tube

Figure 2-1 Preparation of the clay/sand mixtures

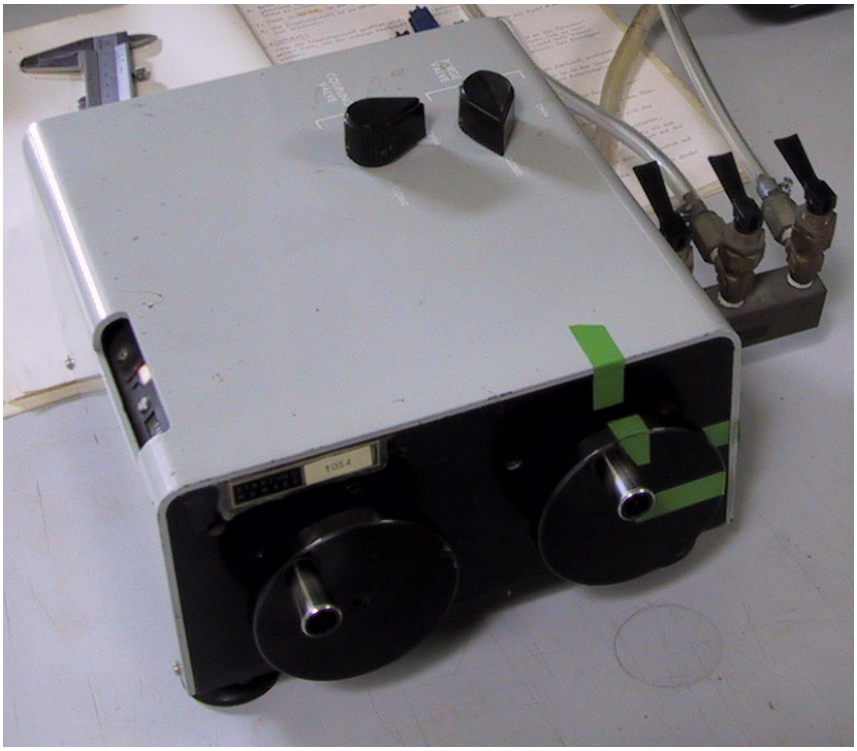

Figure 2-2 Air comparison pycnometer (after Beckman)

2.2.2 Permeability, gas break-through pressure, and swelling pressure

Permeability and gas break-through pressure as well as the swelling pressure of clay/sand mixtures were examined in four newly constructed oedometer cells, as shown in Figure 2-3 /ZHA 04/. Two normal cells allow a sample size of 50 mm diameter and 50 mm length, and two other cells allow a large sample size of 100 mm diameter and 100 mm length.

The general testing procedure was:

1. Installation: The prepared clay/sand mixture were emplaced in the cell and compacted to the similar density achieved in the large tube by vibrating-compaction.

2. Gas injection: Under the installed conditions, gas was injected to the sample for the determination of permeability to gas.

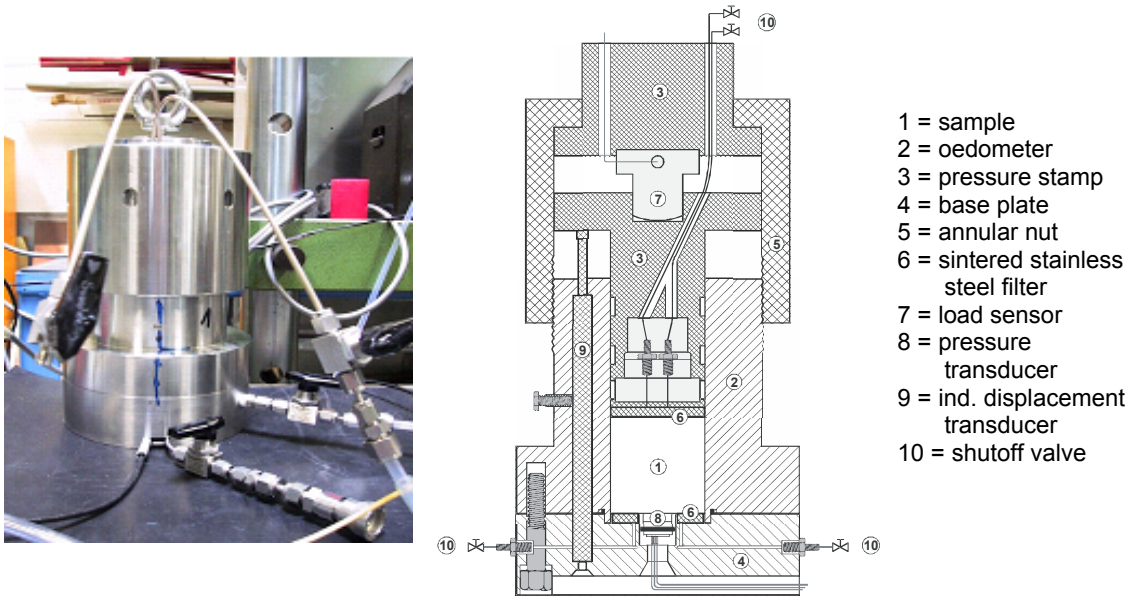

Figure 2-3 GRS oedometer cell

3. Gas injection again: After saturation of the sample, gas was injected again by stepwise increasing the gas pressure, in order to determine the gas break-through pressure. Because this procedure is very time-consuming, another method was applied in further investigations. The gas was injected by the displacement of the gas from a bottle by water at constant flow rate. The constant flow rate of the water was controlled by a HPLC-pump. Due to the capillary entry pressure, the gas injection pressure increased up to the point of gas break-through (gas break-through pressure). At this state, a gas flow through the samples was given. After the break, the gas permeability was measured.

4. Compaction and repeating points 3 and 4: The sample was compacted to 5 MPa. The compacted density is possibly achievable by special techniques for in-situ installation and compaction of the clay/sand mixtures in boreholes and drifts. Under the compacted conditions, the points 3 and 4 were repeated to measure the permeability to water and to gas and the gas break-through pressure at the high density.

Table 2-1 gives the components of the synthetic Opalinus clay solution used in the test.

Table 2-1 Composition of the used Opalinus clay solution (pH value: 7.6) /PEA 03/

Na	K	Ca	Mg	Cl	SO_4
mmol/l	mmol/l	mmol/l	mmol/l	mmol/l	mmol/l
235	1.7	25	16	287	14

The gas permeability was determined with nitrogen. For the evaluation, the extension of Darcy's law to compressible media was applied for steady-state flow (compare section 2.1). The water permeability, measured with the synthetic Opalinus clay solution, was calculated by the Darcy's for incompressible media (compare section 2.2):

By water uptake the materials swell, which leads to a reduction of porosity and permeability. The swelling capacity was determined at saturation with the synthetic Opalinus clay solution. At the smaller specimens, the swelling pressure was measured directly at the samples using a pressure transducer installed inside at the bottom of the oedometer. In further investigations on samples with 100 mm diameter and 100 mm length, the swelling pressure was determined by a load sensor installed between the pressure stamps at the top of the cell (Figure 2-3). The upper part of the pressure stamp in combination with the annular nut effects as a support. Considering the cross section area of the pressure stamp, which is in contact with the specimen and the load, the resulting pressure was calculated according to:

$$p = \frac{F}{A} \tag{2.12}$$

with:

p resulting pressure, N/m^2
F load, N
A cross section area, m^2

To determine the swelling pressure, the influence of the injection pressure on the resulting pressure was considered in both cases.

2.2.3 Saturation

For prediction of the time needed for full saturation of the mock-up and in-situ experiments, a series of saturation tests were conducted on the clay/sand mixtures in steel cylinders of 50 mm diameter and 100 mm length (Figure 2-4).

In a first group of the tests, samples with a clay/sand ratio of 35/65, 50/50 and 70/30 were saturated with the Opalinus clay solution at the atmosphere pressure. For each clay/sand mixture, the tests were last for two time intervals of one and three months. After the saturation phase, the samples were cut in small discs. The water contents and densities of the discs were measured and their distributions along the sample length were determined.

Figure 2-4 Experimental setup for saturation tests

The discs were dried at 105 °C to constancy of mass which is assumed to represent the completely dry state of the sample. The water content and the degree of water saturation were calculated according to equations (2.5 – 2.8).

Considering possibly application of high water pressures to the seals to accelerate their saturation in the mock-up and the in-situ tests, additional saturation tests on the small samples were carried out with clay/sand mixtures of 35/65 and 50/50 at an injection pressure of about 1 MPa. After the saturation, the water permeability and the gas break-through pressure were determined on each sample (section 2.2.2).

2.3 Results of the preceding laboratory investigations

In order to determine the achievable installation densities, two procedures, compaction by hand and by vibrator, were tested. The investigations on the hydraulic behaviours were carried out on samples compacted by hand and, in one case after an additional compaction of the same samples, at wet conditions. The results achieved are described in the following.

2.3.1 Installation density and porosity

The seal material consists of bentonite powder (Calcigel) and ordinary sand. The grain size distribution of the sand is shown in Figure 2-5. The sand is available at each commercial sand pit.

The bentonite (Calcigel) is a product of the Süd-Chemie AG. The place of origin is Bavaria (Germany). The mineralogical composition (Table 2-2) is described in the "Product information of Calcigel" /NN 01/ as followed:

Table 2-2 Mineralogical composition of Calcigel after Süd-Chemie AG 2001

Mineralogical component	Percentage
montmorillonite	60 -70 %
quartz	6 -9 %
feldspar	1 – 4 %
kaolinite	1 – 2 %
mica	1 – 6 %
other minerals	5 – 10 %

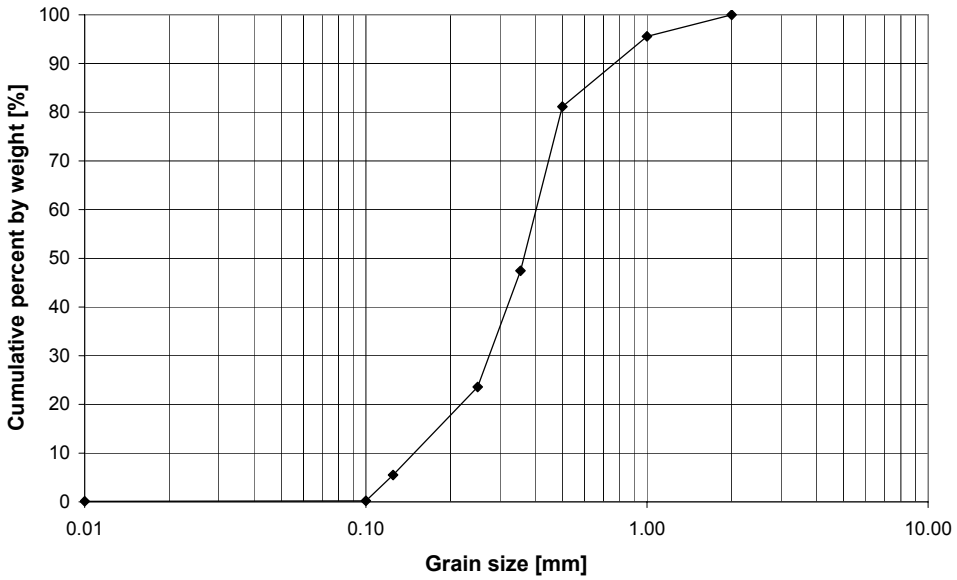

Figure 2-5 Grain size distribution of the sand

The grain densities of the sand, the bentonite, and of the mixtures were determined at state of delivery as well as after drying at 105 °C up to constancy of weight. The results are summarized in Table 2-3 and Table 2-4. Considering the water content of the clay and the sand, the bulk (or installation) densities and porosities were calculated for the state of delivery and at the dry state as well.

A comparison of the samples compacted by hand and by vibration shows that the densities are in a similar order of magnitude for the mixtures with 35 % and 50 %. On the other hand, the densities of the sample with the highest clay content of 70 % were lower. This result might be explained by the higher clay content, which possibly acts as a buffer and hinders further compaction.

2.3.2 Permeability, gas break-through pressure, and swelling pressure

For the determination of the hydraulic parameters, the clay/sand mixtures were installed in the oedometer cells. The installation densities corresponded to the densities described in chapter 2.3.1. The water contents of the materials were determined by drying in an oven according to DIN 18121-1.

Table 2-3 Parameter values obtained from the investigations of achievable installation densities; material compacted by hand

Sample	Grain density (dry)	Grain density (state of delivery	Bulk density (dry)	Bulk density (state of delivery)	Porosity (dry)	Porosity (state of delivery)
Clay/sand ratio	ρ_g	ρ_g	ρ_{bd}	ρ_b	Φ_d	Φ
	g/cm³	g/cm³	g/cm³	g/cm³	%	%
35/65	2.672	2.578	1.816	1.869	32.0	27.5
50/50	2.676	2.572	1.756	1.821	34.4	29.2
70/30	2.696 *	2.573	1.603	1.680	40.5	34.7
Calcigel	2.706	2.491	n.d.	n.d.	n.d.	n.d.
Sand	2.672	2.65	n.d.	n.d.	n.d.	n.d.

* calculated by grain densities of the pure sand and Calcigel

Table 2-4 Parameter values obtained from investigations of achievable installation densities; material compacted by vibrator

Sample	Grain density (dry)	Grain density (state of delivery	Bulk density (dry)	Bulk density (state of delivery)	Porosity (dry)	Porosity (state of delivery)
Clay/sand ratio	ρ_g	ρ_g	ρ_b	ρ_b	Φ	Φ
	g/cm³	g/cm³	g/cm³	g/cm³	%	%
35/65	2.672	2.578	1.876	1.930	29.8	25.1
50/50	2.676	2.572	1.668	1.73	37.7	32.7
70/30	2.696*	2.573	1.394	1.461	48.0	42.4
Calcigel	2.706	2.491	n.d.	n.d.	n.d.	n.d.
Sand	2.672	2.65	n.d.	n.d.	n.d.	n.d.

* calculated by grain densities of the pure sand and Calcigel

Under the installed conditions of the sealing material compacted by hand, the gas permeabilities were measured. After the measurement of the gas permeability, the samples were saturated with clay solution and the swelling pressure as well as the water permeability was determined. For the measurement of the gas break–through pressure, gas was injected by increasing the gas pressure applied to the saturated samples. The results of the hydraulic measurements as well as the swelling pressures are described in Table 2-5.

With respect to requirements described in chapter 1.2 and concerning an acceptable saturation time of some months, the clay/sand mixtures 35/65 and 50/50 were found to be the most suited material mixtures.

For the investigation of the hydraulic properties of higher compacted densities, possibly achievable by special techniques for in-situ installation, the same clay/sand samples as described above were compacted at 5 MPa at wet condition. After the determination of the water permeability, the gas break-through pressure was measured and the gas permeability was calculated from the flow rates measured after the gas break-through (Table 2-6).

To confirm previous results and to complete the data especially with respect to swelling pressure and gas break-through pressure, further investigations in the oedometer cell were performed on samples 35/65 and 50/50 compacted by hand. The pressure history during the saturation is depicted in Figure 2-6. The Figure shows the injection pressures and the resulting pressure response at the sensors installed outside the cells.

Table 2-5 Parameter values of SB samples obtained from investigations of hydraulic properties; material compacted by hand (sample sizes: 50 mm diameter, 50 mm length)

Sample	**Bulk density (state of delivery)**	**Gas permeability**	**Water permeability**	**Gas break-through pressure**	**Swelling pressure**	**Water content**
Clay/sand ratio	ρ_b	k_g	k_w	p_{bth}	p_s	w
	g/cm^3	m^2	m^2	MPa	MPa	wt%
35/65	1.869	1.23E-13	9.02E-18	0.4	0.2-0.4	2.9
50/50	1.821	7.48E-14	1.79E-18	0.4	0.3-0.5	3.7
70/30	1.680	1.16E-15	5.50E-19	1	0.4-?	4.8
Calcigel	n.d.	n.d.	n.d.	n.d.	n.d.	6.07
Sand	n.d.	n.d.	n.d.	n.d.	n.d.	1.11

n.d.: not determined

Table 2-6 Hydraulic parameters of SB samples after compaction of wet mixtures at 5 MPa (sample sizes: 50 mm diameter, 50 mm length)

Sample	Water permeability	Gas break-through pressure	Gas permeability (after break-through)
Clay/sand ratio	k_w	p_{bth}	k_g
	m^2	MPa	m^2
35/65	1.50E-17	2.36	6.70E-17
50/50	3.08E-20	n.b.	n.b.
70/30	6.45E-20	ca. 10	7.26E-19

The remaining pressure (after disconnecting and reducing the injection pressure down to atmospheric conditions) is assumed to represent the swelling pressure, which is marked in Figure 2-6 by the horizontal broken line. The vertical dotted lines mark the points of water outflow of the samples. After saturation, the water permeability was measured. The results are summarized in Table 2-7.

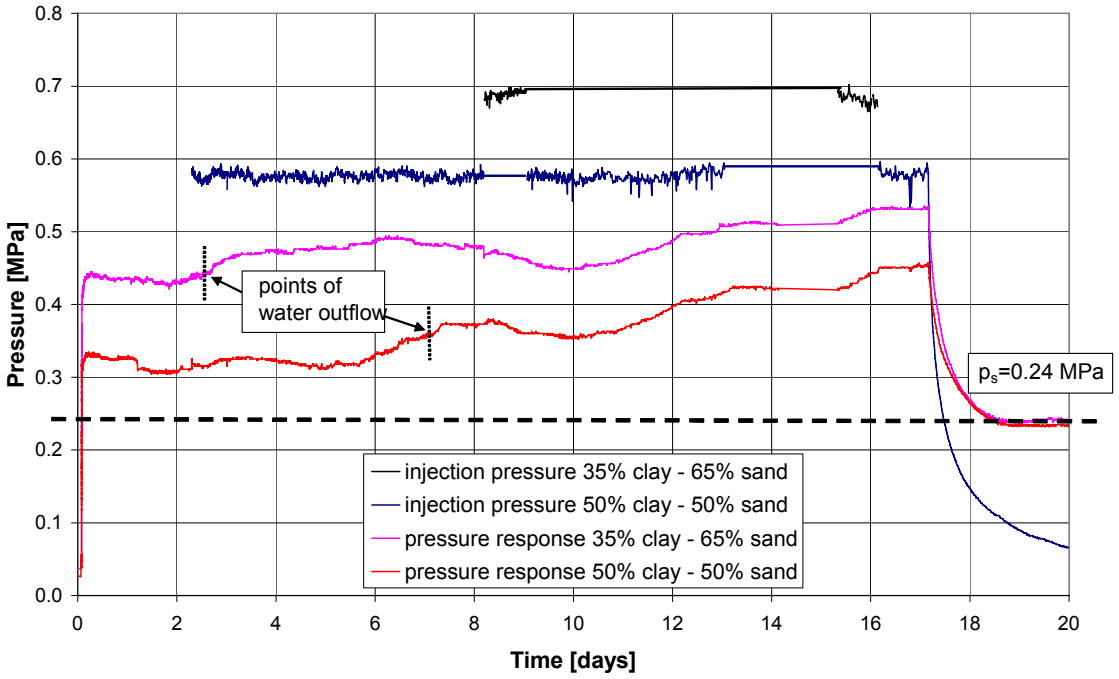

Figure 2-6 Pressure history of clay/sand samples 35/65 and 50/50 at saturation phase for determination of the swelling pressure

Table 2-7 Results of the second oedometer tests (sample size: 100 mm diameter, 100 mm length)

	Bulk density (state at delivery)	**Water permeability**	**Swelling pressure**
Clay/sand sample	[g/cm^3]	[m^2]	[MPa]
35/65	1.903	4.73E-18	0.24
50/50	1.703	4.26E-18	0.24

2.3.3 Saturation

All investigations on saturation were performed on samples compacted by hand.

In a first group of tests, samples were saturated with Opalinus clay solution at atmospheric pressure, only.

The investigations show, that saturation increases somewhat with increasing clay content. Furthermore, a dependence on time of the distribution of the saturation along the samples is observed. It is trivial that highest saturations were measured near the contact of the water with the samples. The results are plotted in Figure 2-7.

The saturation > 100 % is a principal problem of clay and can be explained by the method of determination of the densities and preparation of the samples and a deposition of water between the intermediate layers of the mica minerals as well. According to eq. (2.8), the saturation was calculated by the water content and the grain and bulk densities, both determined after drying at 105 °C. Depending on the degree of dryness, a changing of the grain densities and the bulk densities can be observed. With increasing dryness, the grain density increases too, and the bulk density decreases (see Table 2-3 and Table 2-4). The saturation, however, increases up to > 100 %.

The evolution of the dry density is presented in Figure 2-8. The investigations show a decrease of the dry densities with increasing clay content. This result may be explained by the higher clay content, which possibly acts as a buffer and hinders further compaction during the preparation procedure. At the front of the samples, where the

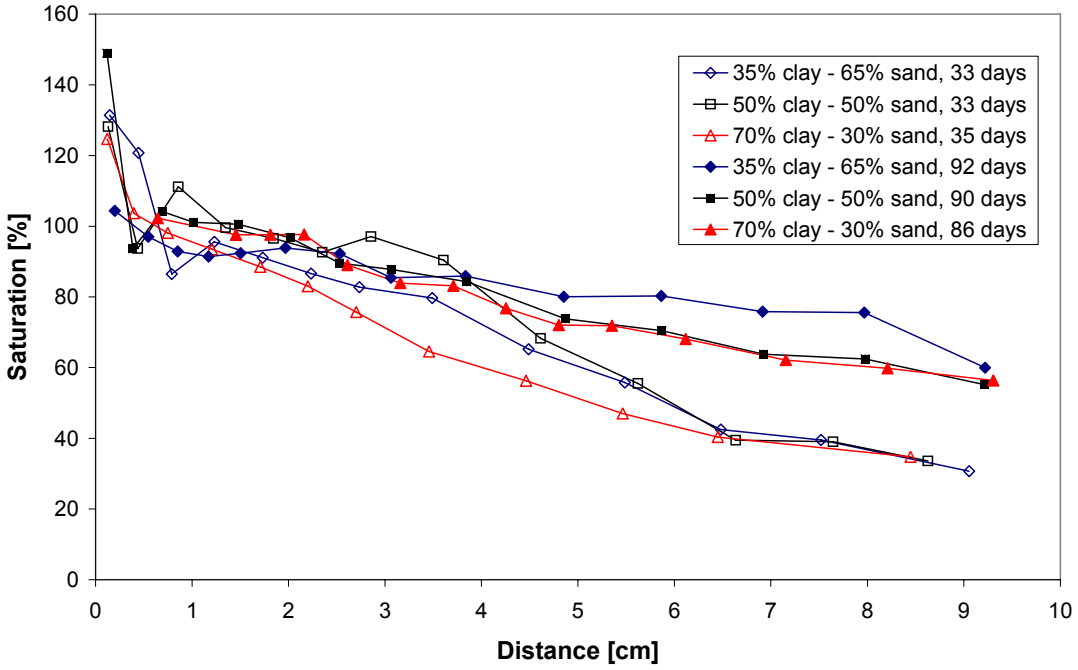

Figure 2-7 Distribution of saturation along the samples

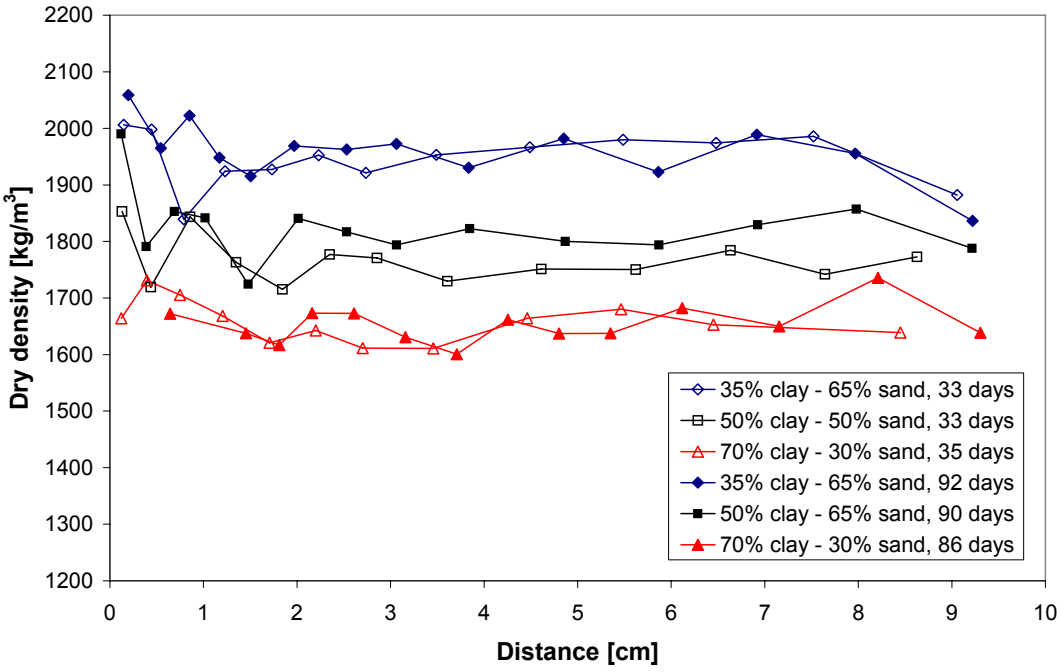

Figure 2-8 Distribution of the densities along the samples

sample contacts the water, a slight increase of density was determined for the samples with lower clay contents of 30 % and 50 %. This increase was not observed at the

samples with the highest clay content of 70 %. A significant dependence on time was not observed. The variations of density along the samples may be explained by inhomogeneity due to the preparation procedure.

In a second group, samples with a clay/sand ratio of 35/65 and 50/50 were saturated with Opalinus Clay solution at an increased injection pressure of 1 MPa. The measurements were performed to investigate the influence of pressure on the saturation process and to determine the water permeability as well as the gas break-through pressure.

After saturation, the water permeability (for the Opalinus Clay solution) was measured. The results, summarized in Table 2-8, show that the permeability of the samples with the lower clay content of 35 % was somewhat higher than the permeability with the clay content of 50 %.

A first test on a clay/sand mixture 35/65 (sample 35/65 (1)) with a relatively high constant flow rate of 10 ml/min at the HPLC-pump shows, that the increasing of the resulting pressure was too fast, so that the point of break-through could not be identified. In Figure 2-9 the gas flow at the outlet of the sample and the injection pressure are shown.

Due to the observation of the first sample, the investigations of the gas break-through pressure were continued with a second clay/sand sample 35/65 (2) and two further samples 50/50 (sample 50/50 (1), sample 50/59 (2)) with reducing the flow rate of the HPLC-pump to 0.2 ml/min. The results are plotted in Figure 2-10 to Figure 2-12. At the point of gas break-through, marked by a dotted line, the gas flow rate at the outlet side of the samples increases rapidly. This effect was very distinct, especially at the samples with the higher clay content of 50 %. At saturated state, the higher clay content causes a higher swelling capacity and leads to an increased flow resistant and to a higher capillary entry pressure as well. This process hinders the continuous inflow of the gas.

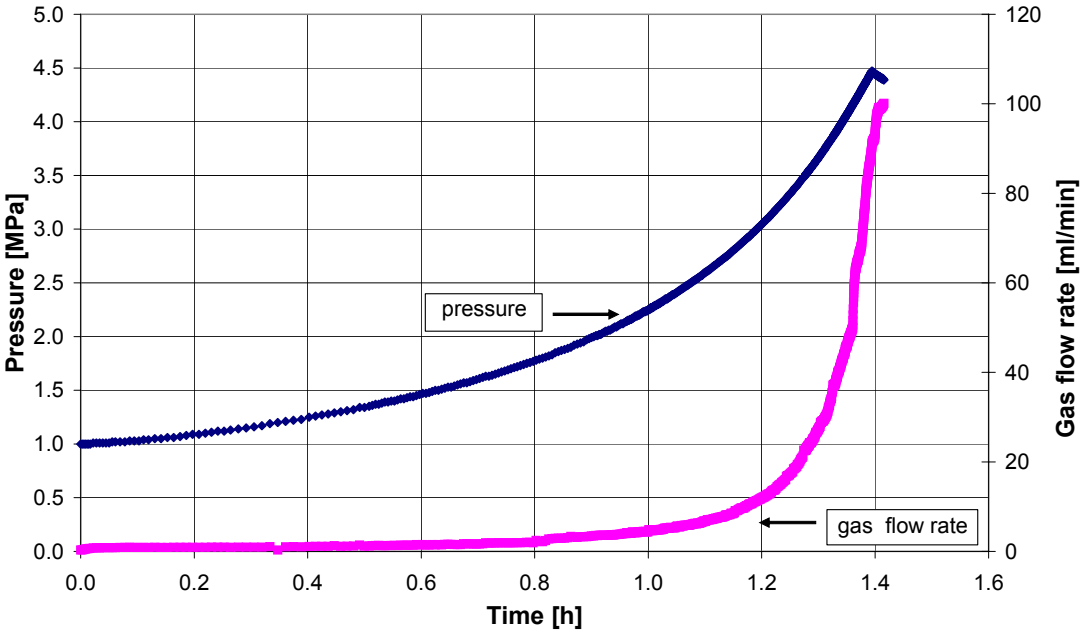

Figure 2-9 Development of pressure and gas flow rate at the outlet side of the clay/sand sample 35/65 (1); (rate of HPLC-pump: 10 ml/min)

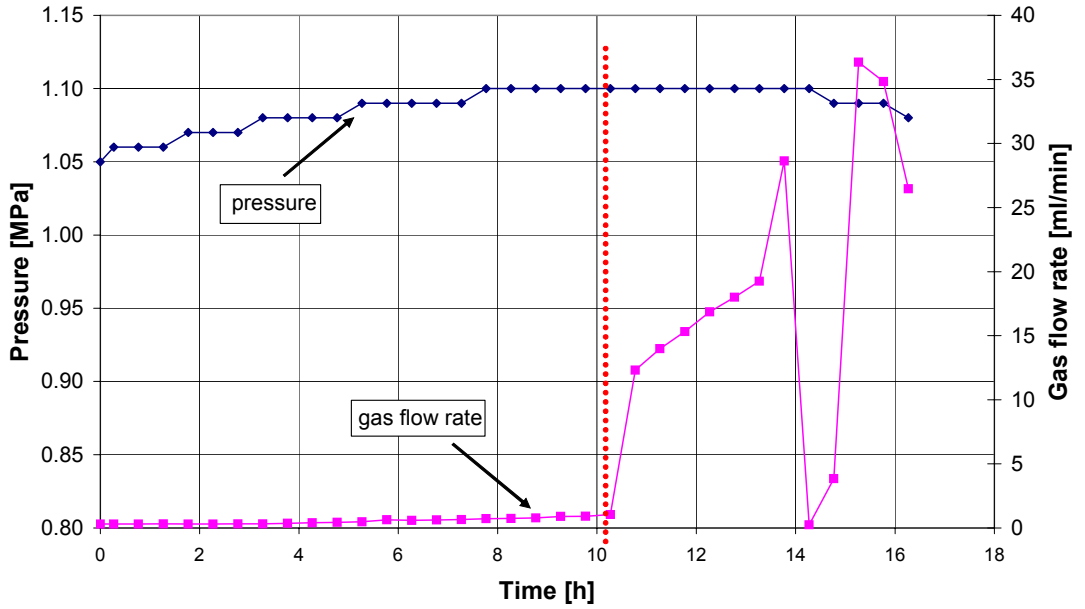

Figure 2-10 Development of pressure and gas flow rate at the outlet side of the clay/sand sample 35/65 (2); dotted line: point of gas break-through (rate of HPLC-pump: 0.2 ml/min)

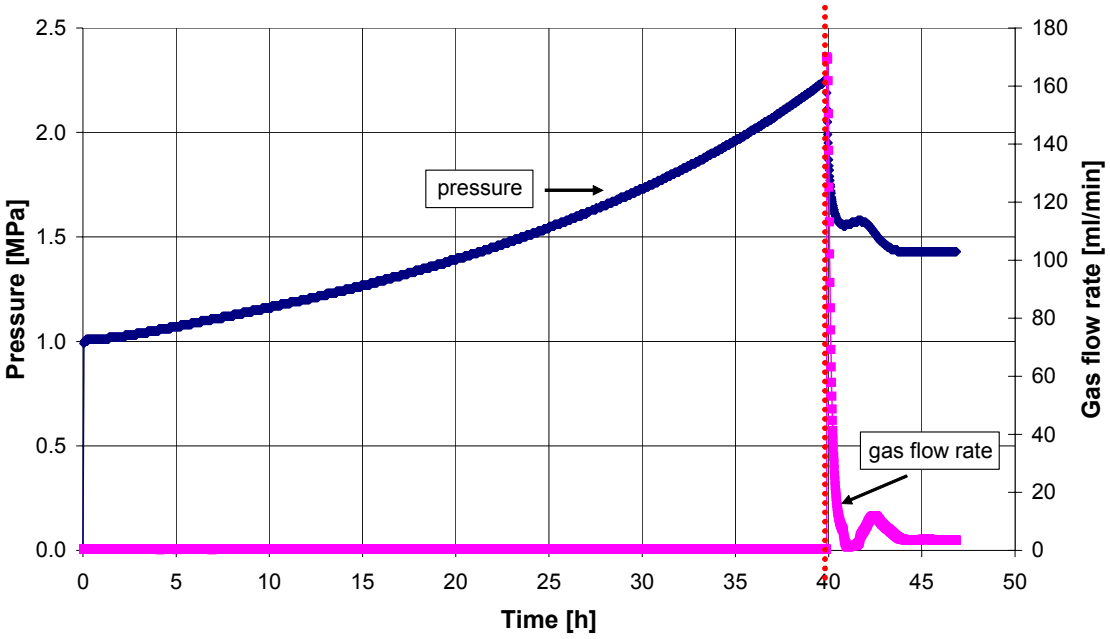

Figure 2-11 Development of pressure and gas flow rate at the outlet side of the clay/sand sample 50/50 (1); dotted line: point of gas break-through (rate of HPLC-pump: 0.2 ml/min)

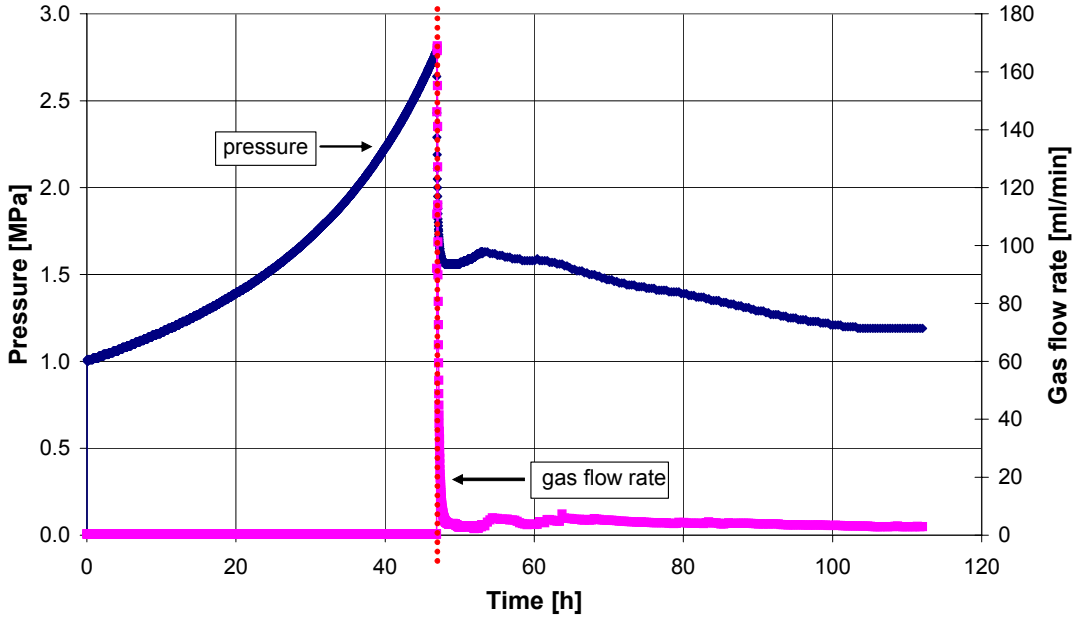

Figure 2-12 Development of pressure and gas flow rate at the outlet side of the clay/sand sample 50/50 (2); dotted line: point of gas break-through (rate of HPLC-pump: 0.2 ml/min)

Anyway, immediately after the pressure has reached the point of break-through, the gas flows into the sample. The determined gas break-through pressures are summarized in Table 2-8.

Table 2-8 Results of the saturation experiments at increased water injection pressure

Sample	Bulk density (state of delivery)	Water permeability	Gas break-through pressure	Gas permeability after break-through	Water content after break-through
Clay/sand mixture	g/cm^3	[m^2]	[MPa]	[m^2]	[%]
35/65 (1)	1.901	3.3E-18	n.d.	1.6E-17	n.d.
35/65 (2)	1.900	3.9E-18	1.1	1.1E-17	16
50/50 (1)	1.704	1.1E-18	2.3	5.5E-18	n.d.
50/50 (2)	1.703	1.8E-18	2.8	6.2E-18	21.4

n.d.: not determined

In comparison to sample 35/65 with a gas break-through pressure of 1.1 MPa, the gas break-through pressure of samples 50/50 clearly increased with values ranging between 2.3 MPa and 2.8 MPa.

After gas break-through, the gas permeability was measured and the corresponding water content for one sample of both clay/sand mixtures was determined (Table 2-8). Due to higher clay content, a lower permeability of the samples 50/50 was measured. The remaining water content of the 35/65 clay/sand mixture was 16 % and of the 50/50 clay/sand mixture 21.4 %. The higher water content of the samples 50/50 can be explained by a better absorption of water due to higher clay content.

2.3.4 Selection of suitable clay/sand mixtures for the SB experiment

In order to select suitable clay/sand mixtures for the SB experiment at MTRL, preceding laboratory experiments were performed on clay/sand mixtures with clay contents of 35 %, 50 % and 70 %. The most important material properties as criteria are installation density and porosity, respectively, water permeability, gas break-through pressure, and gas permeability after break-through.

Table 2-9 summarizes ranges and mean values (in parentheses) of the determined properties for the investigated clay/sand mixtures and compares them to the requirements described in section 1.2. It is obvious that the 35clay/65sand and 50clay/50sand mixtures meet the requirements completely. It can be expected that the gas break-through pressure may reduce further in the case of significantly lower gas generation rates which are to be considered in a real repository. The extrapolation of test results to mixtures with clay contents less than 50 % suggests that the 70clay/30sand mixture may have higher swelling pressure and gas break-through pressure than the given upper limit.

Table 2-9 Comparison of the measured parameters to the requirements (averages in parentheses)

Measured parameters at installation conditions					
	Gas permeability under dry conditions	Initial water permeability at full saturation	Gas break-through pressure	Gas permeability after gas break-through	Swelling pressure
Sample	m^2	m^2	MPa	m^2	MPa
35/65	1.2E-13	3.3E-17 - 9E-18 (5.2E-18)	0.4 - 1.1 (0.75)	1.1E-17 - 1.6E-17 (1.4E-17)	0.2 - 0.4 (0.28)
50/50	7.5E-14	1.1E-18 - 4.3E-18 (2.2E-18)	0.4 - 2.8 (1.83)	5.5E-18 - 6.2E-18 (5,9E-18)	0.3 - 0.5 (0.35)
70/30	1.2E-15	5.5E-19	1	n.d.	0.4-?
Requirements					
	Gas permeability under dry conditions	Initial water permeability at full saturation	Gas break-through pressure	Gas permeability after gas break-through	Swelling pressure
	high	1E-17 - 1E-18	2	high	2

From those results, the clay/sand mixtures with the ratios of 35/65 and 50/50 are selected for further mock-up and in-situ tests.

3 Modelling Work

One of the objectives of the SB project is to achieve an improvement or confirmation of existing THM computer codes and THM models, respectively by comparing modelling and test results of the SB-experiment. GRS will apply the code CODE_BRIGHT developed by the Technical University of Catalonia (UPC) in Barcelona. The theoretical framework employed in the code is presented in /OLI 96/, /UPC 02/ and reviewed in /GEN 98/, /ALO 02/, /ZHA 04/. Modelling work envisaged for the project includes:

- determination of material parameters for selected clay/sand mixtures and the host rock,
- scoping calculations for design of mock-up and in-situ tests,
- simulation and interpretation of the experimental results.

In the framework of the SB pre-project, scoping calculations for designing mock-up and in-situ tests have been conducted by using material parameters preliminarily determined during the preceding laboratory tests on clay/sand mixtures and taken from literature.

3.1 Determination of material parameters

From the results of preceding laboratory tests mentioned in section 2, two clay/sand mixtures with clay contents of 35 % and 50 % were selected to be used for mock-up and in-situ tests. In scoping calculations for designing the tests, material parameters for the selected mixtures were preliminarily established from the preceding laboratory tests which aimed at selecting seal materials for the SB experiment. The parameters for the Opalinus clay were taken from literature /ZHA 04/.

3.1.1 Petrophysical properties

Mean values of the petrophysical properties of clay/sand mixtures and Opalinus clay are summarised in Table 3-1.

Table 3-1 Physical properties of clay/sand mixtures and Opalinus clay

Property	Symbol	Unit	Opalinus clay	Clay/sand 35/65	Clay/sand 50/50	Clay/sand 70/30
Grain density	ρ_s	kg/m^3	2710	2672	2676	2680
Dry density	ρ_d	kg/m^3	2340	1900	1700	1450
Void ratio	e_o	-	0.190	0.406	0.574	0.848
Porosity	ϕ_0	-	0.160	0.289	0.365	0.459
Water content	w_0	%	7.2	2.9	3.7	4.8
Initial suction	s_0	MPa	0	1.2	1.8	3.6
Degree of saturation	S_{l0}	%	100	17	17	17

3.1.2 Hydraulic models and parameters

The constitutive models and parameters considered for the hydraulic behaviour of clay/sand mixtures and Opalinus clay are given below.

Liquid and gas flow follow Darcy's law:

$$\mathbf{q}_l = -\mathbf{K}_l (\nabla P_l - \rho_l \mathbf{g}) \tag{3.1a}$$

$$\mathbf{q}_g = -\mathbf{K}_g (\nabla P_g - \rho_g \mathbf{g}) \tag{3.1b}$$

where $\mathbf{K}_\alpha = \mathbf{k}\, k_{r\alpha} / \mu_\alpha$ is the permeability tensor. The intrinsic permeability tensor (**k**) depends on the pore structure of the porous medium. $k_{r\alpha}$ is the value of relative permeability that controls the variation of permeability in the unsaturated regime and μ_α denotes the dynamic viscosity. α stands for either l or g depending on whether liquid or gas flow is considered. **g** is the gravity vector. The variation of intrinsic permeability with porosity is given by

$$\mathbf{k} = \mathbf{k}_0 \frac{\phi^3}{(1-\phi)^2} \frac{(1-\phi_0)^2}{\phi_0^3} \tag{3.2}$$

where ϕ_0 is a reference porosity. The relative permeabilities of the liquid and gaseous phases are dependent on the degree of liquid saturation according to

$$S_e = \frac{S_l - S_{lr}}{S_{ls} - S_{lr}} \tag{3.3}$$

$$k_{rl} = S_e^{1/2} \cdot \left[1 - (1 - S_e^{1/\beta})^{\beta}\right]^2 \qquad S_e \le 1 \tag{3.4}$$

or power law $$k_{rl} = A \cdot S_e^B \tag{3.5}$$

$$k_{rg} = 1 - k_{rl} \tag{3.6}$$

where S_l, S_{lr}, S_{ls}, S_e are the actual, residual, maximum and effective saturation of liquid, respectively, and β, A and B are parameters.

It is necessary to define the retention curve of the materials relating the degree of saturation to suction $(s = P_g - P_l)$. The expression of Van Genuchten is selected

$$S_e = \left[1 + \left(\frac{P_g - P_l}{P_0}\right)^{1/(1-\beta)}\right]^{-\beta} \qquad P_g - P_l \ge 0 \tag{3.7}$$

where P_0 is a material parameter.

The molecular diffusion of vapour in air is governed by Fick's law:

$$\mathbf{i}_g^w = -\mathbf{D}_g^w \nabla \omega_g^w = -(\phi \ \rho_g S_g \tau \ \mathbf{D}_m^w \ \mathbf{I} \ + \ \rho_g \ \mathbf{D}_g') \ \nabla \omega_g^w \tag{3.8}$$

where $\mathbf{i}_g^w$ is the non-advective mass flux of water in gas, $\mathbf{D}_g^w$ is the dispersion tensor, ω_g^w is the mass fraction of water in gas, τ is the tortuosity and $\mathbf{D}_g'$ is the mechanical dispersion tensor. Usually, a constant dispersion coefficient corresponding to the molecular diffusion of vapour in air is assumed:

$$D_m^w = 5.9 \cdot 10^{-12} \cdot \frac{(273.15 + T)^{2.3}}{P_g} \qquad (m^2 / s) \tag{3.9}$$

P_g is given in MPa. $\mathbf{D}_g'$ can be neglected if air flow is insignificant.

The mass of water vapour per unit volume of gas (θ_g^w) is determined via the psychrometric law:

$$\theta_g^w = (\theta_g^w)^0 \exp\left[\frac{-(P_g - P_l)M_w}{R(273.15+T)\rho_l}\right] \tag{3.10}$$

where P_l and P_g are liquid and gas pressures, respectively, $(\theta_g^w)^0$ is the vapour density in the gaseous phase in contact with a planar surface (i.e. when $P_g - P_l$ = 0), M_w is the molecular mass of water (0.018 kg/mol), R is the gas constant (8.314 J/mol K) and T is the temperature (°C). $(\theta_g^w)^0$ is dependent on temperature. The vapour partial pressure is computed by means of the ideal gas law.

The solubility of air in water is controlled by Henry's law:

$$\omega_l^a = \frac{P_a}{H}\frac{M_a}{M_w} \tag{3.11}$$

where ω_l^a is the mass fraction of air in the liquid, P_a is the partial pressure of air, M_a is the molecular mass of air (0.02895 kg/mol) and H = 10000 MPa is Henry's constant. According to the definition of partial density, $\theta_l^a = \omega_l^a \rho_l$.

Based on the preceding test results, hydraulic parameters for the clay/sand mixtures and the Opalinus clay were determined (Table 3-2). The retention curves for the mixtures with clay contents of 35 %, 50 % and 70 % were established by extrapolation of the two-phase flow data obtained on the compacted clay/sand mixtures with clay contents of 10 % and 25 % in the KENTON project /JOC 00/, /MIE 03/, as shown in Figure 3-1. The test data obtained on 20bentonite/80sand mixture by Alonso et al. /ALO 02/ vary in the range between curves of mixtures with clay contents of 10 % and 25 %. Application of the extrapolated retention curves to the simulation of a saturation test on clay/sand mixtures in a cylinder of 50 mm diameter and 100 mm length at an injection pressure of 1 MPa led to a reasonable saturation time of about 2 days for the 35clay/65sand mixture and 6 days for the 50clay/50sand mixture, which is in good agreement with the observed times of 2 – 5 days and 5 – 13 days, respectively. The retention curve of the Opalinus clay is taken from /ZHA 04/ and presented in Figure 3-2. The intrinsic permeability of the clay/sand mixtures was measured by using

the Opalinus clay solution. Figure 3-3 shows the relationship between intrinsic permeability and porosity for the mixtures and the Opalinus clay. The permeability decreases with decreasing porosity. In the tests, it was found that clay/sand mixtures with clay contents higher than 50 % after compaction at 5 MPa exhibit very low permeability of 10^{-20} m^2 which is comparable to that of the intact clay rock. The relative liquid and gas permeability for the mixtures are given as a function of degree of water saturation in Figure 3-4. First, they are assumed equal for all mixtures because of a lack of test data. Figure 3-5 compares the relative permeability of the Opalinus clay and the Serrata bentonite.

Table 3-2 Hydraulic parameters for the clay/sand mixtures and the Opalinus clay

Parameter in equation	Symbol	Unit	Opalinus clay	Clay/sand 35/65	Clay/sand 50/50	Clay/sand 70/30
(3.2)	ϕ_0	-	0.16	0.274	0.331	0.384
(3.2)	k_o	m^2	$2 \cdot 10^{-20}$	$4 \cdot 10^{-18}$	$1 \cdot 10^{-18}$	$5 \cdot 10^{-19}$
(3.3)	S_{lr}	-	0.01	0.01	0.01	0.01
(3.4)	S_{ls}	-	1.0	1.0	1.0	1.0
(3.5)	A	-	1			
(3.5)	B	-	5			
(3.4), (3.7)	β	-	0.4	0.9	0.9	0.9
(3.7)	P_o	MPa	20	1.0	1.5	3
(3.8)	τ	-	0.8	1	1	1

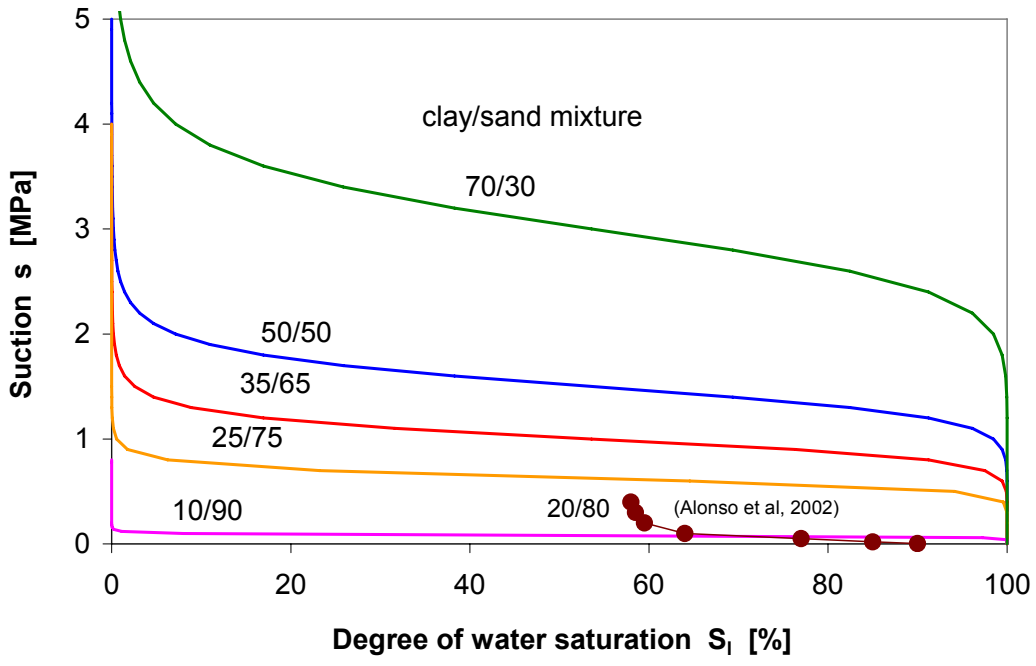

Figure 3-1 Retention curves for different clay/sand mixtures

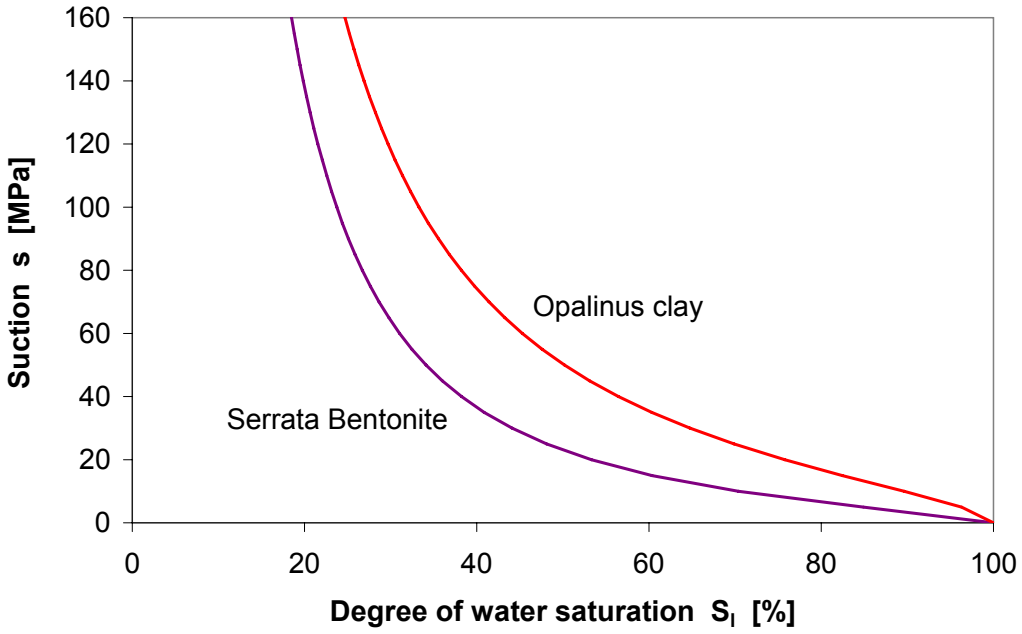

Figure 3-2 Retention curves for the Opalinus clay and Serrata bentonite /ZHA 04/

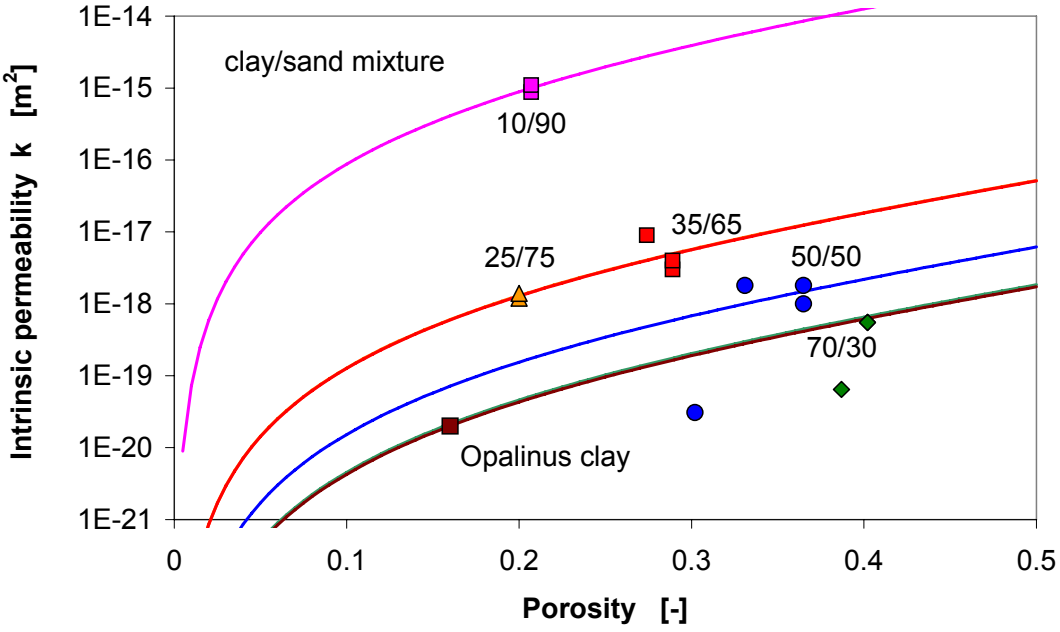

Figure 3-3 Intrinsic permeability as a function of porosity for different clay/sand mixtures and the Opalinus clay

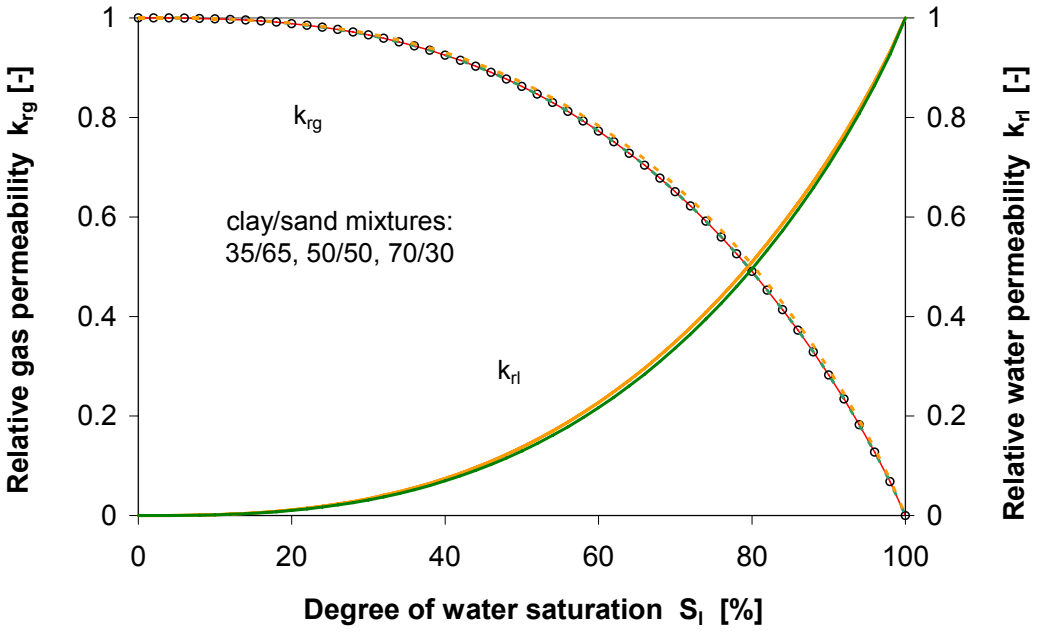

Figure 3-4 Relative water and gas permeability as a function of saturation for the clay/sand mixtures

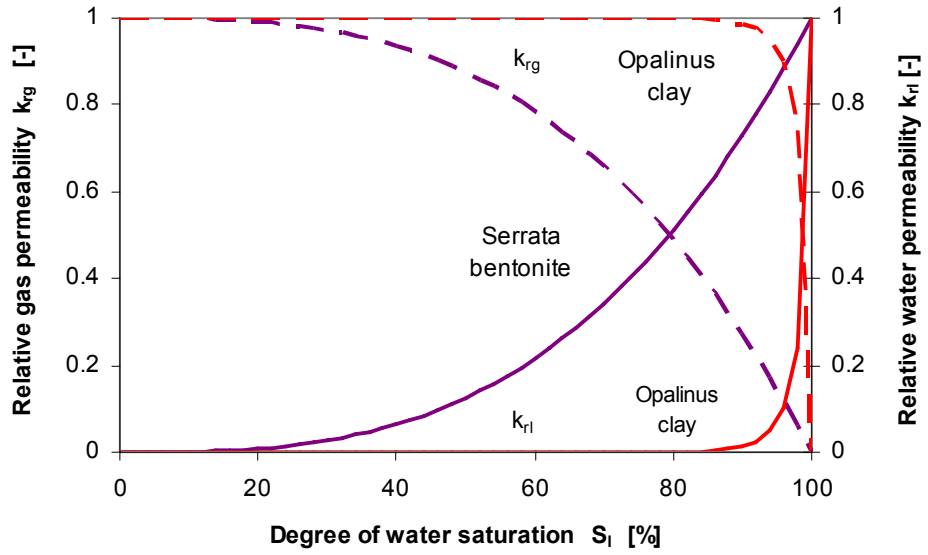

Figure 3-5 Relative water and gas permeability as a function of saturation for Opalinus clay and Serrata bentonite /ZHA 04/

3.1.3 Mechanical model and parameters

The Barcelona Basic Model (BBM) implemented in CODE_BRIGHT is an elasto-plastic model able to represent many mechanical features of unsaturated soils in a consistent and unified manner. For scoping calculations it was used for the description of the mechanical behaviour of the sealing materials and the Opalinus clay. The constitutive relationships are listed in Table 3-3a, whereas mean values of the parameters are given in Table 3-3b. The latter ones were determined from a few limited compaction tests on the clay/sand mixtures in oedometer cells and the parameters for the Opalinus clay were taken from /ZHA 04/.

Figure 3-6 compares the compaction results obtained on clay/sand mixtures with the modelling curves, whereas Figure 3-7 illustrates the swelling behaviour of clay/sand mixtures. The mixtures swell with increasing water saturation due to the existence of clay minerals. However, the assumed swelling capacity seems to be low. The maximum swelling strain of $\Delta e = 0.0003$ to 0.0007 is reached after saturation.

Table 3-3a BBM model for the mechanical behaviour of unsaturated materials

Constitutive model	Expression	Equation
Elastic volumetric strain	$d\varepsilon_v^e = d\varepsilon_{vp}^e + d\varepsilon_{vs}^e$	(3.12)
	$d\varepsilon_{vp}^e = \frac{k_i}{v}\frac{dp'}{p'}$	(3.13)
	$k_i = k_{io}(1+\alpha_i s)$	(3.14)
	$d\varepsilon_{vs}^e = \frac{k_s}{v}\frac{ds}{s+p_{at}}$	(3.15)
	$k_s = k_{so}\left(1+\alpha_{sp}\ln\left(\frac{p'}{p_{ref}}\right)\right)\exp(\alpha_{ss}s)$	(3.16)
Elastic deviatoric strain	$d\varepsilon_q^e = \frac{G}{3}dq$	(3.17)
	$G = \frac{3(1-2\nu)}{2(1+\nu)}\frac{(1+e)}{k_i}p'$	(3.18)
Yield locus	$q^2 - M^2(p'+p_s)(p_o - p') = 0$	(3.19)
	$p_s = p_{so} + k\cdot s$	(3.20)
	$p_o = p^c\left(\frac{p_o^*}{p^c}\right)^{\frac{\lambda(o)-k_{io}}{\lambda(s)-k_{io}}}$	(3.21)
	$\lambda(s) = \lambda(o)[(1-r)\exp(-\beta s) + r]$	(3.22)
	$q = Mp'$	(3.23)
Hardening	$\frac{dp_o^*}{p_o^*} = \frac{v}{\lambda(o)-k_{io}}d\varepsilon_v^p$	(3.23)

Table 3-3b Parameters for clay/sand mixtures and Opalinus clay

Parameter in equation	Symbol	Unit	Opalinus clay	Clay/sand 35/65	Clay/sand 50/50	Clay/sand 70/30
(3.14)	k_{io}	-	0.0035	0.002	0.002	0.002
(3.14)	α_i	-	0	0	0	0
(3.16)	k_{so}	-	$4 \cdot 10^{-5}$	0.0005	0.0007	0.001
(3.16)	α_{sp}	-		0	0	0
(3.16)	α_{ss}	MPa^{-1}		0	0	0
(3.16)	p_{ref}	MPa		-	-	-
(3.18)	ν	-	0.33	0.35	0.35	0.35
Bulk modulus	K	MPa	3500	80	80	80
Shear modulus	G	MPa	1340	27	27	27
Young's modulus	E	MPa	3570	40	40	40
(3.23)	M	-	1.5	1.5	1.5	1.5
(3.20)	k	-	-0.007	-0.1	-0.1	-0.1
(3.21)	p^c	MPa	0.1	0.1	0.1	0.1
(3.21)	p_o^*	MPa	20.0	1.5	2.0	2.5
(3.21)	$\lambda(o)$	-	0.027	0.05	0.05	0.05
(3.22)	r	-	0.6	0.75	0.75	0.75
(3.22)	ß	MPa^{-1}	0.015	0.05	0.05	0.05

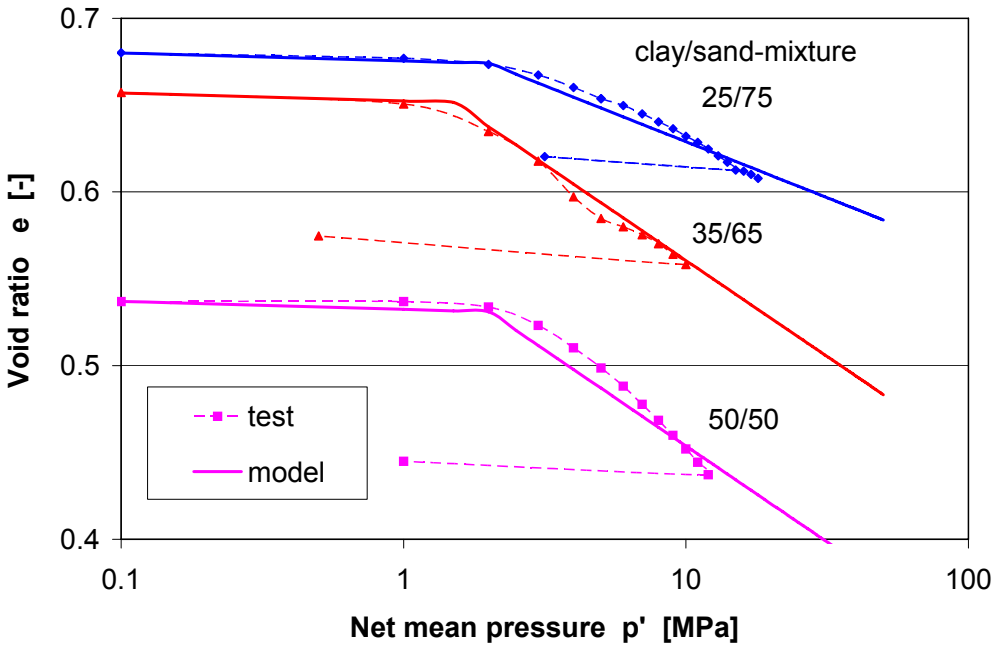

Figure 3-6 Compaction behaviour of clay/sand mixtures

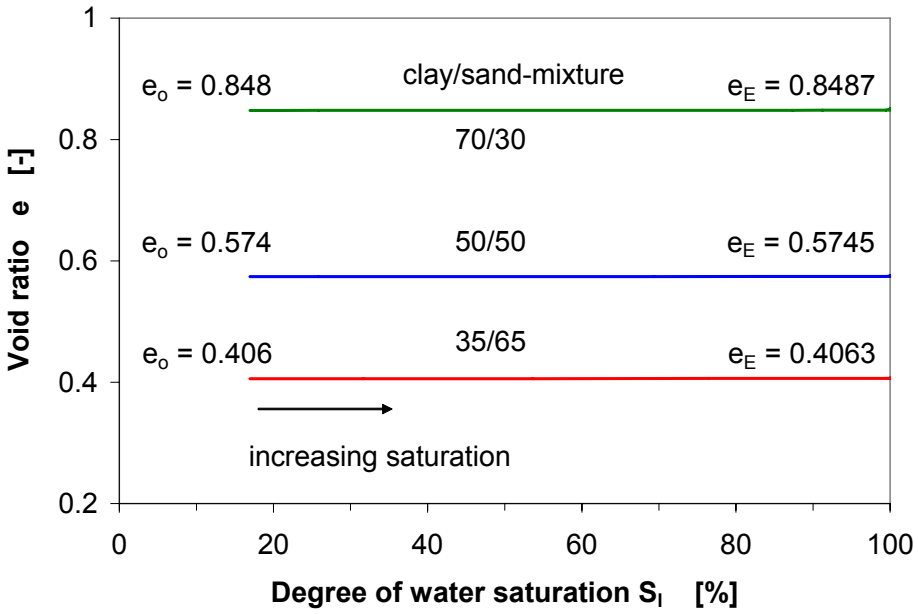

Figure 3-7 Swelling of clay/sand mixtures due to water saturation

3.2 Scoping calculations

For designing mock-up and in-situ tests, scoping calculations have been performed by applying the preliminary parameters mentioned above. The calculations focused on prediction of testing conditions such as injection pressures for water and gas, duration of water saturation, ranges of measuring parameters (gas and water flux, swelling pressure, total pressure etc.), and determination of initial and boundary conditions in the in-situ test field. In the scoping calculations, the materials installed in mock-up and in-situ tests were assumed as homogeneous and isotropic. Possible processes occurring in the materials during the tests were considered as THM coupling processes, so that a series of balance equations was solved:

- Balance of energy:

$$\frac{\partial}{\partial t}\left[E_s \rho_s (1-\phi) + E_l \rho_l S_l \phi + E_g \rho_g S_g \phi\right] + \nabla \cdot (\mathbf{i}_c + \mathbf{j}_{Es} + \mathbf{j}_{El} + \mathbf{j}_{Eg}) = f^E \qquad (3.24)$$

where E_s, E_l and E_g are specific internal energies corresponding to the solid, liquid and gaseous phases, ρ_s, ρ_l and ρ_g are the densities of the three phases, ϕ is porosity, S_l is the volumetric liquid fraction and S_g is the volumetric gaseous fraction

with respect to the pore volume, $S_l + S_g = 1$. $\mathbf{i}_c$ is the non-advective (conductive) heat flux and $\mathbf{j}_{Es}$, $\mathbf{j}_{El}$, $\mathbf{j}_{Eg}$ are the advective energy flux of each of the three phases with respect to a fixed reference system. The most relevant advection energy fluxes correspond to vapour and liquid water motion. f^E is the energy supply per unit volume of the considered medium.

- Balance of water mass:

$$\frac{\partial}{\partial t}(\theta_l^w S_l \phi + \theta_g^w S_g \phi) + \nabla \cdot (\mathbf{j}_l^w + \mathbf{j}_g^w) = f^w \tag{3.25}$$

where θ_l^w and θ_g^w are the mass of water per unit volume of liquid and gas, respectively, $\mathbf{j}_l^w$ and $\mathbf{j}_g^w$ denote the total mass flux of water in the liquid and gas phases with respect to a fixed reference system and f^w is the external mass supply of water per unit volume of medium.

- Balance of air mass:

$$\frac{\partial}{\partial t}(\theta_l^a S_l \phi + \theta_g^a S_g \phi) + \nabla \cdot (\mathbf{j}_l^a + \mathbf{j}_g^a) = f^a \tag{3.26}$$

where θ_l^a and θ_g^a are the mass of dry air per unit volume of liquid and gas, respectively, $\mathbf{j}_l^a$ and $\mathbf{j}_g^a$ indicate the total mass flux of air in liquid and gas phases with respect to a fixed reference system, and f^a is the external mass supply of air per unit volume of medium.

- Balance of momentum (equilibrium):

$$\nabla \cdot \sigma + b = 0 \tag{3.27}$$

where $\boldsymbol{\sigma}$ represents the stresses and **b** the body forces.

In the scoping calculations, the following physical phenomena were taken into account:

- Water flow is controlled by advection (Darcy's law), vapour diffusion in air (Fick's law) and phase changes (psychrometric law);

- Air and vapour are considered to behave as ideal gases and air flow is controlled by advection (Darcy's law) and solution in liquid water (Henry's law);
- Heat transport is dominated by conduction (Fourier's law) through the media and by advection of liquid water and vapour flow;
- The mechanical behaviour of both materials are described by the BBM elasto-plastic model with the main features of swelling.

The modelled results will be presented in section 4 for design of the mock-up tests and in section 5 for the in-situ tests, respectively.

3.3 Further modelling work

3.3.1 Improvement of parameter certainty

The preliminarily established parameters presented in section 3.1 are based on the very limited test results obtained in the preceding laboratory programme and some of them are assumed without data base. So there is an uncertainty with the use of the parameters for modelling the SB experiments. To increase the quality of further modelling results it is necessary to conduct additional laboratory tests on selected clay/sand mixtures under consideration of relevant mock-up and in-situ testing conditions, so that the certainty of the parameters will be improved. For this purpose, the following tests have to be carried out:

- **Water saturation tests on unsaturated clay/sand mixtures at injection pressure:** The **Retention curve** (eq. 3.7) controls water saturation of an unsaturated material. The associated parameters for the clay/sand mixtures were preliminarily determined by extrapolation of the gas injection tests on the highly compacted mixtures with clay contents of 10 % and 25 % /JOC 00/, /MIE 03/, but not based on any tests on the materials themselves. Therefore, it is necessary to conduct saturation tests for the determination of retention curves for selected materials. The saturation tests will be carried out on samples of 50 mm diameter and 100 mm length in a steel cylinder with the Opalinus clay solution at relevant injection pressures (see also section 2.1.3). At different saturation times, the samples will be cut in small discs and their water contents will be measured and, finally, the distribution of water content along the sample length will be determined.

By simulation of saturation tests, the parameters of retention curves will be optimised. After reaching full saturation, the **intrinsic water permeability** (eq. 3.2) will additionally be measured on some samples.

- **Gas injection tests on saturated clay/sand mixtures:** Gas transport through barriers after full saturation is one of the most important issues for designing engineered barrier systems in repositories. In the case of investigated clay/sand mixtures which will not be compacted very strongly, gas flow through them after saturation may displace partially the pore water. This mechanism implies a two-phase flow. Therefore, relative liquid and gas permeability as a function of water saturation (eqs. 3.4, or 3.5, 3.6) have to be determined for the selected materials by means of gas injection tests. The tests will be carried out in a steel cylinder of 50 mm diameter and 100 mm length. The initially unsaturated samples will firstly be injected with nitrogen to measure the gas permeability at mostly dried conditions. Secondly, they will be saturated by injection of the Opalinus clay solution. In the third phase, nitrogen gas will be injected into the samples with a controlled flow rate to examine the **gas break-through pressure**. Afterwards the gas pressure will be increased stepwise to measure the **gas permeability** and the **water content** (degree of water saturation), so that the parameters of equations 3.4 to 3.6 for relative permeabilities as a function of saturation can be identified. Additionally, the **retention curve** (eq. 3.7) **for the gas injection path** can also be determined from the measurements. Finally, the samples will be cut in small discs and the distribution of water content along the sample length will be examined.

- **Compaction behaviour**: For determination of the BBM parameters, compaction tests in oedometer and triaxial cells will be performed on selected materials under suction controlled conditions.

- **Swelling behaviour**: To examine the swelling capacity of selected clay/sand mixtures and to determine the BBM parameters associated with the suction effect on the mechanical behaviour, swelling pressure and swelling strain will be investigated in swelling cells by wetting the samples under constant volume or constant load, respectively.

The above determined parameters will first be applied to numerical simulations of the mock-up tests. By comparing the modelled results with the measurements, the parameters will be calibrated and then used to simulate the in-situ experiments. Based

on the in-situ measurements and the post-test investigations on representative samples drilled from the seal and the surrounding rock, the parameters will be calibrated again, if necessary.

3.3.2 Modelling the mock-up tests

By using the above determined parameters, the mock-up tests will be numerically simulated. By comparing the modelling results with the measurements, the parameters will be calibrated and applied again in second calculations of the mock-up tests. The modelling results will be used for interpretation of the observations in the mock-up tests.

3.3.3 Modelling the in-situ tests

The calibrated parameters mentioned above will be employed for modelling the in-situ experiments. The in-situ observations will be explained by support of the modelling results.

Finally, it is necessary to evaluate the suitability of the models used during the modelling work, especially on the basis of in-situ measurements and post-test investigations on representative samples drilled from the seal and the surrounding rock. If necessary, the models will be improved with the assistance of the code developer UPC.

4 Mock-up Tests

For the successful conduction of in-situ experiments proper installation techniques assuring the required installation densities are extremely important. In addition, the saturation time of the seal has to be considered in the design of in-situ experiments. Before going in situ, both, installation technique and saturation time will be tested and investigated for different material mixtures in large-scale mock-up tests in the GRS geotechnical laboratory at Braunschweig, respectively.

4.1 Objectives and design of mock-up tests

The mock-up tests will be performed in vertically arranged steel tubes with the same diameter of 0.3 m as the in-situ boreholes. The tube length will be 2.5 m and the sealing material will be installed in thin layers of about 5 to 10 cm in a similar way as in-situ. Different techniques (hand stamping, vibrator technique) will be tested and the achievable density determined. Additionally, gas permeability, saturation velocity, water permeability, gas break-through pressures and gas permeability after the break-through will be determined in order to provide adequate experiences for the design of in-situ experiments at Mont Terri.

The detailed objectives of the mock-up tests are listed below:

1. development and testing of an adequate method for mixing 100 litre of a clay/sand mixtures with adequate homogeneity,

2. development and testing of methods to install the clay/sand mixture at a borehole depth of 2 m with the pre-determined dry density and without segregation,

3. determination of the saturation velocity of the clay/sand seal at different water injection pressures as well as the permeability to water and gas at different stages of water saturation,

4. testing of pre-selected instrumentation and of a data collection system for measuring the parameters described in section 5.2 (gas and water injection, gas and water pressure, gas and water flow, swelling pressure),

5. selection and testing of a porous medium which is to be emplaced in the boreholes above and below the clay/sand seal

6. select and test a filter material at the boundary between the porous medium and the seal which avoids penetration of the bentonite into the porous medium and which ensures a homogeneous flow of water and gas through the seal.

Figure 4-1 shows the planned arrangement of altogether four test tubes in the laboratory together with the data collection system and further equipment needed for running the tests.

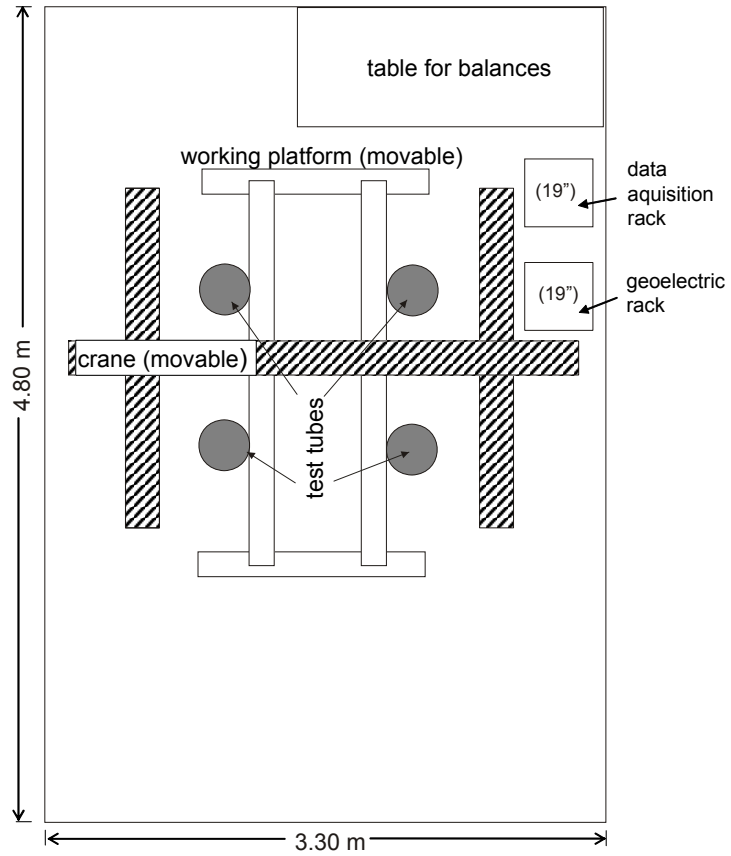

Figure 4-1 Principle layout of a mock-up test with four test tubes and the equipment for running the experiments

Two types of test tubes will be set up in the surface laboratory.

Tube Type 1 will be instrumented to allow all necessary investigations and measurements with regard to the objectives listed above. Two test set-ups will be assembled to enable the investigation of the saturation time for two types of material mixture at constant injection pressure. An overview of this tube type with the planned test instrumentation is shown in Figure 4-2.

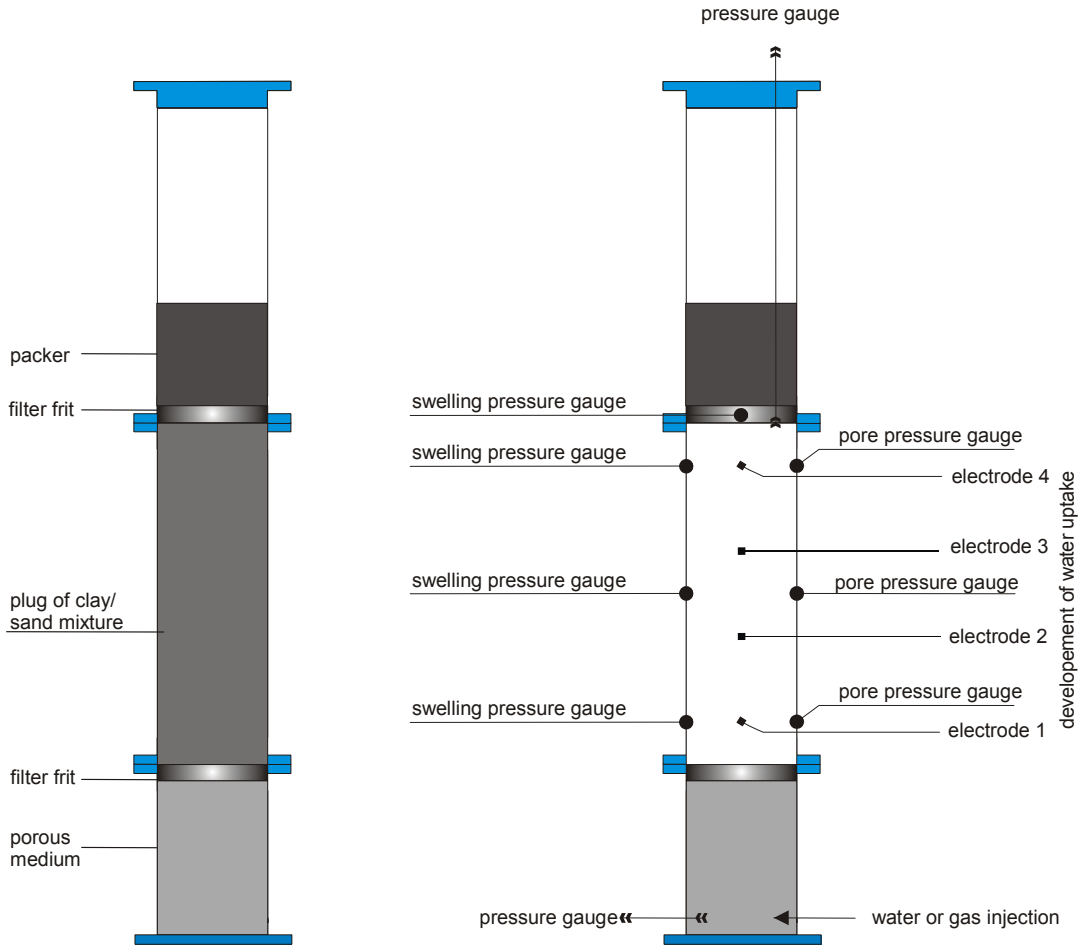

Figure 4-2 Principle layout of test tubes type 1 with the locations of possible measuring sensors

Tube Type 2 (Figure 4-3 and Figure 4-4) will mainly be instrumented for performing the same investigations as in the type 1-tubes, but without any instrumentation to avoid any negative influence of the instrumentation on the test results. The injection pressure, however, will be limited to a low injection pressure to test impact of injection pressure on the saturation time.

In the described way it will be possible to investigate the installation techniques and the saturation time for two different material mixtures at two different injection pressures.

In addition, both tube types, the instrumented and the non-instrumented type will be equipped at the inlet and the outlet with some pressure and flow sensors to enable determination of the material permeability to gas and water as well as the gas break-through pressure and the effective permeability to gas as a function of water saturation.

Additionally, the data collection system, which will be used at Mont Terri, will be tested in the mock-up tests in Braunschweig. All electronic sensors will be connected to a data collection system and data from the different sensors will be recorded and evaluated.

Table 4-1 shows all envisaged mock-up tests and the measuring parameters.

4.2 Test tube design

Each test tube consists of three prefabricated parts with welded flanges. At the flanges they are fitted together gas and water tight. The tubes are seamless with an outer diameter of 323.9 mm and a wall thickness of 7.1 mm. They are licensed for pressures of 1.6 MPa. The bottom part has a length of 500 mm with a welded blind flange the tube stands on at the floor. The centre tube as well as the top tube each have a length of 1000 mm. They stand on top of each other and they are fitted together by 12 bolts of 20 mm. For gas and water injection or extraction the bottom part and the top part have two holes of 20 mm at the wall for installation of valves. The whole test tube has a total length of 2500 mm. It is mounted to a working platform (Figure 4-1) to allow a better installation of all components and to avoid a fall over.

Table 4-1 Overview of the envisaged measurements in four mock-up tests

	test tube type 1	test tube type 1	test tube type 2	test tube type 2
Clay/sand mixture	35/65	50/50	35/65	50/50
Injection pressure [MPa]	1	1	0.5	0.5
Envisaged measurement/investigation				
1. Testing of inst. techniques	X	X	X	X
2. Gas permeability	X	X	X	X
3. Seal saturation	X	X	X	X
4. Water permeability	X	X	X	X
5. Swelling pressure	X	X		
6. Pore pressure	X	X		
7. Gas break-through pressure	X	X	X	X
8. 2-Phase flow measurements	X	X	X	X
9. Instruments at or in seal	X	X		
10. Data collection system	X	X	X	X

The bottom part with a length of 500 mm will be filled with the porous medium (either stone chips, gravel, or sand) to guarantee homogeneous gas and water injection into the seal. A filter frit will be installed at the top in order to avoid penetration of the bentonite into the porous medium.

The central part with a length of 1000 mm will be filled with the compacted seal (clay/sand mixture) with a filter frit at the top.

The upper part with a length of 1000 mm will be filled again with the porous medium of 500 mm height and a packer with a lead-through tube which is connected to a pressure gauge and a flow meter for gas or water.

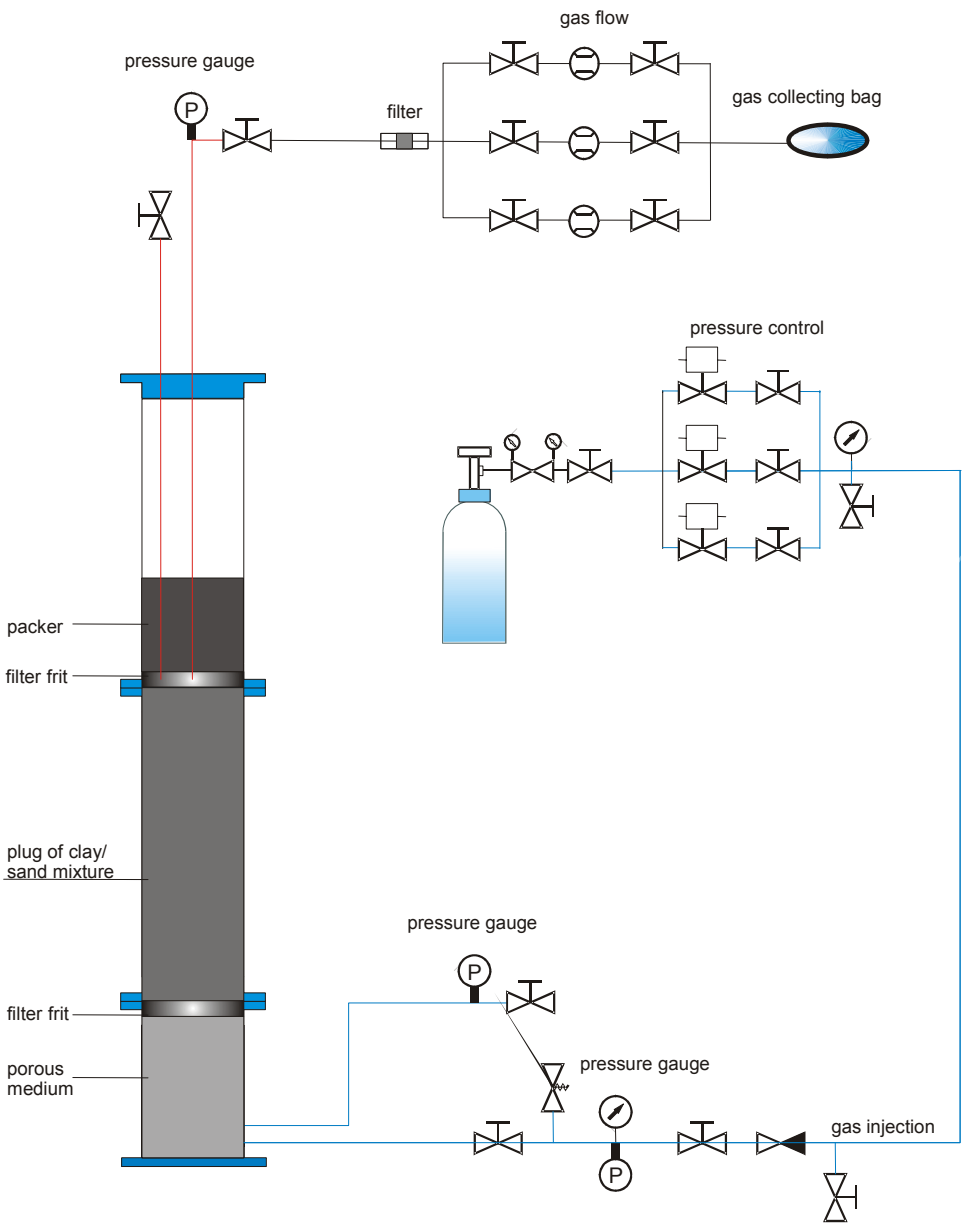

Figure 4-3 Principle layout of tube type 2 for gas injection and gas flow determination

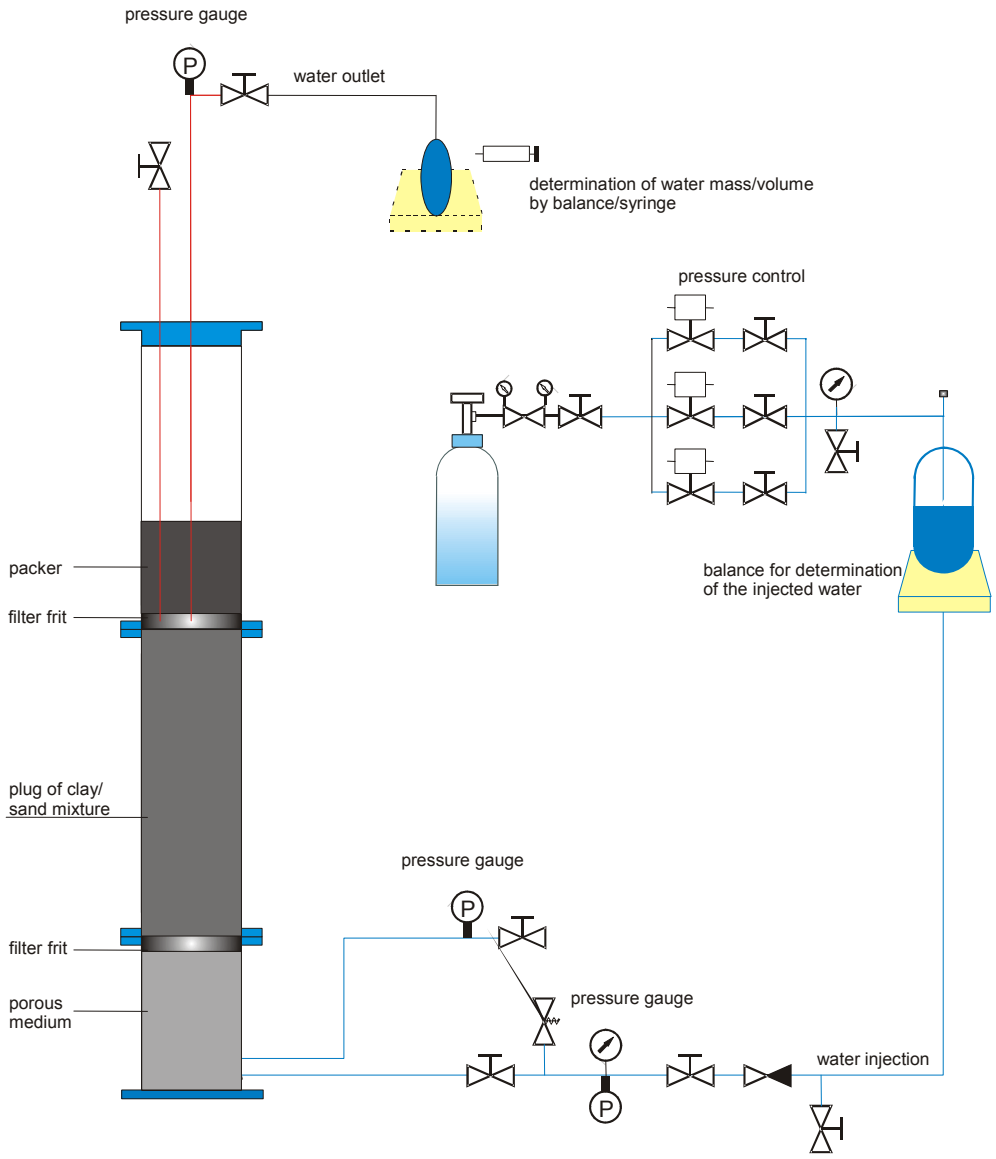

Figure 4-4 Principle layout of test tube 2 for water injection and water flow determination

4.3 Set up of mock-up tests

For developing and testing the emplacement conditions in the test field all materials (the porous medium and the seal) will be installed through the top of the 2500 mm high test tube via a feeding hopper and a hose. The hose always has to reach down to the final level of installation to avoid dust and segregation.

In order to have laminar gas and water flow in the whole cross section of the central tube the bottom tube (500 mm) will be filled with a porous medium of stone chips or

gravel. This porous medium has to be brought in by four layers of 100 to 150 mm. Each layer has to be compacted by hand stamping or by an electric vibrator. On top of the porous volume a filter frit of stainless steel is installed to avoid penetration of clay particles.

The central part of the test tube (1000 mm) above the filter frit will be filled with the clay/sand mixture and the achieving of the pre-determined installation density will be tested by using either the method of compaction by hand stamping or by using an electric vibrator. The clay sand mixture will be brought in layers of 50 to 100 mm. Each layer has to be compacted up to the predetermined density. The density is calculated by the amount of the mixture installed and the volume of the compacted layer. On top of the seal again a stainless steel filter frit will be installed.

The top part will be filled again with 500 mm of the porous medium in the same way as at the bottom. Finally, the system will be sealed with a packer with a lead-through.

4.4 Test procedure and measurements

In the mock-up tests the following processes will be accompanied by measurements to enable the determination of the saturation velocity of the borehole seal at different water injection pressures, the permeability to water after saturation and the permeability to gas after break-through the saturated seal.

4.4.1 Gas injection

The gas will be injected via one of the two inlets at the bottom tube (Figure 4-2). In general, the gas tests will be performed with nitrogen from a gas bottle. From the pressure reduction valve at the gas bottle a tube to the injection volume passing an additional valve, a pressure gauge, and an overpressure valve adjusted to 1.6 MPa which is the licensed pressure of the steel tube. If useful, an electronic gas flow meter could be installed. The gas flow will be measured by determining the loss in weight of the gas bottle with time. A further pressure gauge and a valve will be connected to the second inlet to determine the gas pressure inside the injection volume. The second inlet may also serve as a gas outlet, if necessary.

4.4.2 Gas flow and pressure determination at the outlet

For determining the gas flow passing the seal a capillary of 6x2 mm is mounted to the lead-through of the packer. This capillary passes an overpressure valve, a pressure gauge, and a reduction valve and runs to three electronic flow meters with different measuring ranges arranged in parallel. The reduction valve is installed to generate a gas pressure at the outlet above atmospheric pressure.

In the case of stationary gas flow the amount of gas injected into the inlet and extracted at the outlet should be identical. However, in the in-situ experiment it cannot be excluded that a certain amount of gas may migrate into the surrounding host rock. In order to determine this gas flow it is essential to measure the amount of gas injected and extracted.

The gas injection as well as the equipment for the flow and pressure determination is shown in Figure 4-3.

4.4.3 Water injection

For the water injection a gastight water bottle is added into the injection capillary (Figure 4-4). The water pressure is generated by the gas pressure above the water level. The amount of water is determined by weighing the water bottle. All the other equipment is the same as for gas injection.

4.4.4 Water flow and pressure determination at the outlet

The test tube for water flow determination is identical to the gas flow determination, except for the flow meters for gas for which an electronic flow meter for water is installed. If the water flow rate is very low an electronic flow meter will not work. In that case a gas and water tight sampling bag will be connected to the outlet. The amount of water will be collected for longer time periods and the amount will be determined by weighing.

The water injection as well as the equipment for the flow and pressure determination is shown in Figure 4-4.

4.5 Scoping calculations for the mock-up tests

To enable proper selection of measuring instruments and to predict durations of the mock-up tests, some scoping calculations have been performed by use of CODE_BRIGHT and the preliminary parameters given in section 3 under consideration of the test procedure described in section 4.4. The theoretical considerations and assumptions in the calculations were presented previously in section 3.2.

4.5.1 Numerical model

Regarding the conclusions drawn from the preceding laboratory experiments (section 2.3), the selected clay/sand mixtures with clay contents of 35 % and 50 % were considered in the calculations. The average properties and parameters of the materials given in Table 3-1, 3-2 and 3-3b were applied in the calculations. The selected materials are installed in steel tubes of 0.3 m diameter and 1.0 m length. Due to the symmetry of the steel tubes, only half of the construction (seal, injection chamber and filter) was considered in the axisymmetric model shown in Figure 4-5.

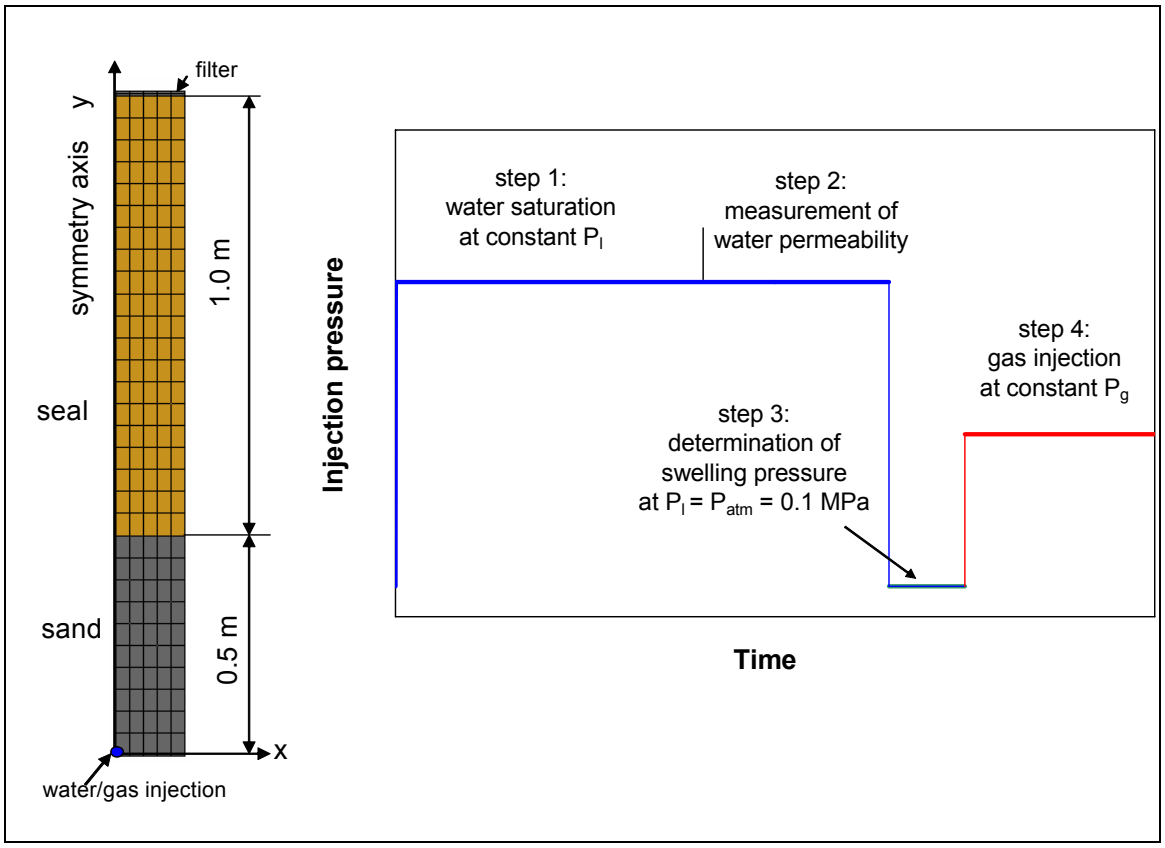

Figure 4-5 Numerical model and calculation steps

According to the envisaged test procedure (section 4.4), the following steps were considered in the calculations (Figure 4-5):

Step 1: Water injection at constant water pressure to determine evolution of water saturation and time needed for full saturation;

Step 2: Water flow through the saturated seal at constant injection pressure and measurement of water outflow;

Step 3: Reduction of the water pressure down to atmospheric pressure to examine the swelling pressure (remaining total stress) in the seal;

Step 4: Gas injection into the saturated seal at constant flow rate to determine gas break-through pressure and gas outflow.

The following initial and boundary conditions were prescribed in the calculations:

- The initial stress in the seal $\sigma_{10} = \sigma_{20} = \sigma_{30}$ = 0.1 MPa induced by compacting the seal material in the steel tube;
- No displacement of all boundaries ΔU = 0 due to confinement of the seal in the stiff tube;
- No water and gas outflow through the circumferential surface $Q_w = Q_g$ = 0, because of the tight steel tube;
- Water injection at the bottom of the seal at given pressure P_l;
- Gas injection at the bottom of the seal at given flow rate $\dot{Q}_g$;
- Atmospheric pressure $P_g = P_{atm}$ = 0.1 MPa at top boundary of the seal.

In the calculations, the water injection pressure and the gas injection rate are varied as follows: P_l = 0, 0.2, 0.5, 1.0 MPa; $\dot{Q}_g$ = 0.02, 0.2 ml/min.

Note that real values (gauge values) of water and gas pressure as well as stress are equal to the calculated values minus the atmospheric pressure P_{atm} = 0.1 MPa.

4.5.2 Modelling results

4.5.2.1 Water saturation and flow

Water saturation and flow was calculated for both selected mixtures under different injection pressures between 0 and 1 MPa. Figure 4-6a and 4-6b show the distribution and evolution of water saturation in the 35clay/65sand seal at an injection pressure of 1 MPa, whereas the calculation results for the 50clay/50sand mixture at the same injection pressure of 1 MPa are illustrated in Figure 4-7a and 4-7b. The seals are saturated from the bottom to the top. The time needed to reach a full saturation at 1 MPa injection pressure is about 6 month for the 35clay/65sand seal and 19 month for 50clay/50sand seal. Table 4-2 summarises the saturation times for both seals at different pressures. Figure 4-8 and 4-9 show the evolution of pore water pressures at different locations in the seals. After full saturation, the water flux at the outlet was predicted for both seals at 1 MPa injection pressure to $\dot{Q}_w = 2.9 \cdot 10^{-4}$ ml/min for the 35clay/65sand seal and to $\dot{Q}_w = 9.0 \cdot 10^{-5}$ ml/min for the 50clay/50sand seal. To collect a water volume of 10 ml in a steady flow state, the time needed is about 25 days for the 35clay/65sand seal and 80 days for the 50clay/50sand seal.

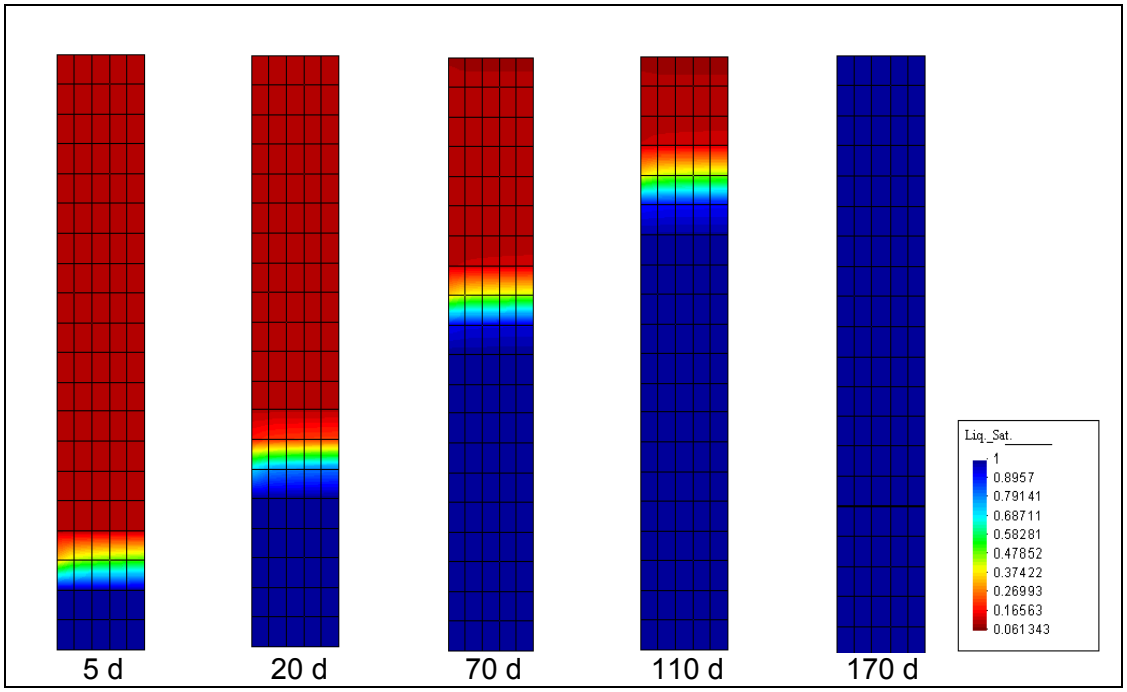

Figure 4-6a Distribution of water saturation in 35clay/65sand seal at an injection pressure of 1 MPa

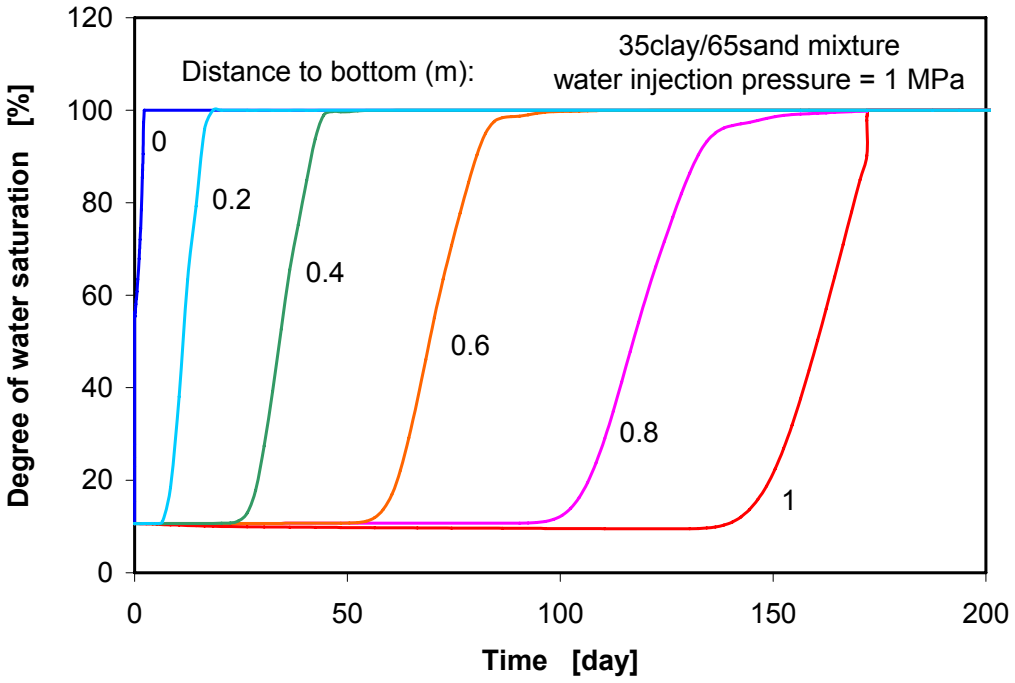

Figure 4-6b Evolution of water saturation in 35clay/65sand seal at an injection pressure of 1 MPa

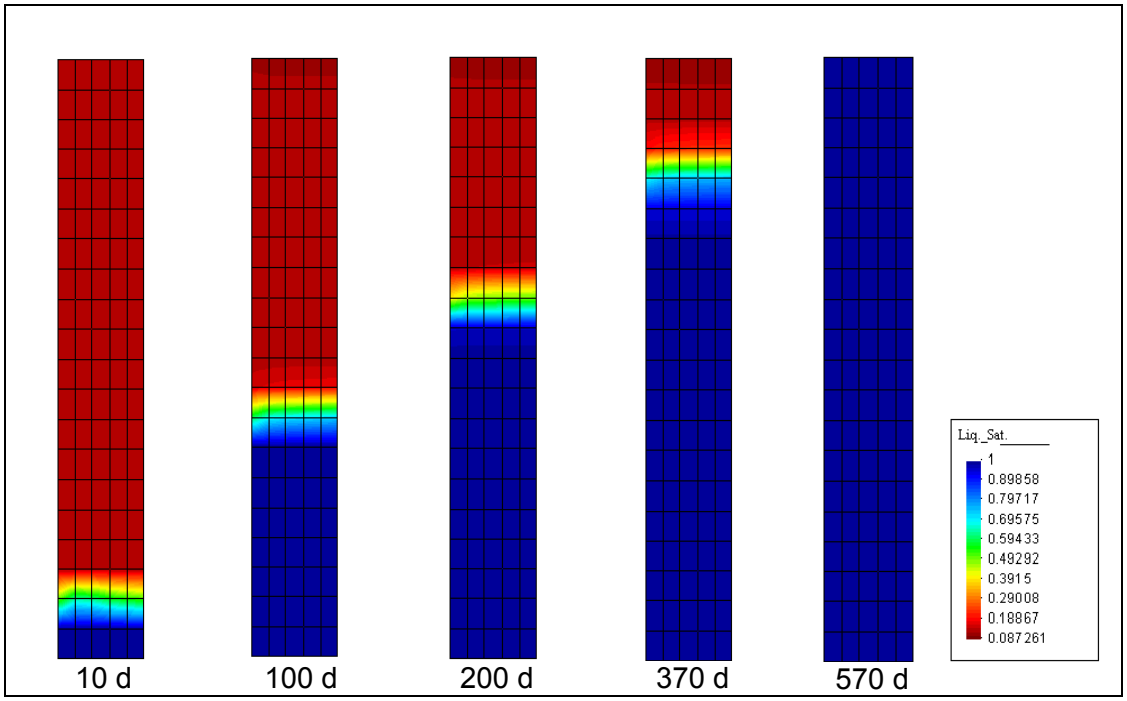

Figure 4-7a Distribution of water saturation in 50clay/50sand seal at an injection pressure of 1 MPa

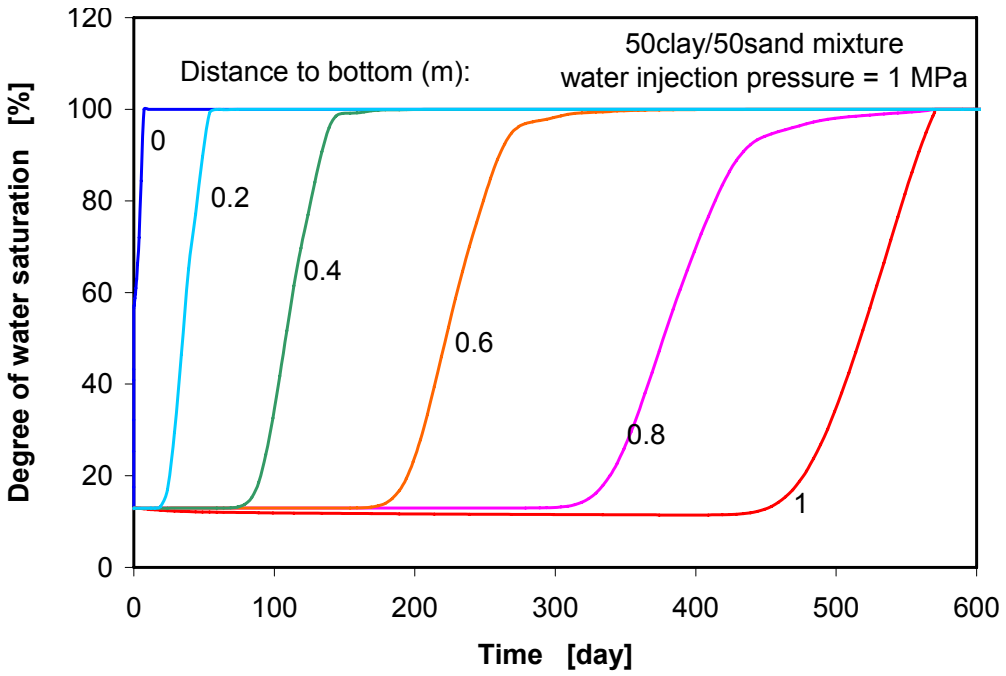

Figure 4-7b Evolution of water saturation in 50clay/50sand seal at an injection pressure of 1 MPa

Table 4-2 Time needed for a full saturation of the seals at different pressures

Clay/sand seal	Injection pressure [MPa]	0.0	0.2	0.5	1.0
35/65	Time [day]	380	300	240	170
50/50	Time [day]	900	840	700	570

4.5.2.2 Gas break-through pressure and flow

Gas flow through the fully saturated seals was simulated by injecting dry gas at constant rate of 0.02 and 0.2 ml/min. Figure 4-10a and 4-10b show the development of pore gas pressures in the 35clay/65sand seal during the gas injection with the constant injection rates, while the evolution of pore gas pressures in the 50clay/50sand seal is depicted in Figure 4-11a and 4-11b. It is obvious that the gas pressure at the bottom of the seals builds up rapidly and then more or less keeps constant until gas breaks through the initially saturated seals. The maximum gas pressure observed at the bottom is defined here as the gas break-through pressure. Slow gas injection generates a low gas break-through pressure. The gas outflow after the gas break-through was predicted as well. Table 4-3 summarises the modelled results of gas break-through pressure, gas outflow rate, time needed until breaking and time needed for collecting a normal gas volume of 100 ml at the outlet after the gas break-through.

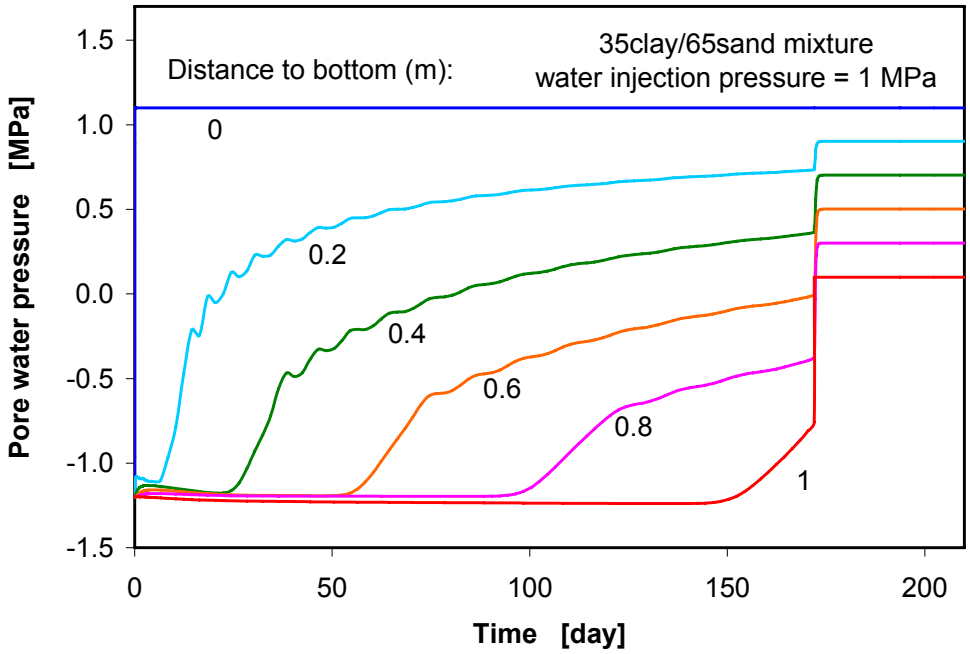

Figure 4-8 Evolution of pore water pressure in 35clay/65sand seal at an injection pressure of 1 MPa

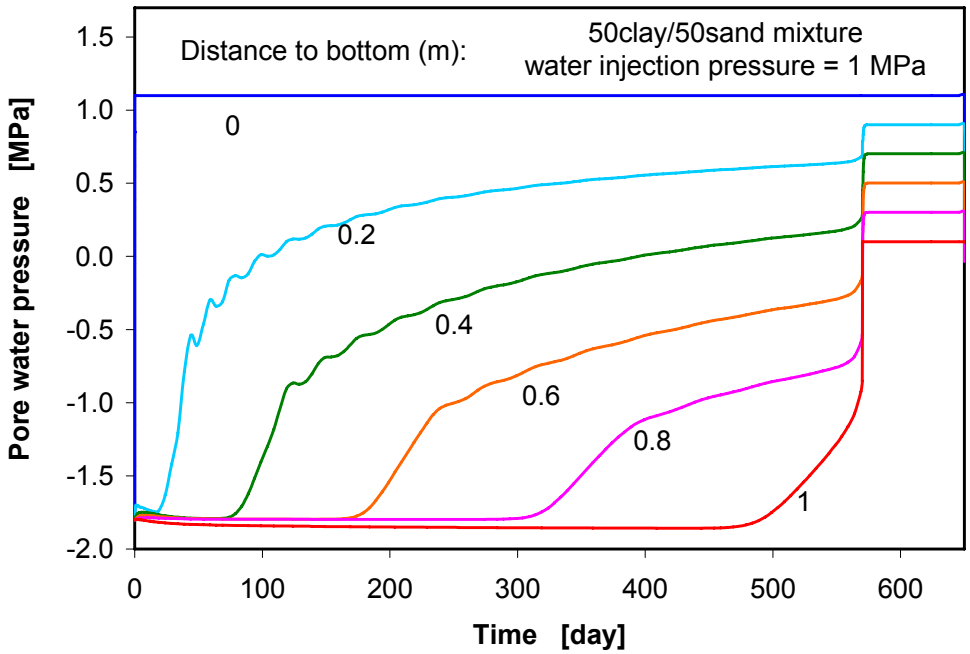

Figure 4-9 Evolution of pore water pressure in 50clay/50sand seal at an injection pressure of 1 MPa

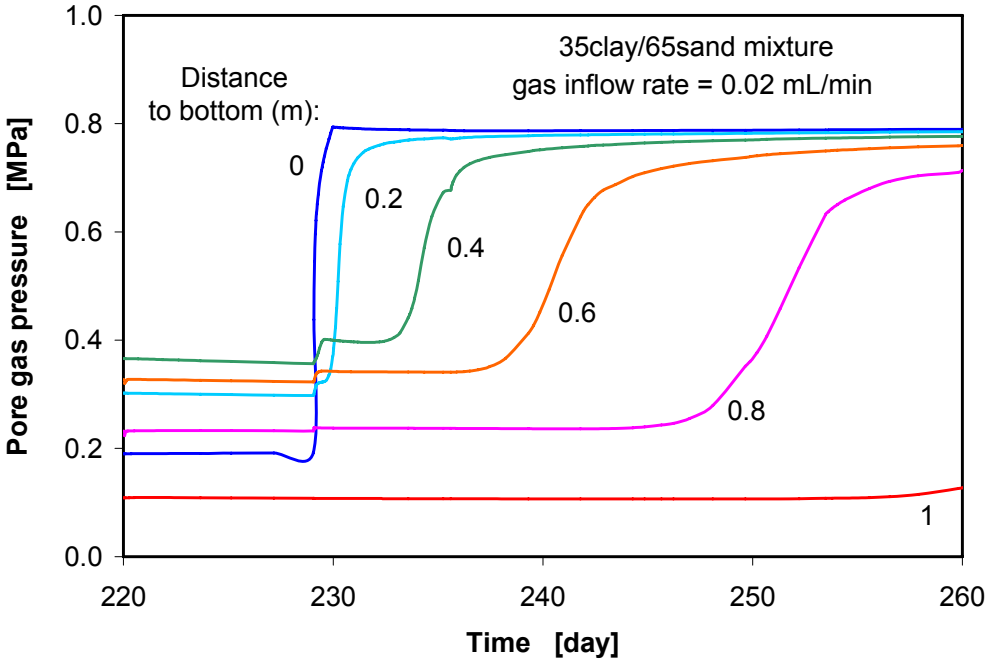

Figure 4-10a Evolution of pore gas pressure in 35clay/65sand seal during gas injection at an injection rate of 0.02 ml/min

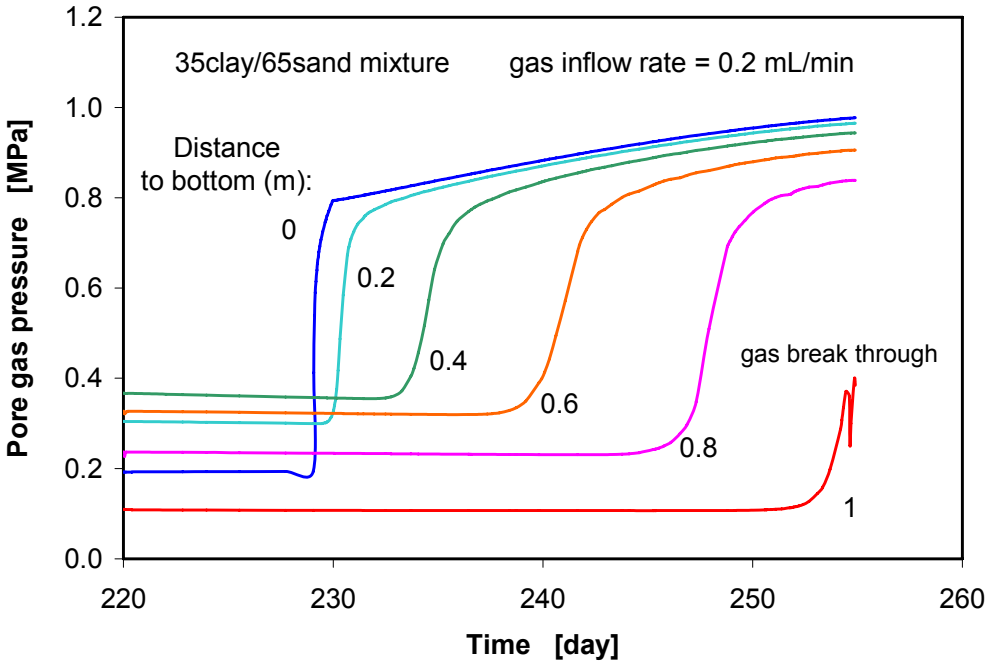

Figure 4-10b Evolution of pore gas pressure in 35clay/65sand seal during gas injection at an injection rate of 0.2 ml/min

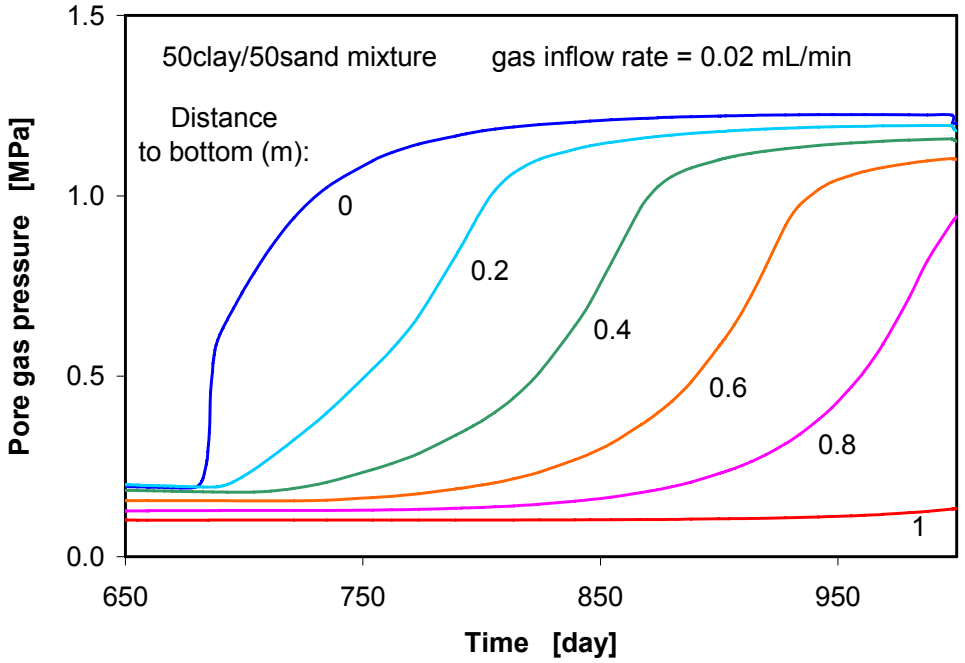

Figure 4-11a Evolution of pore gas pressure in 50clay/50sand seal during gas injection at an injection rate of 0.02 ml/min

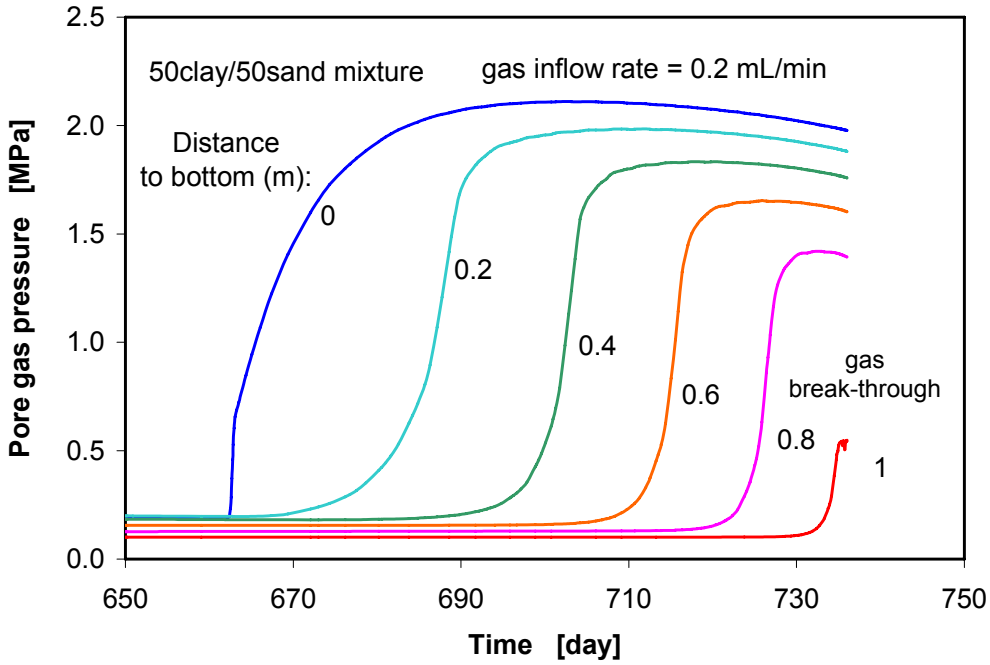

Figure 4-11b Evolution of pore gas pressure in 50clay/50sand seal during gas injection at an injection rate of 0.2 ml/min

The time for the gas break-through of the 35clay/65sand seal varies between 25 and 35 days, whereas the gas break-through of the 50clay/50sand seal occurs after 80 days at the injection rate of 0.2 ml/min and after about 1 year at the rate of 0.02 ml/min. To collect a normal gas volume of 100 ml at a steady state flow, the time needed is about 1 to 2 days for the 35clay/65sand seal and 10 to 200 days for the 50clay/50sand seal.

Table 4-3 Gas break-through pressure and outflow rate after break-through

Clay/sand seal	**35/65**	**35/65**	**50/50**	**50/50**
Gas injection rate [ml/min]	0.02	0.2	0.02	0.2
Gas break-through pressure [MPa]	0.7	0.9	1.1	2.0
Gas outflow rate [ml/min]	$4.3 \cdot 10^{-2}$	$9.6 \cdot 10^{-2}$	$1.4 \cdot 10^{-4}$	$6.6 \cdot 10^{-3}$
Time for gas break-through [d]	35	25	340	80
Time for collecting 100 ml gas [d]	1.6	0.7	198	10.5

4.5.2.3 Total stress and swelling pressure

Figure 4-12a and 4-12b illustrate the development of radial and vertical total stress in the 35clay/65sand seal during the whole test at a water injection pressure of 1 MPa and a gas injection rate of 0.02 ml/min, while the modelled results for the 50clay/50sand seal under the same conditions are shown in Figures 4-13a and 4-13b. In case of the tests without applying external loads, the total stress σ is taken to be the sum of the swelling pressure P_s induced by expansion of clay minerals and the pore water or gas pressure P_l or P_g. Comparing the resulting total stresses with the water saturation (Figures 4-6a,b and 4-7a,b) and the pore water pressure (Figures 4-8 and 4-9), it can be seen that the total stresses increase with water saturation and pore water pressure. Figures 4-12a,b and 4-13a,b show also that the radial total stress varies in dependence of location in the seal because of the water pressure gradient and the maximum is reached at the bottom. The vertical total stress is the same in the whole seal. After reaching full saturation, the water injection pressure is adjusted to be constant for measurement of the water permeability. In this phase, the total stress

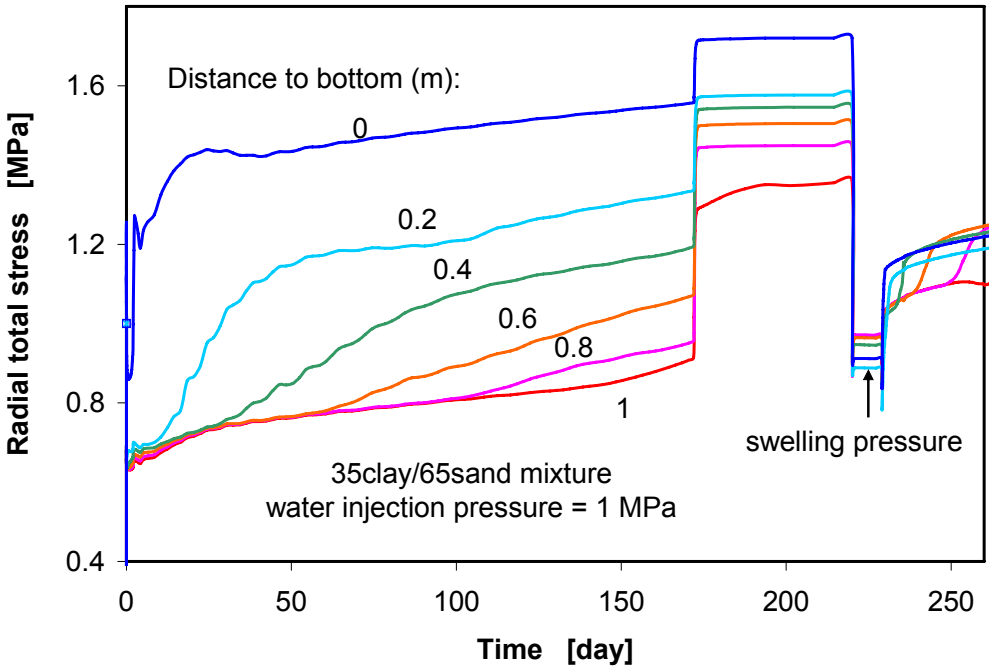

Figure 4-12a Development of radial total stress in 35clay/65sand seal at a water injection pressure of 1 MPa and a gas injection rate of 0.02 ml/min

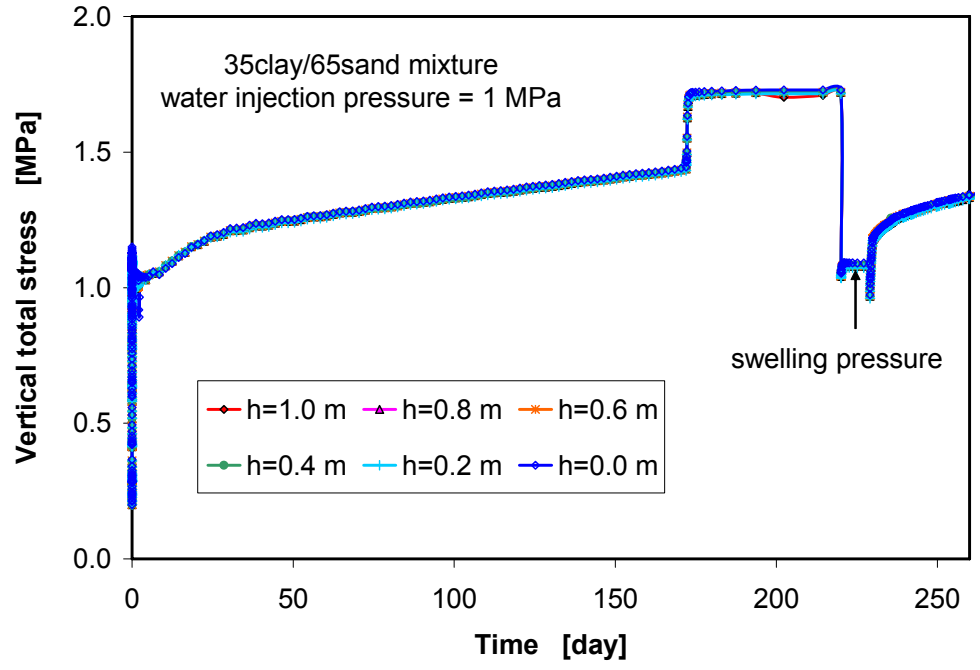

Figure 4-12b Development of vertical total stress in 35clay/65sand seal at water injection pressure of 1 MPa and gas injection rate of 0.02 ml/min

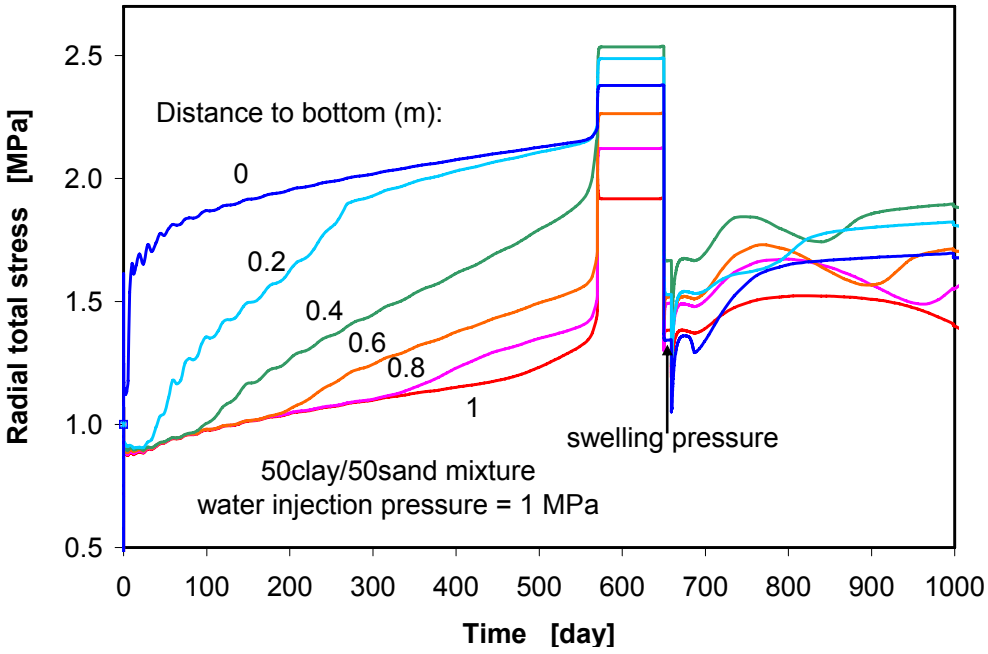

Figure 4-13a Development of radial total stress in 50clay/50sand seal at water injection pressure of 1 MPa and gas injection rate of 0.02 ml/min

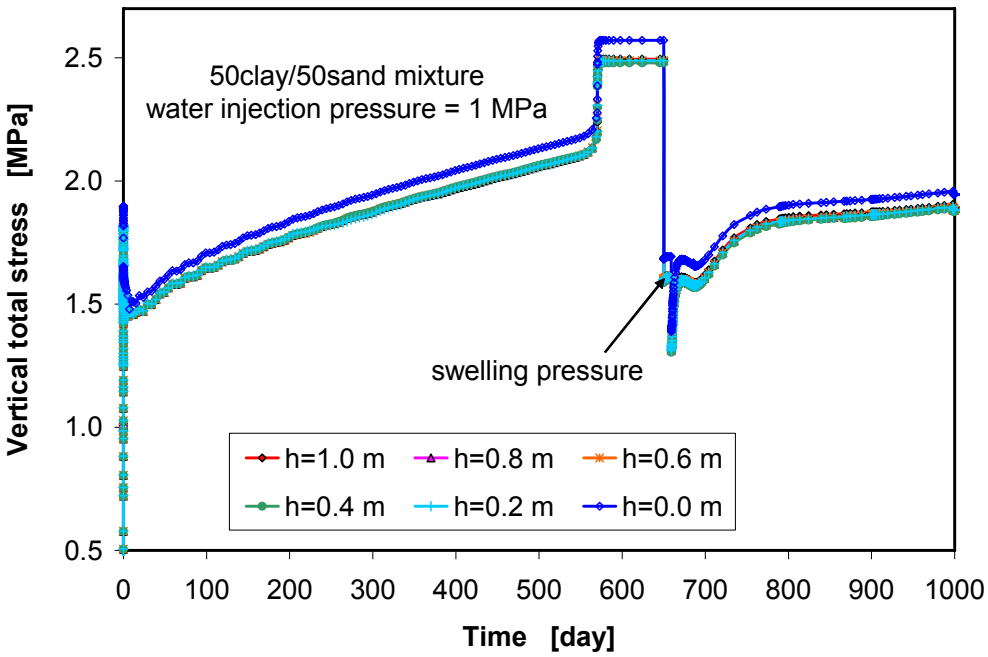

Figure 4-13b Development of vertical total stress in 50clay/50sand seal at a water injection pressure of 1 MPa and a gas injection rate of 0.02 ml/min

reaches the maximum level: $\sigma_{r\text{-}max} = \sigma_{v-max}$ = 1.6 MPa for the 35clay/65sand seal and $\sigma_{r\text{-}max} = \sigma_{v-max}$ = 2.4 MPa for the 50clay/50sand seal. At a water injection pressure of 0.5 MPa, the maximum total stress is lower: $\sigma_{r\text{-}max} = \sigma_{v-max}$ = 1.0 MPa for the 35clay/65sand seal and $\sigma_{r\text{-}max} = \sigma_{v-max}$ = 1.4 MPa for the 50clay/50sand seal.

In the third test phase, the water injection pressure is dropped down to zero to determine the pure swelling pressure, as depicted in Figures 4-12a,b and 4-13a,b. It can be seen that the resulting swelling pressure in radial direction depends on the location due to the variation of porosity, as shown in Figures 4-14 and 4-15. The water saturation results in local swelling in a region near the water inlet, causing compaction in the remaining domain. The radial swelling pressure in the 35clay/65sand seal varies in a small range of 0.8 to 0.85 MPa, whereas the radial swelling pressure in the 50clay/50sand seal lies between 1.25 and 1.55 MPa. The vertical swelling pressure is independent on the location: $P_{s\text{-}v}$ = 1.0 MPa for the 35clay/65sand seal and $P_{s\text{-}v}$ = 1.5 MPa for the 50clay/50sand seal.

The total stress does not change significantly during the gas injection. The swelling pressure may reduce due to de-saturation in this phase. Therefore, the pore gas pressure may dominate the total stress.

4.5.3 Conclusions and recommendations for the mock-up tests

Because of a lack of test data, some of the material parameters adopted are not precise and therefore the modelled results are of preliminary character. Precise parameters will be determined in further laboratory investigations and used in additional calculations, in which coupled hydro-mechanical processes in the seals including water saturation, two-phase-flow, swelling pressure etc. will be analysed and compared with the test results.

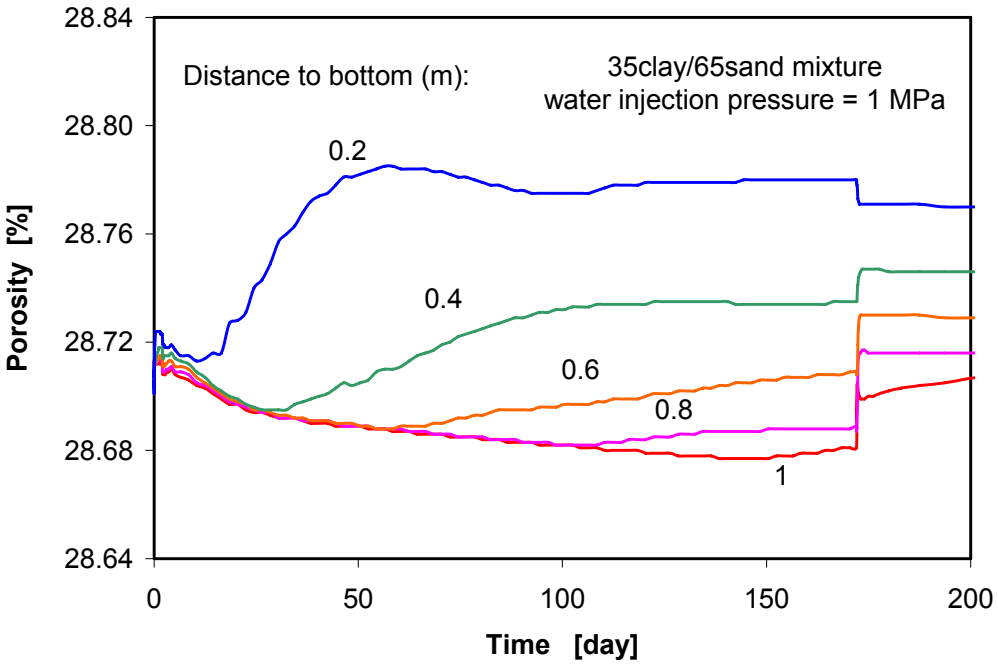

Figure 4-14 Porosity change in 35clay/65sand seal during water saturation at an injection pressure of 1 MPa

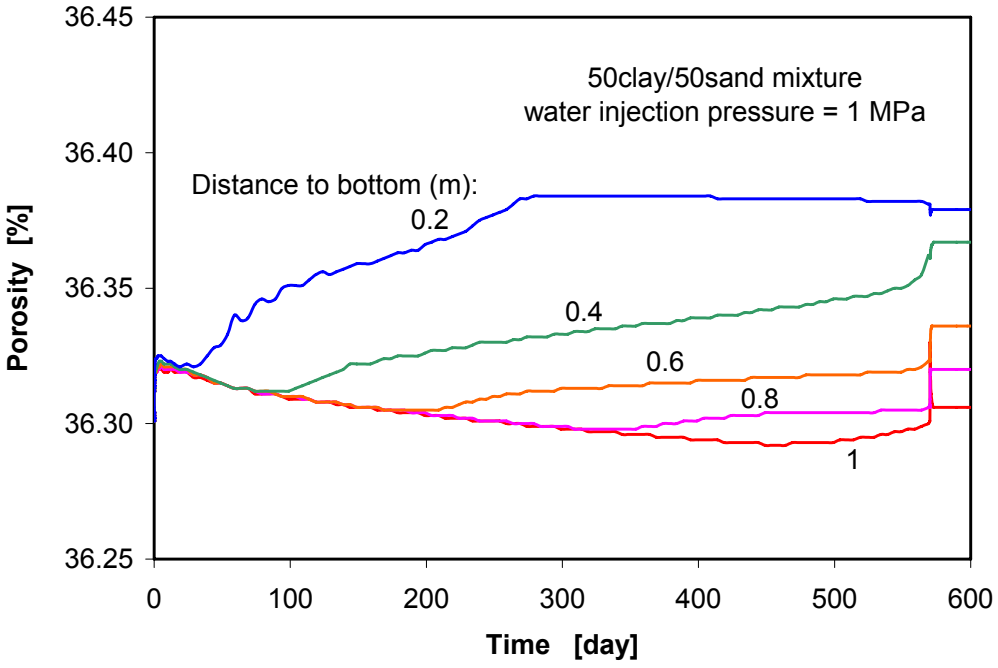

Figure 4-15 Porosity change in 50clay/50sand seal during water saturation at an injection pressure of 1 MPa

From the modelled results, the testing procedure and conditions are recommended for the mock-up tests and summarised in Table 4-4 with predictions of some important measuring parameters and testing durations. To avoid possible fracturing of the host rock during water injection to the seals in the in-situ experiment and also to minimise possible perturbations of the seal, the injection pressure shall be limited to below 1 MPa. An additional reason for the low injection pressures is that the groundwater pressure acting on seals in the clay formations during the saturation phase may be very low. To investigate the effect of the water injection pressure on the saturation time, water injection pressures of 0.5 and 1 MPa shall be applied in the mock-up tests. The modelled swelling pressures of 0.5 to 1.5 MPa are overestimated for both clay/sand mixtures in comparison with the preliminary test results of 0.2 to 0.5 MPa. Therefore, the total stress of 2.4 MPa calculated for test 4 with 50clay/50sand mixture may be lower in reality. In test 2 on the 50clay/50sand seal, the high gas injection rate of 0.2 ml/min may cause a high gas break-through pressure of 2 MPa. Under consideration of the maximum permitted pressure of 1.6 MPa for the steel tube, it is strongly recommended that the water injection pressure, the build-up of gas pressure and the total stress on the tube wall must be monitored and controlled to maintain it below the allowable limits of the testing system during the whole test procedure. The prediction suggests that the tests with the 35clay/65sand mixture may be finished within 1 year, and the conduction of the tests with 50clay/50sand mixture may need about 3 years. For instance, to reduce the testing duration of the 50clay/50sand mixture, it is recommended to reduce the seal length to 0.5 m. In this case, all the tests may be finished within 2 years.

Table 4-4 Prediction of the mock-up tests

Mock-up test	Test 1	Test 2	Test 3	Test 4
Tube type	Type 1	Type1	Type 2	Type 2
Clay/sand mixture	35/65	50/50	35/65	50/50
Phase 1: Water saturation of the unsaturated seals				
Water injection pressure [MPa]	0.5	0.5	1.0	1.0
Saturation time [day]	240	700	170	570
Phase 2: Water through the saturated seals				
Water injection pressure [MPa]	0.5	0.5	1.0	1.0
Maximum total stress [MPa]	1.0	1.4	1.6	2.4
Water outflow rate [ml/min]	$1.5 \cdot 10^{-4}$	$4.5 \cdot 10^{-5}$	$2.9 \cdot 10^{-4}$	$9.0 \cdot 10^{-5}$
Time for 10 ml water [day]	50	160	25	80
Phase 3: Determination of swelling pressure				
Water injection pressure [MPa]	0.0	0.0	0.0	0.0
Swelling pressure [MPa]	0.7-0.9	0.5-1.2	0.8-1.0	1.2-1.5
Time [day]	15	15	15	15
Phase 4: Gas injection through the saturated seal				
Gas injection rate [ml/min]	0.2	0.2	0.02	0.02
Break-through pressure [MPa]	0.9	2.0	0.7	1.1
Gas outflow rate [ml/min]	$9.6 \cdot 10^{-2}$	$6.6 \cdot 10^{-3}$	$4.3 \cdot 10^{-2}$	$1.4 \cdot 10^{-4}$
Time until gas break [day]	25	80	35	340
Total testing time [day]	330	955	245	1005

5 In-situ Experiment at Mont Terri

This work package will be conducted in a specially excavated niche at the MTRL. In up to four boreholes drilled and instrumented sequentially, the sealing materials pre-tested in the laboratory will be tested again and their functioning demonstrated under in-situ conditions. After seal installation, measurements to test and determine the gas and water permeability, the gas break-through pressure in the saturated stage and the two-phase parameters in interaction with the surrounding rock will be performed. The principles of test design were already described in section 1.3. In the following, information is presented with regard to the test procedures envisaged so far:

5.1 Test procedure

The experiments will be conducted in five stages:

- Installation and instrumentation of the test boreholes,
- determination of the initial installation density of the seal,
- water injection to simulate the groundwater flow to the seals,
- gas injection to simulate the gas generation in the boreholes,
- post-test investigations for determination of the achieved final properties of the seals.

During the test stages, the following hydro-mechanical parameters of the sealing system will be measured or adjusted, respectively: gas and water flow rate and accumulated volume, gas and water injection pressure, permeability to gas and water, gas break-through pressure, and swelling pressure of the seals.

All actions necessary to prepare and operate the tests are given in detail in the following paragraphs:

- Preparation of the in-situ test field: A suitable test location will be selected in co-operation with interested project partners. A test room of 5 m width, 4 m height and 8 m length will be excavated in the MTRL. During the excavation a number

of rock samples will be taken from the test field for the accompanying surface laboratory programme. Careful geological mapping and chemical-mineralogical characterization of the surrounding rock in the test field is foreseen.

- **Drilling of the Boreholes:** A first phase will be started with operating two boreholes to examine the applicability of installation and measuring techniques which have been tested in preceding mock-up tests in the GRS laboratory (see section 5). If necessary, the techniques will be improved. In a second phase, the remaining boreholes (two or four) will be equipped by using the improved installation techniques.

- **Installation and instrumentation of the boreholes:** Immediately after drilling of the boreholes, the lower porous injection chamber, the sealing material, the upper porous collection chamber, and the packer will be installed by using the techniques tested and eventually improved. On the basis of measured material masses and volumes the initial properties of the testing components will be determined: **clay/sand ratio, bulk density, water content, porosity**. All the test equipments, instruments, and measuring systems will be tested and calibrated during the mock-up tests in advance to the in-situ experiments.

- **First gas injection:** At the beginning, dry nitrogen gas will be injected via the injection tube inserted into the lower injection chamber. The injection pressure will be adjusted to below 0.1 MPa to avoid a possible flow of fine clay grains out of the seal. The amount of the gas inflow and outflow will be monitored at the inlet and the outlet of the seal. Comparing the inflow and outflow makes it possible to examine if gas is lost into the surrounding rock. Once steady state flow is achieved, the **gas permeability** of the seal representing the upper limit of the sealing properties will be determined.

- **First water injection:** After installation, the seal in a repository will take up water from the host rock until full-saturation is reached. In contrast to this, the surrounding rock may be firstly desaturated due to insufficient water supply from the far region and then resaturated in a longer period of time. To accelerate the saturation process in the envisaged experiments, the seal at Mt. Terri will be flooded with synthetic Opalinus clay solution from (both the upper and) the lower porous chambers. The external water pressure will be adjusted to below 1 MPa. The amount of injected water and the pressure in both porous volumes will be monitored. Since the water content as well as the water saturation will not be measured in situ, it will be estimated by comparing the in-situ data to well known

laboratory data and modelled results. Under the applied pressure gradient, full-saturation of the seal can be expected. At steady state flow, the **water permeability** of the sealing-system will be measured.

- **Second gas injection:** After saturation of the sealing-system, nitrogen gas will be injected again into the lower porous volume to determine the gas break-through pressure of the saturated seal system. After gas break-through, the effective gas permeability will be measured. To determine the two-phase flow parameters of the seal as a function of saturation, the injection pressure is increased stepwise in defined increments. At each pressure step, the effective permeability to gas is measured as a function of saturation.

- **Second water injection:** After the second gas injection, the Opalinus clay solution will be injected again from the lower porous chamber to measure the **water permeability after the gas break-through**. Comparing the value to that obtained in the first water injection phase, the **resealing effectiveness** of the system can be evaluated.

- **Post-test investigations:** After termination of the last phase, representative samples will be drilled from the seal and the surrounding rock for post investigations on the achieved in-situ state (density, porosity, water content…). The data can be used for analyses of the in-situ measurements and for calibration of the modelling parameters.

The test duration is strongly determined by the saturation phase which has preliminarily been estimated in the scoping calculations (section 5.2.2.2). The duration of each borehole-sealing test shall be limited to less than one year. If necessary, the testing parameters such as clay/sand ratio, water injection pressure, and even the length of the seals have to be readjusted.

5.2 Scoping calculations for the in-situ tests

As explained previously, scoping calculations were necessary to gain a first estimation of initial and boundary conditions, water and gas injection pressures as well as duration of the SB experiment. Due to excavation and ventilation of the SB niche, the hydro-mechanical state of the surrounding rock will be disturbed. Additionally, there may be also hydro-mechanical interactions between the boreholes drilled down from the floor of the SB niche (Figures 1-1, 1-2). During injection of water and gas to the seals,

coupled hydro-mechanical processes will not only occur in the seals but also in the surrounding rock. Considering the problems to be solved, coupled THM calculations have been performed by solving a set of balance equations of energy, water mass, air mass and momentum for prediction of the in-situ tests. The theoretical considerations and constitutive models used were already presented in section 3.

5.2.1 Numerical model

Regarding the envisaged layout of the boreholes in the SB niche, a 2D plane strain model in a plane normal to the axis of the SB niche was adopted by axisymmetric geometry. The modelling region extends by 40 m x 40 m. The lower and upper boundary are located at distances of -20 m and +20 m from the niche floor, respectively. In the model the SB niche is 2.5 m wide and 5 m high. A test borehole of 300 mm in diameter is drilled from the niche floor down to 3 m depth. The borehole axis is located 1 m distant to the niche wall. The borehole is filled sequentially from the bottom with sand representing the injection chamber of 0.3 m height, one of the selected clay/sand mixtures as seal of 1 m height, one sintered filter of 10 mm thickness, one packer of 1 m height and concrete of 0.7 m to seal the upper part of the borehole. Figures 5-1 shows the finite element mesh, the boundary conditions and the different materials installed in the borehole in detail.

In the model, the materials were assumed homogeneous and isotropic. Both clay/sand mixtures with clay contents of 35 % and 50 % were considered in the calculations. The average properties and parameters of the materials given in Table 3-1, 3-2 and 3-3b were adopted. Because of a lack of data for the injection chamber, packer and concrete, the properties and mechanical parameters of the clay rock were assumed for them. A high permeability of 10^{-12} m^2 was applied to the injection chamber, while the packer was assumed impermeable. Such simplifications are considered acceptable for the purpose of the scoping calculations focusing on hydro-mechanical processes in the seal and surrounding rock.

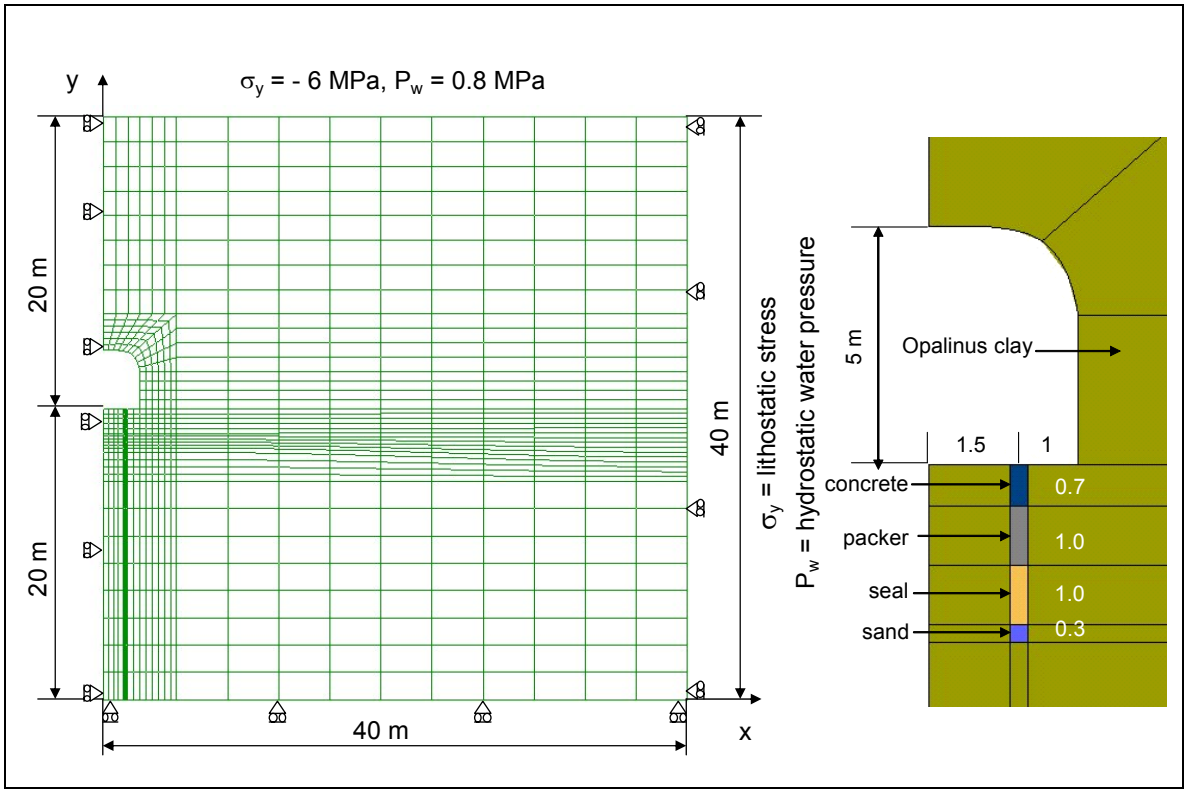

Figure 5-1 Numerical model and materials considered in scoping calculations

In the calculations, the prevailing in-situ conditions at the MTRL were taken into account. The temperature in the rock and in the niche is 17 °C for the initial state. A vertical total stress of 6 MPa applied on the top boundary and the gravity effect result in an initial vertical total stress equal to 6.48 MPa at the level of the niche floor (y = 0). Assumption of the ratio K_o = 0.77 of effective horizontal stress ($\sigma'_x = \sigma_x - P_w$) to vertical stress ($\sigma'_y = \sigma_y - P_w$) leads to an initial total horizontal stress of 5.2 MPa at the floor level. A water pressure of 0.8 MPa supplied to the top boundary and its hydrostatic distribution in the modelling region result in an initial pore water pressure of 1.0 MPa at the floor level. The atmospheric pressure of 0.1 MPa was taken as the initial gas pressure. Flow of water and gas through the other boundaries is not allowed.

According to the envisaged test procedure mentioned in section 5.1, the following steps were simulated by applying suitable conditions:

Step 1: Excavation and ventilation of the SB niche for 180 days to estimate hydro-mechanical state in the surrounding rock, by applying (1) null supporting stress on the niche wall to simulate the niche excavation, and (2) gas flowing

along the niche wall with relative humidity of 85 % (gas density ρ_g = 1.194 kg/m^3, vapour mass fraction ω_g^w =1.005 %) and the turbulence coefficient of 10^{-4} m/s to simulate the niche ventilation.

Step 2: Drilling and ventilation of the SB borehole for 8 days to examine changes of the hydro-mechanical state in the surrounding rock, by applying (1) null supporting stress on the borehole wall to simulate the drilling, and (2) gas flowing along the borehole with relative humidity of 85 % to simulate the ventilation.

Step 3: Installation of the sand, seal, packer and concrete into the SB borehole for 2 days by applying an initial stress of σ_{1o} = σ_{2o} = σ_{3o} = 0.1 MPa to them to represent the compaction effect on the materials.

Step 4: Water injection into the initially unsaturated seal to determine the evolution of saturation and the time needed for full saturation by applying a constant water pressure of 0.5 or 1 MPa to the lower porous chamber.

Step 5: Gas injection into the saturated seal to determine its gas break-through pressure and gas outflow by applying a constant gas injection rate of 0.2 ml/min to the lower porous chamber.

5.2.2 Modelling results

5.2.2.1 Perturbations in the clay rock induced by excavation and ventilation

Mechanical aspect

After the niche excavation, the horizontal stress relaxes in a zone around the niche whereas the vertical stress concentrates in a zone near the niche wall. Figure 5-2 shows the distributions of the horizontal and vertical stresses 180 days after excavation. The redistribution of the stresses causes convergence of the niche. The radial displacement of the wall reaches 7.5 mm, while the roof drops down by 6.7 mm and the floor rises up by 7.1 mm, as shown in Figure 5-3. The envisaged location of the borehole seems to be less disturbed before drilling.

Six months later after the niche excavation, a borehole is drilled from the niche floor down to 3 m depth. The borehole excavation results in an additional perturbation of the mechanical state in the surrounding rock. Figure 5-4 shows the stress distributions 8 days after drilling, whereas the displacement of the rock is illustrated in Figure 5-5. The borehole drilling generates a relaxation of the radial stress around the borehole and contrastively a concentration of the vertical stress at the corner of the borehole bottom. The resulting convergence of the borehole reaches about 10 mm. It should be noticed that the modelled convergence of the borehole may be overestimated because the borehole is modelled as an infinite cut along the niche axis (Figure 5-1) and hence the support effect of the surrounding rock is eliminated in the calculations. This is not a very realistic case.

Hydraulic aspect

The hydraulic response of the rock mass to excavation and ventilation of the niche and borehole is shown in Figure 5-6. Just after the niche excavation, the porosities in the zones over the roof and under the floor of the niche expand somewhat due to the stress relaxation (Figures 5-2, 5-3). This induces a sudden reduction of the pore water pressure even to a negative value (suction) of –1 MPa. In contrast to this, the highly concentrated stress near the lower corner compresses the material and hence generates a high pore water pressure up to 6 MPa, which is close to the minor principal component of the stress. During the ventilation with a relative air humidity of 85 %, the pore water pressure reduces steadily. Six months later, the zone with negative pore water pressure extends to about 1 m from the niche wall into the rock mass. The borehole drilling induces an additional dilatancy of the surrounding rock and hence a higher reduction of the pore water pressure.

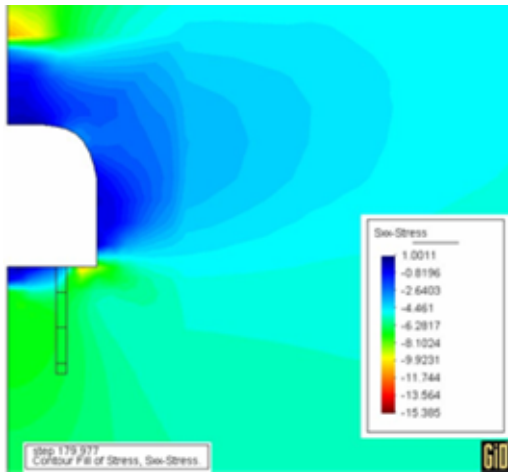

a: horizontal total stress

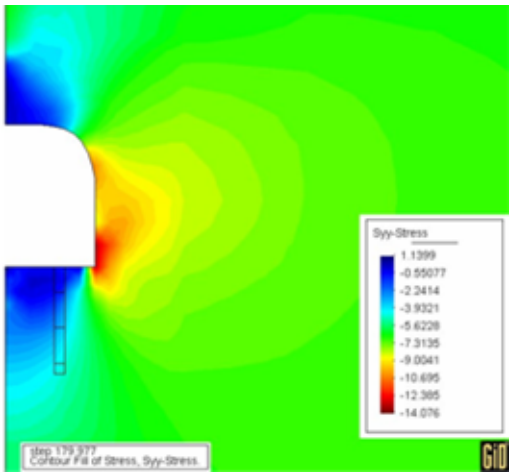

b: vertical total stress

Figure 5-2 Distributions of total stresses 180 days after excavation of the SB niche

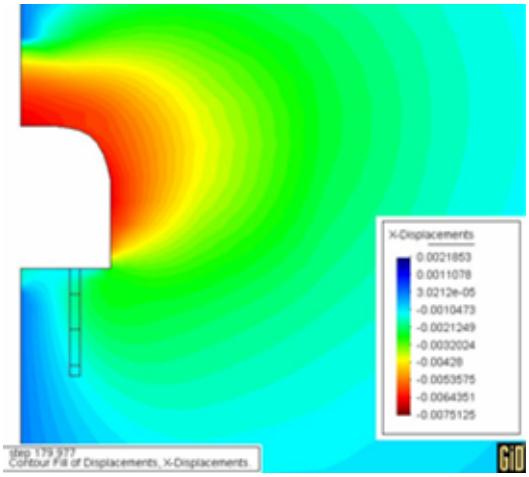

a: horizontal displacement

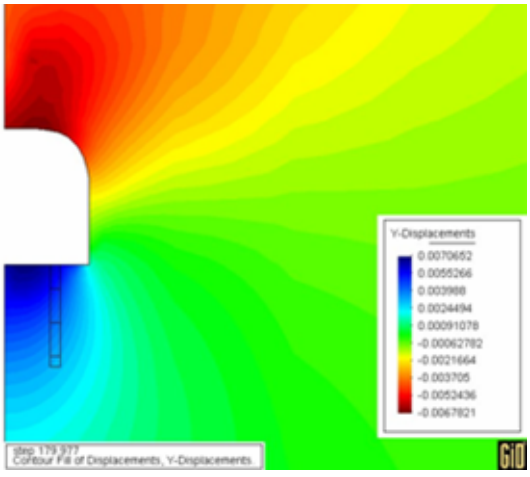

b: vertical displacement

Figure 5-3 Distributions of displacements 180 days after excavation of the SB niche

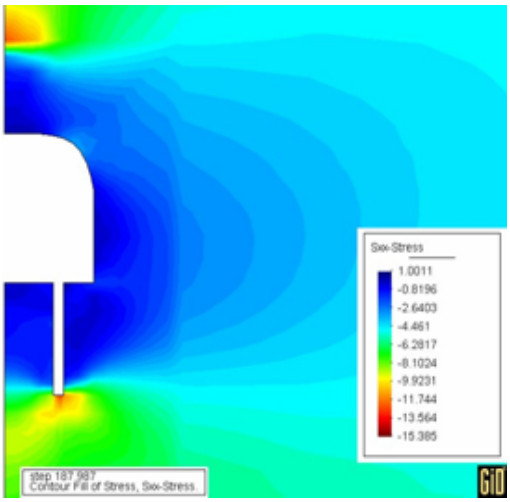

a: horizontal total stress

b: vertical total stress

Figure 5-4 Distributions of total stresses 8 days after drilling of SB borehole

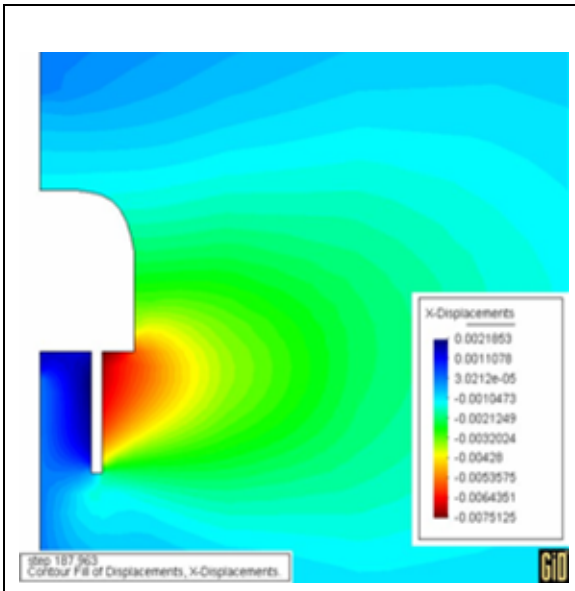

a: horizontal displacement

b: vertical displacement

Figure 5-5 Distributions of displacements 8 days after drilling of the SB borehole

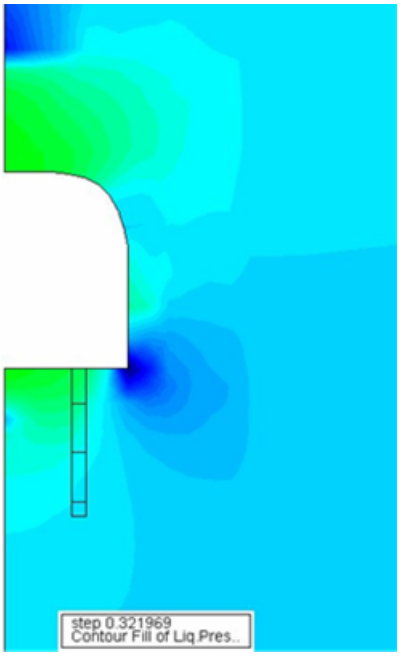

a: just after niche excavation

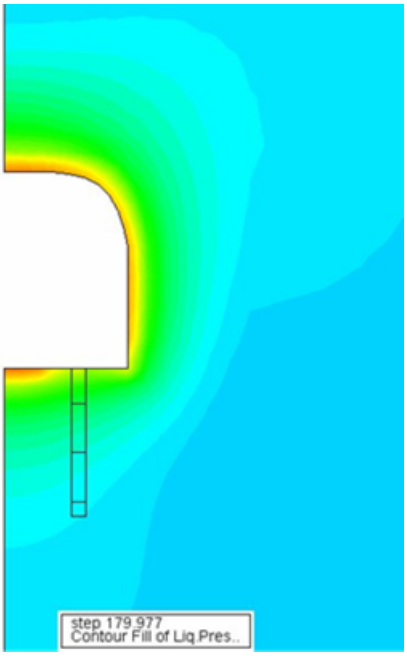

b: 180 days after niche excavation

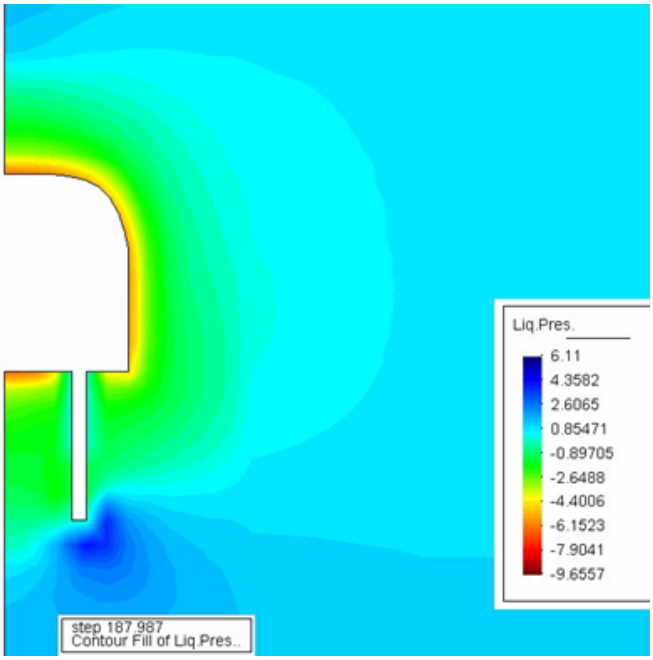

c: 8 days after borehole drilling

Figure 5-6 Redistribution of pore water pressure in the surrounding rock induced by excavation and ventilation of SB niche and borehole

Due to excavation and ventilation of the niche and borehole, the surrounding rock is de-saturated. Figure 5-7 shows the distribution of water saturation in the surrounding rock at the end of the borehole drilling and ventilation. The de-saturated zone with water saturation less than 95 % is limited in 0.5 m to the niche wall. The de-saturation which is mainly caused by the dilatancy of the clay rock is not significant.

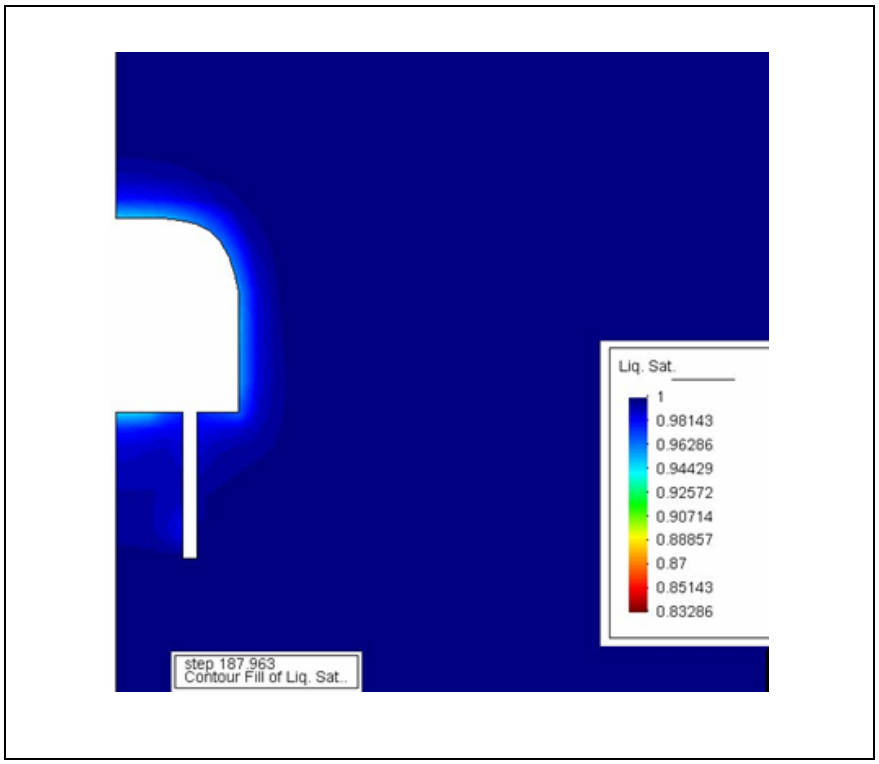

Figure 5-7 Distribution of water saturation in the surrounding rock

5.2.2.2 Water saturation and flow

After the installation of the seal into the borehole, the water injection phase was simulated by applying a water pressure of 0.5 or 1 MPa to the lower porous chamber. Figure 5-8 and 5-9 illustrate the evolution of water saturation at some selected points in both 35clay/65sand and 50clay/50sand seals at an injection pressure of 1 MPa. The seals are saturated from the bottom to the top. The time needed for full saturation at 1 MPa injection pressure is about 10 months for 35clay/65sand mixture and 28 months for 50clay/50sand mixture, which are longer than the saturation times of 6 and 19 months in the envisaged mock-up tests (section 4.5.2.1). When a lower water injection pressure of 0.5 MPa is applied, the saturation phase in the in-situ experiment will then last longer in about 13 and 35 months for 35clay/65sand and 50clay/50sand

seals respectively. Because the permeabilities of the seals are higher than that of the surrounding clay rock (EDZ was not simulated here), the water flow occurs mainly through the seal as shown in Figure 5-10, in which the pattern of the water flow through the 35clay/65sand seal and the surrounding rock is illustrated.

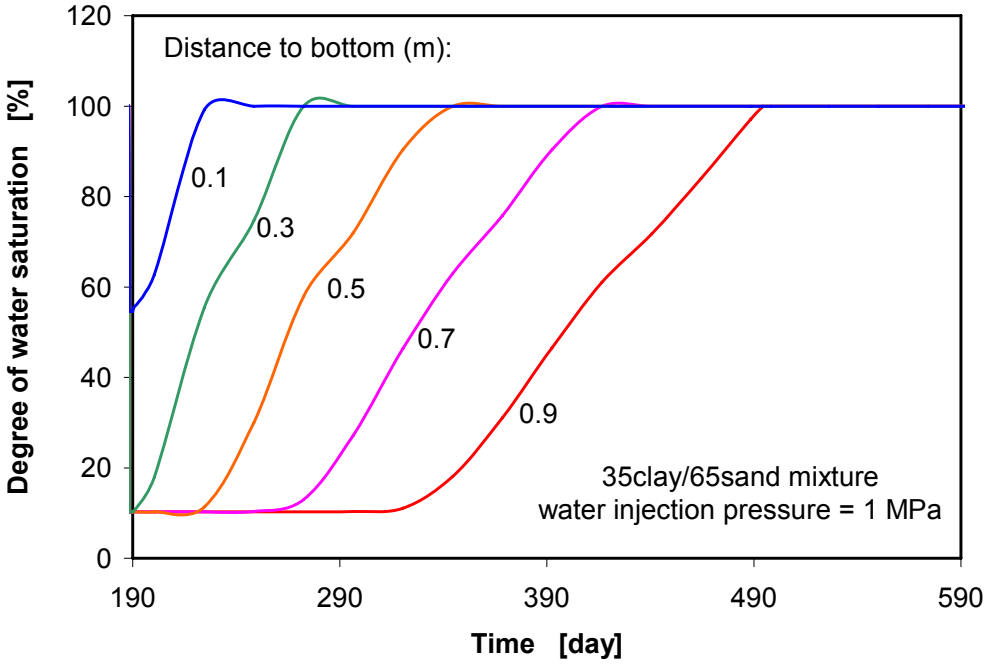

Figure 5-8 Evolution of water saturation in 35clay/65sand seal at an injection pressure of 1 MPa

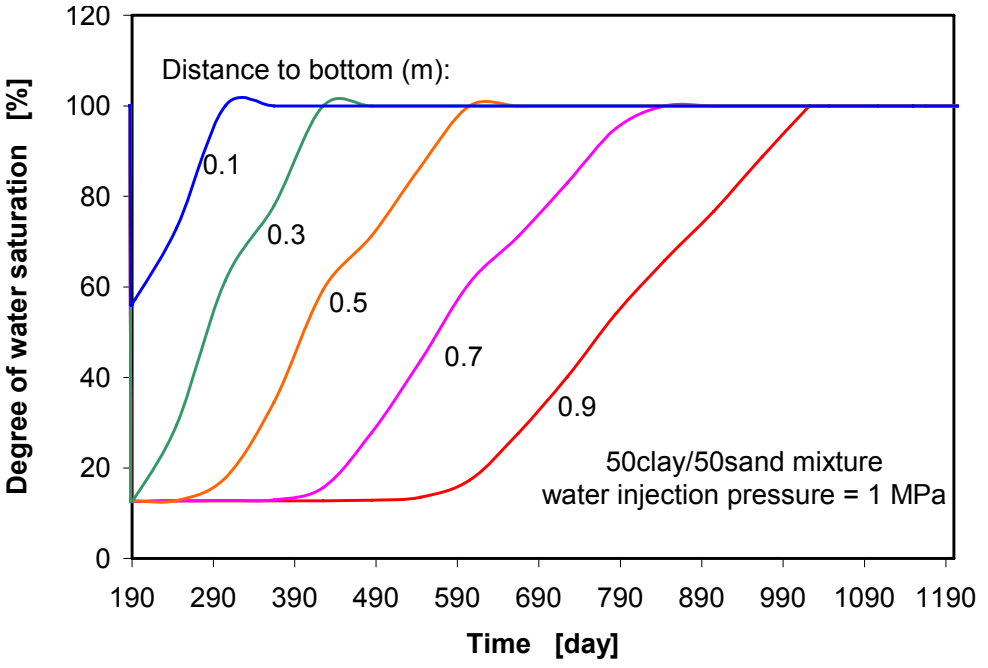

Figure 5-9 Evolution of water saturation in 50clay/50sand seal at an injection pressure of 1 MPa

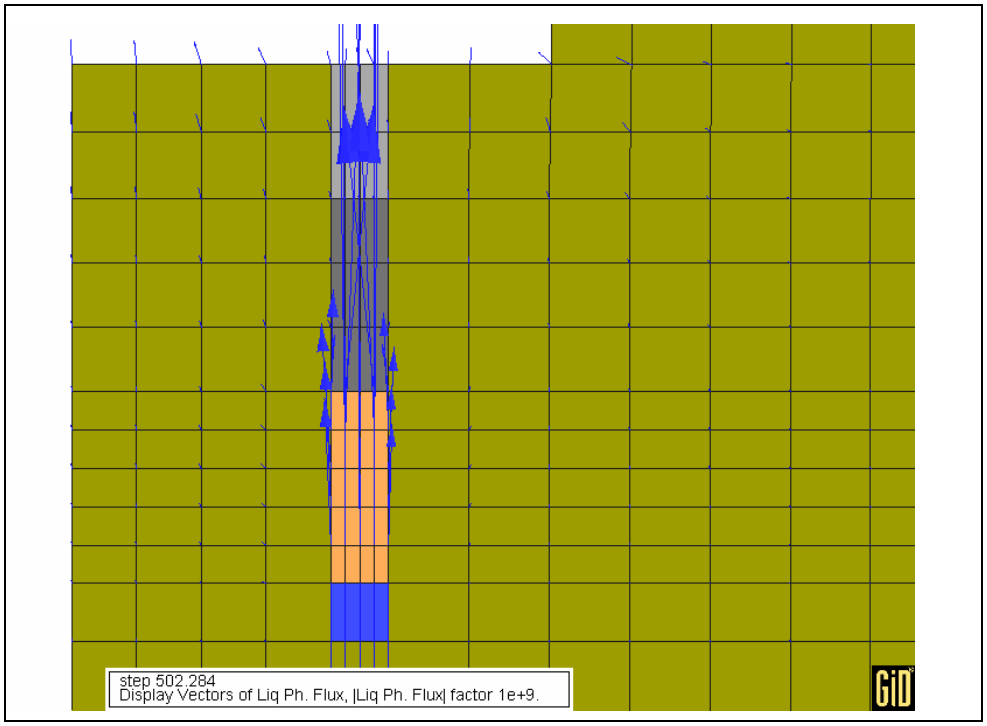

Figure 5-10 Water flow through the rock-seal system (35clay/65sand mixture)

After reaching steady flow state, water outflow rate and time needed for collecting a water volume of 10 ml were predicted for both clay/sand seals at the different injection pressures. The results are summarised in Table 5-1.

Table 5-1 Modelling results for the water injection phase in the in-situ experiment

Clay/sand seal	**35/65**	**35/65**	**50/50**	**50/50**
Water injection pressure [MPa]	0.5	1.0	0.5	1.0
Water outflow after saturation [ml/min]	$4.5 \cdot 10^{-5}$	$9.4 \cdot 10^{-5}$	$1.3 \cdot 10^{-5}$	$6.6 \cdot 10^{-3}$
Time for full saturation [d]	400	300	830	1050
Time for collecting 10 ml water [d]	150	75	530	230
Total time for water injection phase [d]	550	375	1260	1280

5.2.2.3 Gas break-through pressure and flow

Gas injection into the saturated seals was simulated by applying a constant gas inflow rate of 0.2 ml/min to the lower porous chamber. Figure 5-11 and 5-12 show the evolution of the gas pressure at the entry face and the gas outflow rate at the outlet face of the 35clay/65sand and 50clay/50sand seals. With continuous gas injection, the gas pressure at the entry face builds up until a gas break-through occurs. After the

peak point, the gas pressure reduces somewhat and the gas outflow increases further up to a maximum and remains relatively constant. However, for the 50clay/50sand seal the gas break-through occurs later after the peak gas pressure. Generally, the pattern of the computed gas pressure is similar as the laboratory observation on the clay/sand mixtures presented in section 2.3.2. But the significant peak behaviour of the gas outflow observed in the tests is not well represented in the calculations. The calculated gas break-through pressure is about 0.7 MPa for the 35clay/65sand seal and 1.6 MPa for the 50clay/50sand seal at the gas inflow rate of 0.2 ml/min. The time to the gas break-through is about 5 days for the 35clay/65sand seal and 30 days for the 50clay/50sand seal.

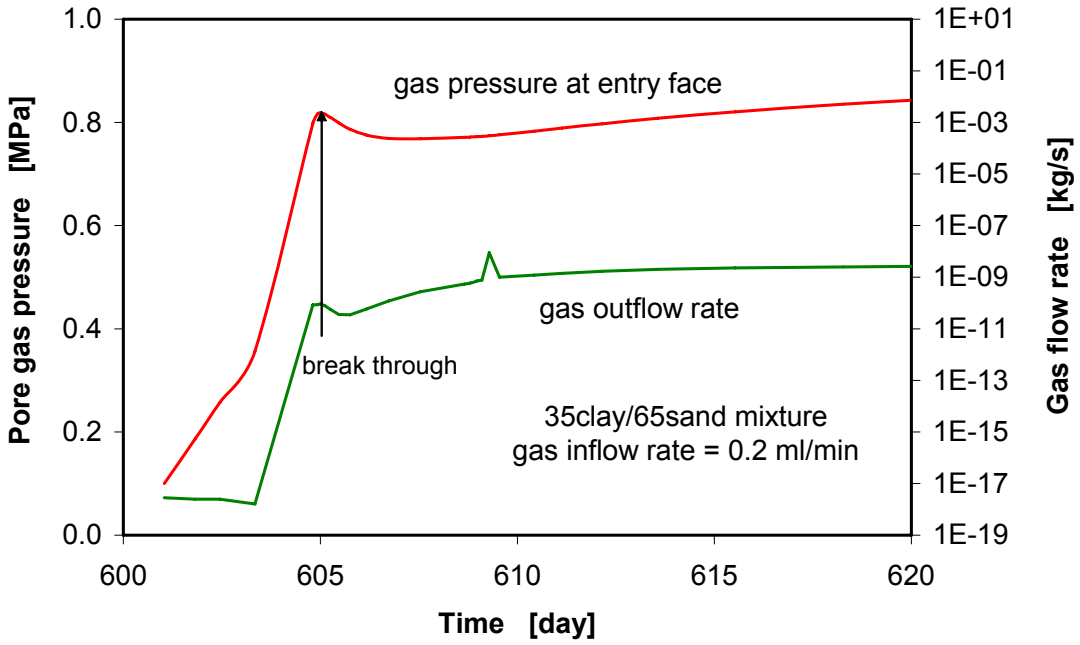

Figure 5-11 Evolution of gas pressure at the entry face and gas outflow rate of 35clay/65sand seal

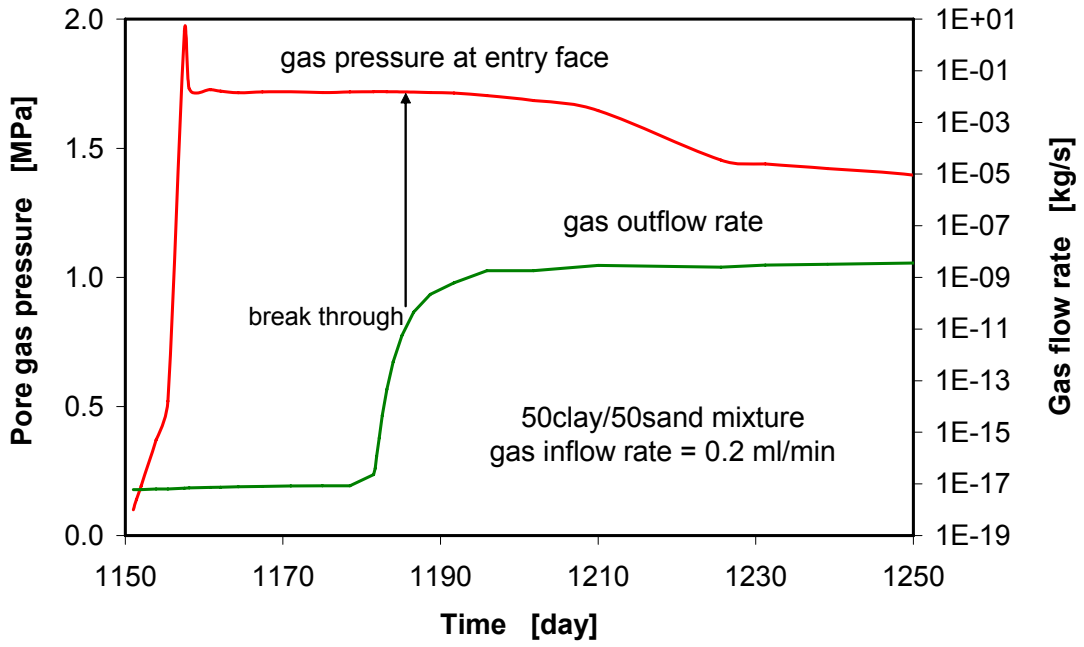

Figure 5-12 Evolution of gas pressure at the entry face and gas outflow rate of 50clay/50sand seal

Figure 5-13 indicates that the gas migration occurs mainly through the saturated seals, not or very limited through the surrounding rock.

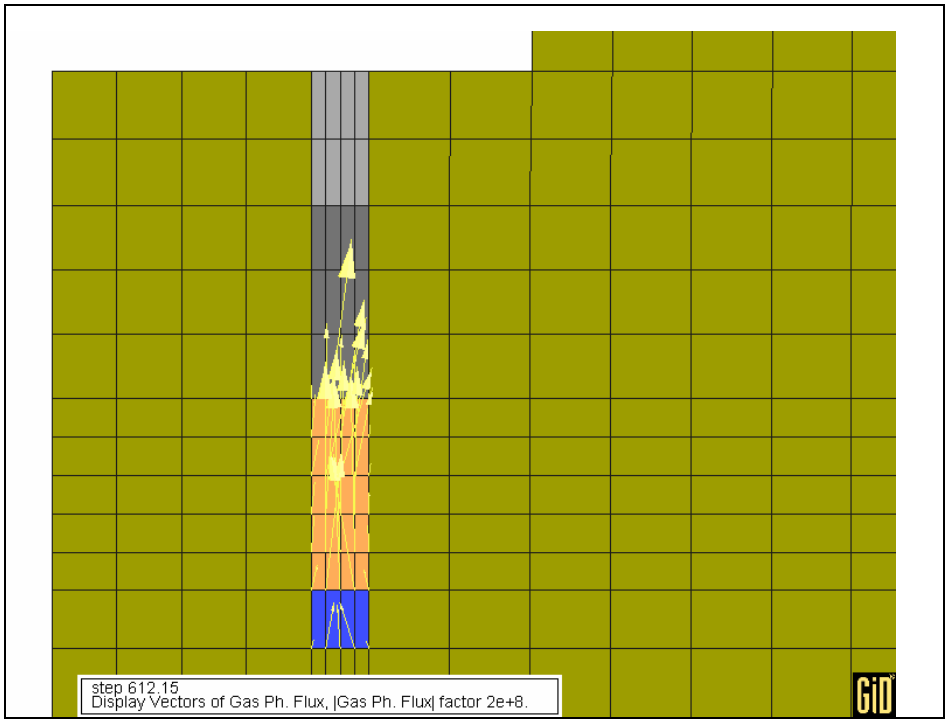

Figure 5-13 Gas migration through the rock-seal system (35clay/65sand mixture)

5.2.2.4 Total stress and porosity

Figures 5-14 shows the evolution of total stresses and porosity near the bottom boundary of the 35clay/65sand seal during the water injection at 1 MPa pressure, whereas the modelling results for the 50clay/50sand seal are illustrated in Figures 4-15. From the figures it can generally be seen that (a) the horizontal and vertical stresses increase due to a coupling effect of the applied water injection pressure, the resulting swelling pressures of the seals and also the clay rock and (b) the porosity increases first with water saturation, then decreases with compaction caused by swelling of other parts of the seal and the surrounding rock, and finally remains relatively constant. It should be noted that the periodical changes of the stresses may be caused by application of unsuitable values of error tolerances to achieve a calculation convergence for the very complete modelling steps.

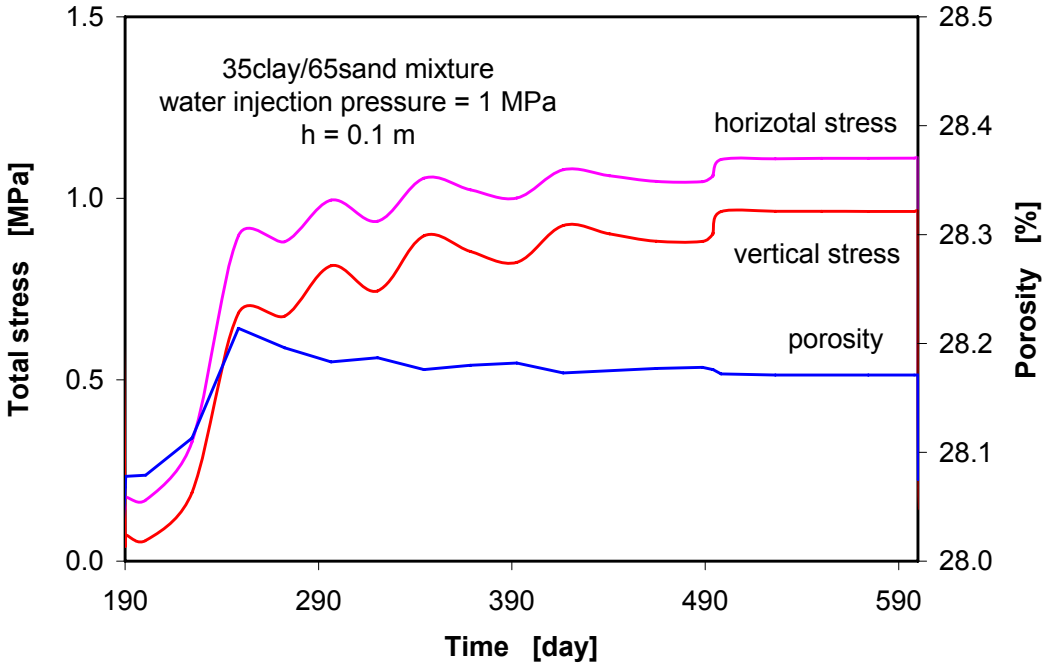

Figure 5-14 Evolution of total stresses and porosity near the bottom and top of 35clay/65sand seal

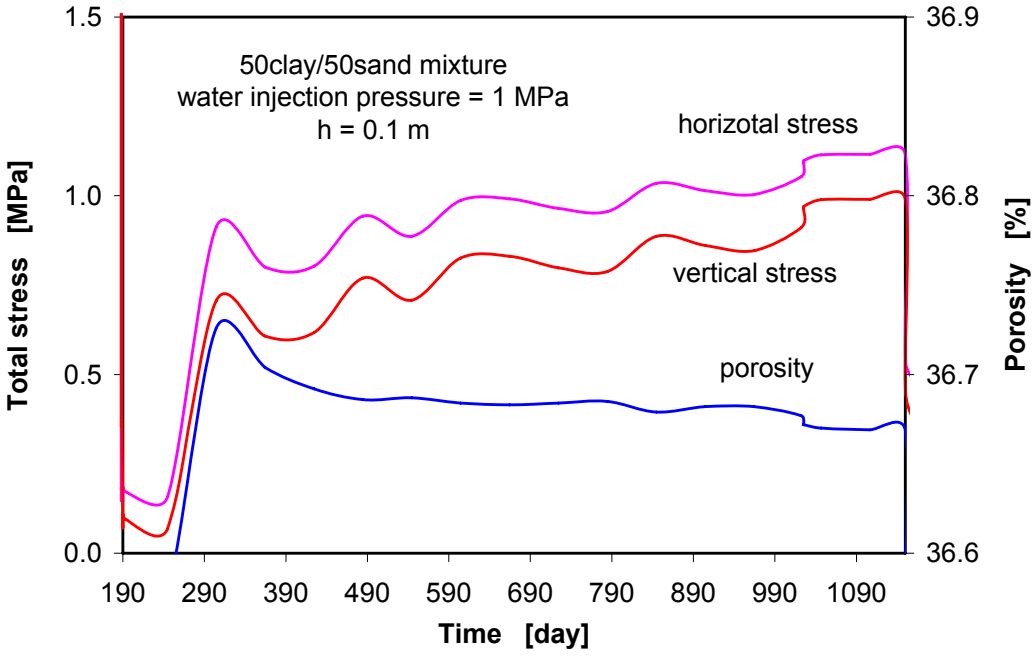

Figure 5-15 Evolution of total stresses and porosity near the bottom and top of 50clay/50sand seal

5.2.3 Conclusions and recommendations for the in-situ experiment

From the scoping calculations the following conclusions and recommendations for the in-situ experiment can be drawn:

- The hydro-mechanical state of the clay rock is disturbed by the excavation and ventilation of the SB niche. Because any material damage process can not yet be modelled with the current version of CODE-BRIGHT, the development of the excavation disturbed zone (EDZ) around the niche and its impact on the hydraulic conductivity can not be identified from the modelling results. On the basis of in-situ observations in the MTRL /BOS 02/, the extension of the EDZ consisting of an air-filled fracture network around the SB niche is probably limited in 1 m and a plastically deformed outer zone in 2 m. This leads to a maximum ratio of the EDZ extension to the drift radius up to 1. The permeability of the EDZ in the MTRL was measured between 10^{-14} and 10^{-17} m^2. The scoping calculations indicated that the desaturated zone with negative pore water pressure extends to about 1 m from the niche wall into the rock mass. To install the clay/sand seals in an undisturbed or less disturbed zone, the boreholes must be drilled down beyond the EDZ. And therefore, the borehole depth of 3 m is suitable.

- The altered hydro-mechanical state after niche excavation is further disturbed by sequentially drilling of the boreholes. Because the boreholes have a smaller diameter of 0.3 m, an EDZ around a borehole can be expected also to be small up to a maximum of 0.3 m. The calculations suggested additionally that the desaturation in the surrounding rock due to the dilatancy of the pores during the borehole drilling is not significant. From the above conclusions, the distance between boreholes shall be larger than about 0.6 m. Therefore, the borehole distance of more than 3 m between the test boreholes in the SB test niche (Figure 1-1) is sufficient.

- The water saturation of the clay/sand seals takes about 1 to 3.5 years for the water injection pressures of 0.5 to 1 MPa. After full saturation, the total stress reaches a maximum of about 1.2 MPa near the bottom. The gas injection with a constant inflow rate of 0.2 ml/min generates a gas break-through pressure of about 0.7 MPa for the 35clay/65sand seal and 1.6 MPa for the 50clay/50sand seal. The gas injection lasts for several weeks to one month. To avoid the high gas pressure of 1.6 MPa, a lower gas inflow rate of 0.02 ml/min, for instance, shall be applied to the 50clay/50sand seal, but the test will then be longer. The total testing time for the 50clay/50sand mixture by applying the above mentioned testing conditions is beyond the time of about 2.5 years which is available for the in-situ experiment within the ESDRED project. Therefore, in the case the 50clay/50sand mixture will be used, the seal shall be reduced to 0.5 m. In that case, the in-situ experiments with both clay/sand mixtures can be finished within the planned testing time of 2.5 years.

6 Summary and conclusions

The GRS-project "Self-sealing Barriers of Clay/Mineral-Mixtures (SB)" represents a continuation of earlier laboratory investigations executed to study the suitability of optimised clay/mineral mixtures as sealing materials in underground repositories for radioactive wastes.

Optimised clay/mineral mixtures exhibit a high gas permeability in the unsaturated state allowing gases generated in disposal rooms to migrate out of the repository. Even after water uptake from the host rock these materials exhibit a comparably low break-through pressure to gas and thus, high gas pressures will not build-up in the repository, neither in the unsaturated nor in the saturated state. On the contrary, after water uptake and swelling of the clay minerals, the permeability to water reduces to very low values and hence, migration of leached radio-nuclides out of the disposal areas is almost impossible.

Based on promising results of the Kenton project /MIE 03/ it is intended to scrutinize the functioning of selected material mixtures in the Mont Terri Rock Laboratory under realistic in-situ conditions.

The SB project has been subdivided in two phases, a pre-project running from January 2003 until June 2004 under contract No. 02E9713 with PtWT+E and the main project running from January 2004 until December 2008 as a cost shared action of PtWT+E (contract No. 02E9894) and the European Commission (contract No. FI6W-CT-2004-508851). This cost shared part of the SB project is also part of the EC Integrated Project ESDRED (Engineering Studies and Demonstrations of Repository Designs).

The main objectives of the pre-project were:

- to conduct preceding laboratory investigations for the final selection of suited material mixtures,
- the develop of a test plan for the envisaged in-situ experiments at the Mont Terri Rock Laboratory (MTL) in Switzerland,
- the preparation of mock-up tests to be performed in advance to the in-situ experiments in the geotechnical laboratory of GRS in Braunschweig, and

- scoping calculations with regard to the assessment of measurement ranges to be expected as well as analyses of saturation time needed by use of different material mixtures.

The investigations in the pre-project were performed on clay/sand mixtures with mixing ratios of 35/65, 50/50, and 70/30.

The investigated clay/sand mixtures with clay contents of 35 % to 50 % meet the sealing requirements completely. The installation technique by vibration generated a dry bulk density of about 1.9 g/cm^3 for the 35/65 mixture and 1.75 g/cm^3 for the 35/65 mixture, corresponding to a porosity of 28 % and 38 %, respectively. The gas permeability of the mixtures measured under dry conditions varies in the range of 10^{-13} to 10^{-14} m^2. The initial water permeability right after saturation under installation conditions was determined to a mean value of $5 \cdot 10^{-18}$ m^2 for the 35clay/65sand mixture and of $2 \cdot 10^{-18}$ m^2 for the 50clay/50sand mixture. Compacting the mixtures at a pressure of 5 MPa resulted in a significant reduction of the water permeability down to $3 \cdot 10^{-20}$ - $6 \cdot 10^{-20}$ m^2 close to that of the intact Opalinus clay. Gas injection into clay/sand samples of 50 mm diameter and 100 mm length at a gas inflow rate of 0.2 ml/min caused an increase in gas pressure until break-through. The gas break-through pressure of the mixtures with clay contents of less than 50 % is lower than the gas entry pressure of 2 MPa of the Opalinus clay at Mont Terri. The gas permeability of the investigated mixtures after break-through was measured between $6 \cdot 10^{-18}$ and 10^{-17} m^2.

The saturation tests on clay/sand samples of 50 mm diameter and 100 mm length without applying any injection pressure indicated that the distribution of saturation is approximately the same for all the mixtures with clay contents of 35 %, 50 % and 70 % after a saturation time of 90 days, but during that time, the samples were not fully saturated. The time needed to reach full saturation observed at an increased injection pressure of 1 MPa varies in a range of 2 – 5 days for the 35clay/65sand mixture and 5 - 13 days for the 50clay/50sand mixture.

Under consideration of the required sealing properties and the testing time available in the project, the mixtures with clay contents of 35 % and 50 % have been selected for both, the mock-up and the in-situ tests.

For designing the mock-up and in-situ tests, a series of scoping calculations by use of CODE_BRIGHT were performed. Material parameters were derived from the

preliminary laboratory tests on the clay/sand mixtures and from literature. Because some of the parameters adopted are not precise due to a lack of test data, the scoping calculations are in a certain sense of preliminary character. In the scoping calculations, the same size of seals of 0.3 m diameter and 1 m length installed in the steel tube in the mock-up tests and in the boreholes in the in-situ tests were considered. The test procedure with four phases of water injection, water flow under a constant pressure, reduction of the injection pressure, and gas injection was simulated for the mock-up tests, while for the in-situ tests the additional phases of niche excavation and ventilation as well as of test borehole drilling were modelled for the determination of the initial and boundary conditions of the in-situ experiment.

On the basis of scoping calculations and considering other relevant conditions, it is recommended that two clay/sand mixtures with ratios of 35/65 and 50/50 shall be used for the mock-up and also for the in-situ tests. The most important testing conditions are the water injection pressure and gas injection rate. The recommendations for both are as follows:

1. To reduce the saturation time, water saturation of the initial unsaturated clay/sand mixtures shall be initiated by applying a constant injection pressure of 0.5 or 1 MPa;

2. Gas injection into the saturated seals shall be carried out at a constant gas inflow rate as low as possible, for instance 0.02 or 0.2 ml/min, to simulate representative gas generation rates in real repository;

For the 50clay/50sand mixture, the tests will last for more than 3 years. To reduce the testing time, the seal length should be shortened to about 0.5 m. Provided this is realized, both the mock-up and the in-situ tests can be finished within the available project duration as planned.

References

/ALO 02/ Alonso, E.E.; Olivella, S.; Delahaye, C.(2002): Gas Migration in Clays. Environmental Geomechanics – Monte Verita 2002, 83-94.

/BOS 02/ Bossart, P., Meier, P., Moeri, A., Trick, T., Mayor, J.-C., (2002): Geological and hydraulic characterization of the excavation disturbed zone in the Opalinus Clay of the Mont Terri Rock Laboratory. Engineering Geology 66, pp 19 – 38, Elsevier Science B.V.

/FRE 93/ Fredlund, D.G.; Rahardjo, H. (1993): Soil Mechanics for Unsaturated Soils. John Wiley&Sons, INC

/GEN 98/ Gens, A.; Garcia-Molina, A.J.; Olivella, S.; Alonso, E.E.; Huertas, F. (1998): Analysis of a Full Scale in situ Test Simulating Repository Conditions. Int. J. Numer. Anal. Meth. Geomech., 22, 515-548 (1998).

/ISR 81/ ISRM: Rock Characterization Testing & Monitoring – ISRM Suggested Methods, 1981.

/JOC 00/ Jockwer, N., Miehe, R., Müller-Lyda, I. (2000): Untersuchungen zum diffusiven Transport in Tonbarrieren und Tongesteinen. Gesellschaft für Anlagen- und Reaktorsicherheit (GRS) mbH, Köln, GRS-167

/LUX 02/ Lux, K.-H. et al., (2002): "Entwicklung und Fundierung der Anforderung "Günstige gebirgsmechanische Voraussetzungen", Teil A: Grundlegende rechnerische Untersuchungen. Gutachten im Auftrag des AkEnd, Professur für Deponietechnik und Geomechanik – Technische Universität Clausthal, März 2002.

/MIE 03/ Miehe, R., Kröhn, P., Moog, H., (2003): Hydraulische Kennwerte tonhaltiger Mineralgemische zum Verschluss von Untertagedeponien (KENTON). Gesellschaft für Anlagen- und Reaktorsicherheit (GRS) mbH, Köln, GRS-193.

/NAG 02/ NAGRA Technical Report 02-06, (2002): Project Opalinus Clay, Models, Codes and Data for safety Assessment – Demonstration of disposal feasability for spent fuel, vitrified high-level waste and long-lived intermediate-level waste (Entsorgungsnachweis). NAGRA National Cooperative for the Disposal of Radioactive Waste.

/OLI 96/ Olivella, S., Gens, A., Carrera, J., Alonso, E. E., (1996): "Numerical formulation for a simulator (CODE_BRIGHT) for the coupled analysis of saline media. Engineering Computations, Vol. 13 No. 7, pp. 87 – 112, MCB University Press.

/PEA 03/ Pearson, F.J., Arcos, D. Bath, A., Boisson, J.-Y., Fernandes, A.M., Gäbler, H.E., Gaucher, E., Gautschi, A., Griffault, L., Hernán, P., and Waber H.N. (2003): Mont Terri Project – Geochemistry of Water in the Opalinus Clay Formation at the Mont Terri Rock Laboratory.- Reports of the Federal Office for Water and Geology (FOWG), Geology Series No.5, Bern-Ittingen, 2003, Switzerland.

/PEL 99/ Pellegrini, R.; Horseman, S.; Kemp, S.; Rochelle, C.; Boisson, J.-Y.; Lombardi, S.; Bouchet, A.; Parneix, J.-C. (1999): Natural analogues of the thermo-hydro-chemical and thermo-hydro-mechanical response. Final report, EUR 19114 EN.

/ROD 99/ Rodwell, W.R.; Harris, A.W.; Horseman, S.T.; Lalieux, P.; Müller, W.; Ortiz amaya, L.; Pruess, K.: Gas Migration and Two-Phase Flow through Engineered and Geological Barriers for a Deep Repository for Radioactive Waste. A Joint EC/NEA Status Report, European Commission, 1999, EUR 19122 EN

/RÜB 03/ Rübel, A., Nosek, U., Müller-Lyda, I., Kröhn, P., Storck, R., (2004): Konzeptioneller Umgang mit Gasen im Endlager, Gesellschaft für Anlagen- und Reaktorsicherheit (GRS) mbH, Köln, GRS-205.

/SUD 01/ NN (2001): Product information of Calcigel. Süd-Chemie AG, Ostenriederstr. 15, D-85368 Moosburg, state as 2001.

/TIA 99/ Tiab, D.; Donaldson, E.C. (1999): Petrophysics. Theory and Practice of Measuring Reservoir Rock and Fluid Transport Properties. Gulf Professional Publishing, Houston, TX, Copyright 1999.

/THU 99/ Thury, M., Bossart, P., (1999): Mont Terri Rock Laboratory – Results of the Hydrogeological, Geochemical and Geotechnical Experiments Performed in 1996 and 1997. Landeshydrologie und –geologie, Geologische Berichte Nr. 23.

/UPC 02/ CODE-BRIGHT, A 3-D program for thermo-hydro-mechanical analysis in geological media, USER'S GUIDE. 2002.

/ZHA 04/ Zhang, C.-L., Rothfuchs, T., Moog, H., Dittrich, J., Müller, J. (2004): Experiments and Modelling of Thermo-Hydro-Mechanical and Geochemical Behaviour of the Callovo-Oxfordian Argillite and the Opalinus Clay. GRS final report, GRS-202.

List of Figures

List of Tables